2 mu4

NATIONAL AERONAUTICS AND SPACE ADMINISTRATION

Technical Memorandum 33-641

A Study of the Compatibility of Science Instruments With the Solar Electric Propulsion Space Vehicle

Richard H. Parker
Joseph M. Ajello
Alexander Bratenahl
Douglas R. Clay
Bruce Tsurutani

JET PROPULSION LABORATORY
CALIFORNIA INSTITUTE OF TECHNOLOGY
PASADENA, CALIFORNIA

October 15, 1973

Prepared Under Contract No. NAS 7-100
National Aeronautics and Space Administration

PREFACE

The work described in this report was performed by the Space Sciences Division of the Jet Propulsion Laboratory.

ACKNOWLEDGMENT

The authors acknowledge the contributions of many JPL colleagues. These include the Solar Electric Propulsion System Integration Technology (SEPSIT) study team, led by Jack A. Gardner, for their direction and assistance, and the Encke Slow Flyby science team, led by Ray L. Newburn, for the use of preliminary science payload data. We are grateful to Fred W. Taylor for allowing us the use of preliminary comet Encke model data and to David Wiksten, whose SEPSIT Environmental Design Criteria study was used herein.

CONTENTS

CONTENTS (contd)

TABLES

FIGURES (contd) Page

FIGURES (contd)

ABSTRACT

Electromagnetic interference (EMI) and field-of-view constraints are identified as the areas of most concern to science on solar electric propulsion space vehicles.

Several areas in which more detailed data on the space vehicle environment are needed are indicated. In addition, possible means to attain or demonstrate science/space vehicle compatibility are recommended for further iteration between space vehicle design and science payload considerations.

This study uses the space vehicle design developed by the Solar Electric Propulsion System Integration Technology (SEPSIT) effort. Two payload sets for comet Encke missions (a slow flyby and a rendezvous), as well as several instruments which are not included in the two payload sets, are analyzed to determine requirements on the space vehicle imposed by the instruments in order to meet their objectives. Environmental requirements for the sets of instruments are developed and compared to both the SEPSIT design criteria and the environment as it is presently understood.

I. INTRODUCTION AND SUMMARY

Potential advantages offered by solar electric propulsion compared to ballistic trajectory missions have long been recognized. However, during the technology development very few detailed considerations have been made concerning the compatibility of the environment produced by a space vehicle (S/V) using solar electric propulsion (SEP) with the payload science. Qualitative descriptions of potential incompatibilities have been expressed, but little quantitative information has been available. Recently questions concerning the compatibility were raised by the science community and addressed to NASA/OAST Office of Space Propulsion and Power Division. In response the science support activity was enlarged to include a study of science instrument compatibility with the SEP space vehicle. This activity is part of the Solar Electric Propulsion System Integration Technology (SEPSIT) program (Ref. 1).

In order for the SEPSIT study team to perform the system integration, the constraints that the science instruments place on the SEP space vehicle must be available. At the same time, members of the science community (i.e., potential users of a SEP space vehicle) need to know the constraints placed on the payload by the SEP spacecraft itself as well as its benefits. Further in order to perform tradeoffs, the approaches to removing or minimizing incompatibilities need to be studied from both the payload and SEP spacecraft points of view.

A. Objectives and Scope

The objective is to determine the compatibility of science instruments with the SEP space vehicle on the comet Encke rendezvous (Ref. 1) and slow

flyby (Ref. 2) missions. Additional instruments which are not included in the payload sets are also considered as candidates for future non-comet missions (which are not specified) on SEP S/V.

The objective is further limited by a quantitative consideration of two specific questions. First, what is the harshest environment to which each instrument can be subjected and still perform its experimental objectives? Second, what effects will the environment of the SEP space vehicle (as it is presently understood) have on the fulfillment of the experimental objectives, assuming no instrument modifications?

Finally, the differences and incompatibilities shown by the two analyses are further considered in order to seek potential solutions which are then suggested to the SEPSIT study team for consideration. The process is to be reiterated with the Science Compatibility Team (SCT).

The SCT has used configuration 3 of Ref. 1 as the baseline space-vehicle (S/V) for the study (Fig. 1). In addition, both the slow flyby instruments and the various experimental objectives given in Ref. 2 were adopted for use in the SCT activities. The rendezvous payload is a slight modification of the slow flyby payload. The rendezvous payload is an ad hoc selection by the authors, considering the different scientific objectives. To provide more generality, additional instruments have been considered. Section II will describe these instruments and their objectives in greater detail.

For the Encke payloads the instruments are considered as a set (rather than as separate experiments) for both the rendezvous and the slow flyby mission objectives. However, for the additional, non-Encke instruments the compatibility study was performed assuming that each instrument comprised the entire payload. It was further assumed that "typical" experiment objectives were applicable rather than objectives for an Encke mission. It is realized that this approach is not detailed enough for the non Encke instruments since specific objectives are a major compatibility consideration. However manpower and funding limitations demand this limitation, which nonetheless will provide two specific cases with at least an indication of the more general aspects of SEP/science compatibility.

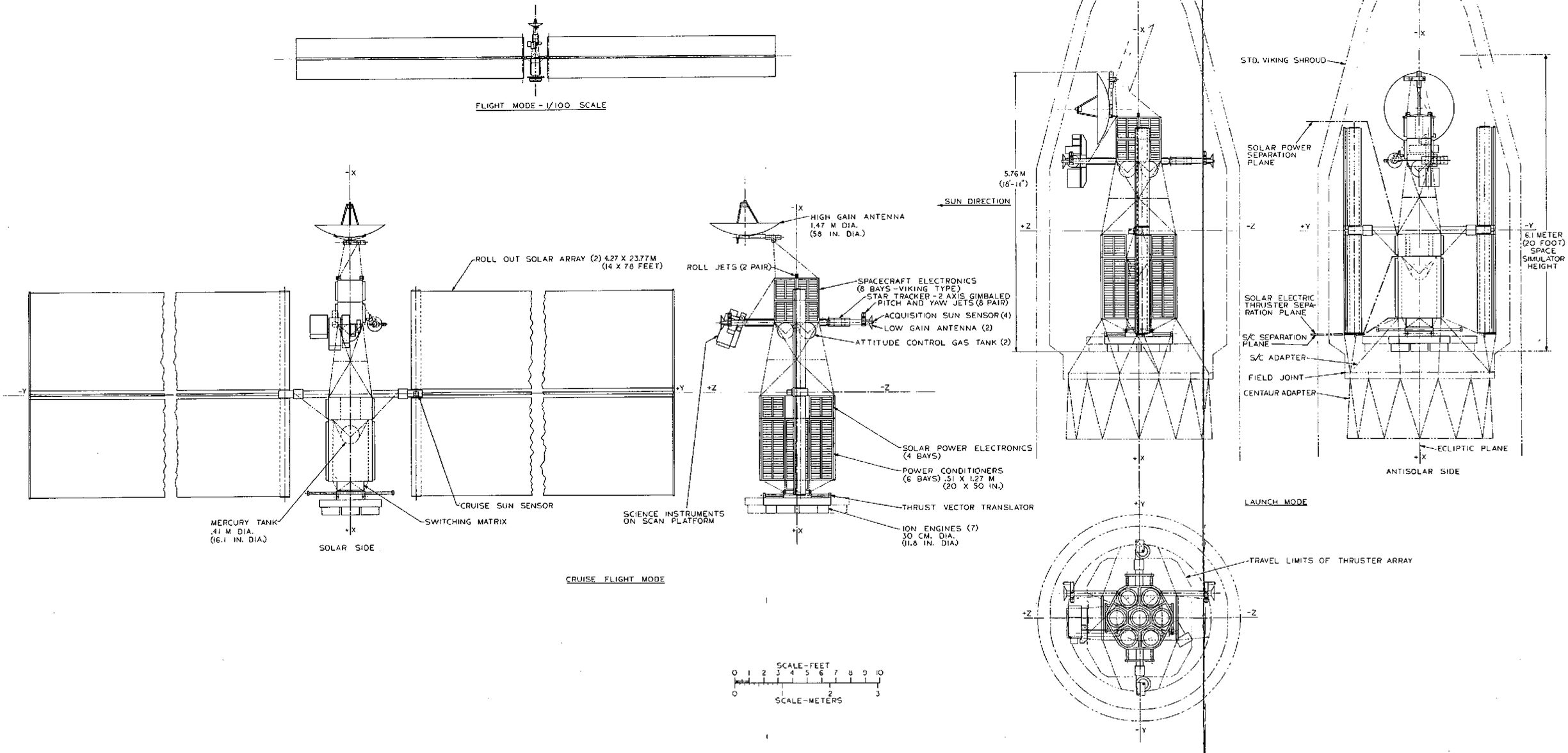

Fig. 1. The SEPSIT configuration 3 schematic. This shows an earlier version of the payload set for a rendezvous mission

FOLDOUT FRAME

FOLDOUT FRAME 2

B. Approach Used in SCT Study

A study team was formed composed of J. M. Ajello, A. Bratenahl (SEPSIT-SCT interface representative), D. R. Clay, R. H. Parker (team leader), and B. T. Tsurutani. The team, after being exposed to the current understanding of the SEP space vehicle environment and the documentation of related studies, compiled a list of compatibility areas of concern (Table 1). Several SCT members were also part of the Encke science payload study activity (Ref. 2) which made for a more thorough and more timely understanding of the Encke slow flyby payload and allowed an extrapolation for the rendezvous mission payload to be made by the SCT.

The various instrument requirements were established by using baseline designs described in Section II. In general, these requirements are obtained by establishing the maximum permissible uncertainty requirement for the most sensitive measurement expected to satisfy the experimental objective (typically ±10% of the minimum parameter expected). If we consider all incompatibilities as noise sources for the experiments, the noise created by the environment on a measurement either can be calculated (or, where available, experimental values are used). This noise should be limited to ±10% of the minimum value to be measured. Where several noise sources can contribute to this maximum allowed value, the rms value of the noises should be limited to ±10%. The design criteria for the environment on the SEP space vehicle are as given in Appendix A. However the EMI picture as currently understood for the SEP space vehicle may be considerably worse than shown in part 1 of Appendix A (see Ref. 3), and this degraded environment has been considered. The variations to the environment design criteria in Appendix A are shown in Table 2. The available plume deposition data was not adequate for the angles and distances envisioned for the instruments on the space vehicle (Refs. 4 and 5) and extrapolations were made as shown in Fig. 2. The extrapolation of this data proved to be optimistic (Ref. 6), and Fig. 3 shows the rather large increase in Hg impingement rates at angles greater than 80 deg from the thrust axis. For 30-cm-diameter thrusters the ion current is 1-4 mA/cm^2 at the exit plane (Ref. 4). Figures 2 and 3 can be coupled with the ion current value for each thruster to obtain the absolute quantity of deposition rates at angles from 0 to 120 deg. The ability to view through the plume has been considered by calculating the total column density. This will be described further in Section III.

Table 1. Compatibility areas of concern

Environment	Instruments affected	Major sources
Magnetic fields	Magnetometer and plasma wave	Thruster magnets, solar panels, PC panels, space vehicle currents, and materials
Conducted electromagnetic interference (EMI)	All instruments	Power conditioning equipment, thrusters arcing and insufficient isolation between subsystems and science
Radiated EMI	Fields and particles instruments	PC and power cables (e.g., arcing), plume plasma
Deposition of Hg and Mo	Cooled instruments and all to some extent	Propellant exhaust
Viewing through plume	UV and visible light-sensitive instruments	Sunlight scattering, $Hg^{0,+,++}$ and $Mo^{0,+,++}$ emission and adsorption lines
Field of view constraints	All instruments	Thrusters, large S/V, solar panels, integration of payload
Others		System integration, other mission types

Table 2. Variations from SEPSIT environmental design criteria for Encke missions

Environment	Design criteria	Level used in study
EMC	See Appendix A	Approximately 100 times higher than Viking levels; see Appendix A
Magnetic Field	5000 γ at TV 0.2 γ at magnetometer	10^4 γ at TV (see Table 18) 1 $\gamma \pm$ 0.1 γ at magnetometer
Meteoroids	$\lesssim$7.5 per 900 days with m $>10^{-6}$g	$\lesssim$8.5 (increased by $\lesssim$1 due to Encke coma events)(Ref. 2)
Vibrations	See Appendix A	Unknown due to uncertainty of boom design, etc.; potentially higher than design criteria
Plume depositions	Not specified	See Figs. 2 and 3
Fields of view	Not specified	See Fig. 1 and discussion in Section III
Radioisotope radiation	Not specified	$\lesssim$0.1 photon/cm^2-s (0.1 keV $\lesssim E_{photon} \lesssim$0.5 MeV) at X-ray spectrometer; $\lesssim \gamma$/cm^2-s (0.5 MeV $\lesssim E\gamma \lesssim$5 MeV) at gamma ray spectrometer

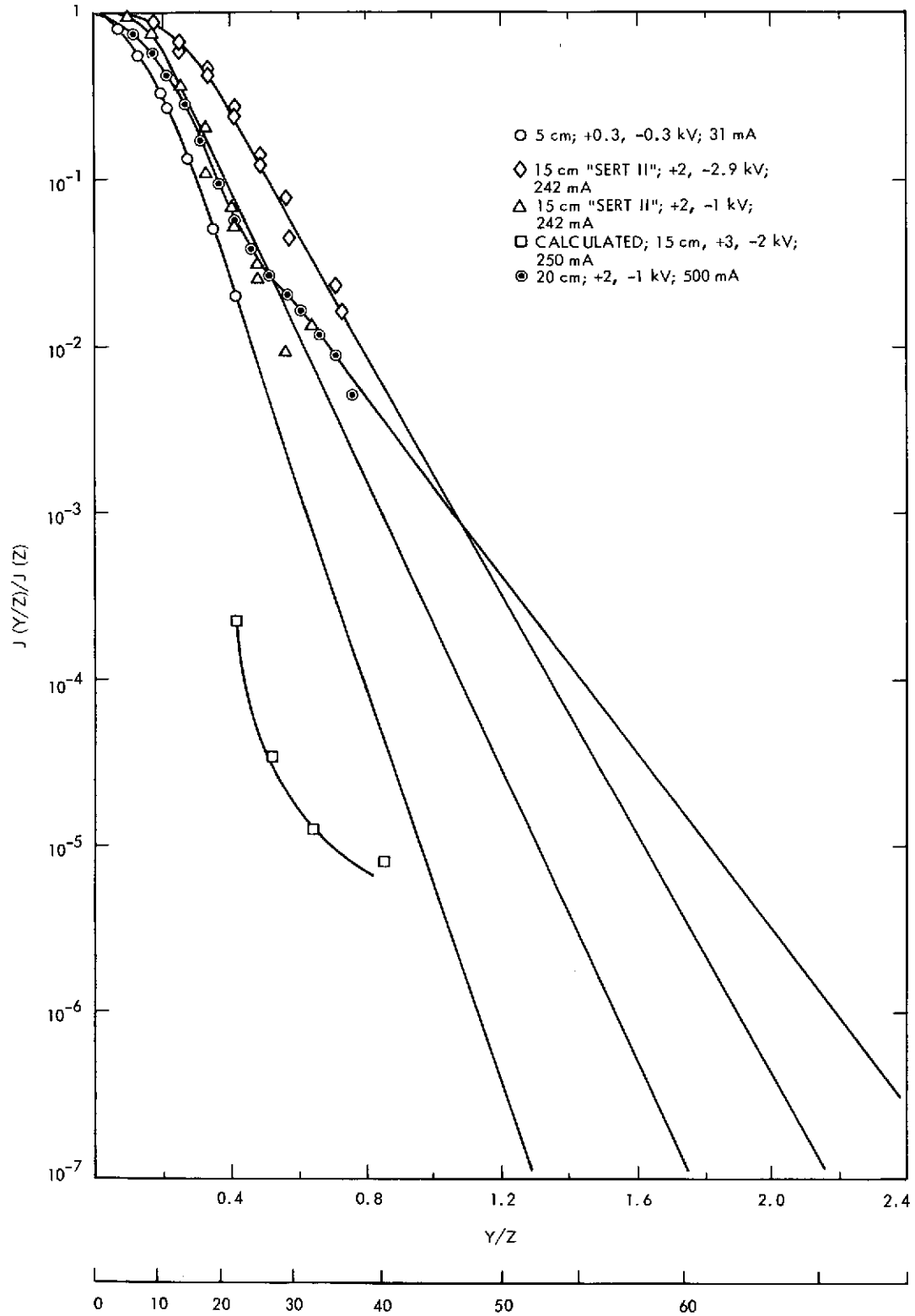

Fig. 2. Ion beam profile data from various Mercury bombardment ion engines with conventional grids. Shows extrapolation to large angles. Adapted from Ref. 4

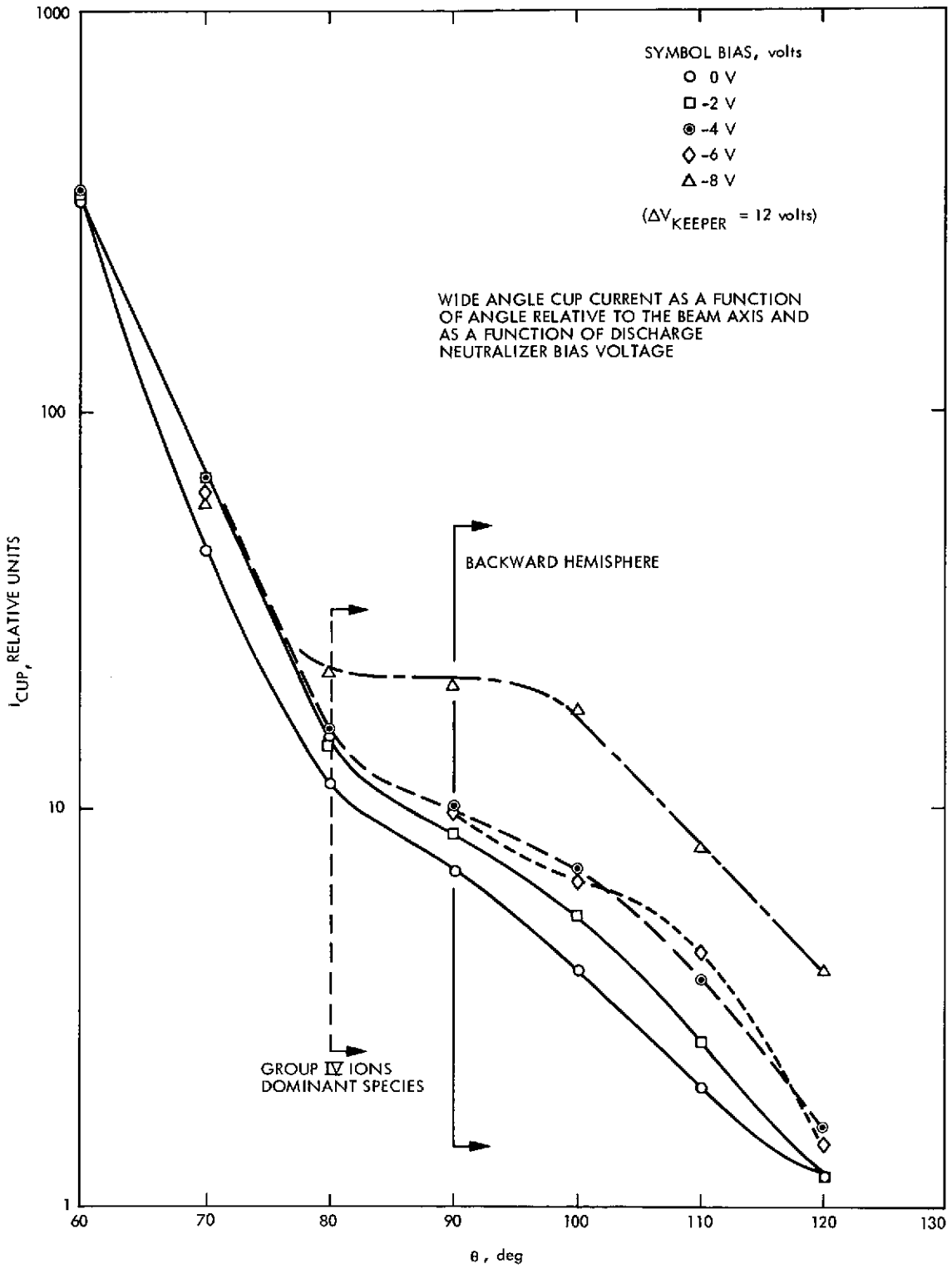

Fig. 3. SEP ion abundance in plume fringes. Faraday cup currents as a function of angle and neutralizer bias. Shows variation in data from earlier extrapolation of Fig. 2. Adapted from Ref. 6

A few brief comments are made as a reference frame for the more detailed discussions in succeeding sections concerning the mission designs and how the types of instruments are affected by specific environments.

Until hardware is actually integrated there is a possibility of undiscovered problems. Also, since only two comet missions have been considered, problems associated with other missions may not be represented in this study.

Some Encke slow flyby and Encke rendezvous trajectory data will be useful in the understanding of detailed problem areas. Figure 4 shows the base trajectories projected onto the plane of the ecliptic with a full scale of 1.6×10^7 km. Also shown are some comet features and the time in days before encounter. The different relative velocities and closest approach distances in the rendezvous and slow flyby missions dominate the types of scientific objectives which may be undertaken. For the rendezvous, detailed nucleus investigations as well as studies of the variations in physical processes (e.g., volatile release rates and constituents) due to large variations in solar distances are possible. For the slow flyby the opportunity to confirm or reject the existence of the nucleus is presented as well as the opportunity to perform in situ measurements on the coma/interplanetary interaction region while the coma is in a relatively steady state since during encounter there will only be small variations in comet solar distances.

Presently thrust analysis for the rendezvous indicates changes in the number of thrusters used at E-20 days ($\sim 8 \times 10^5$ km from nucleus) and again at E-6 days ($\sim 8 \times 10^4$ km from the nucleus). No similar analysis was available for the slow flyby, but for both missions any changes in S/V electrical or thrust conditions lead to uncertainties in analyzing and time-correlating scientific data.

Figure 5 shows (using a smaller scale) the near encounter trajectories from 10^5 km before to 8×10^4 km after encounter in Encke centered coordinates projected onto two orthogonal planes. For the rendezvous mission, an assumed postencounter trajectory is shown in Figure 6. The choice of 100 km altitude represents a tradeoff between safety (which requires large altitudes to reduce micrometeoroid hazard) and the science requirement to view the nucleus from a close distance in order to improve spatial resolution. In particular, the gamma ray spectrometer and the X-ray

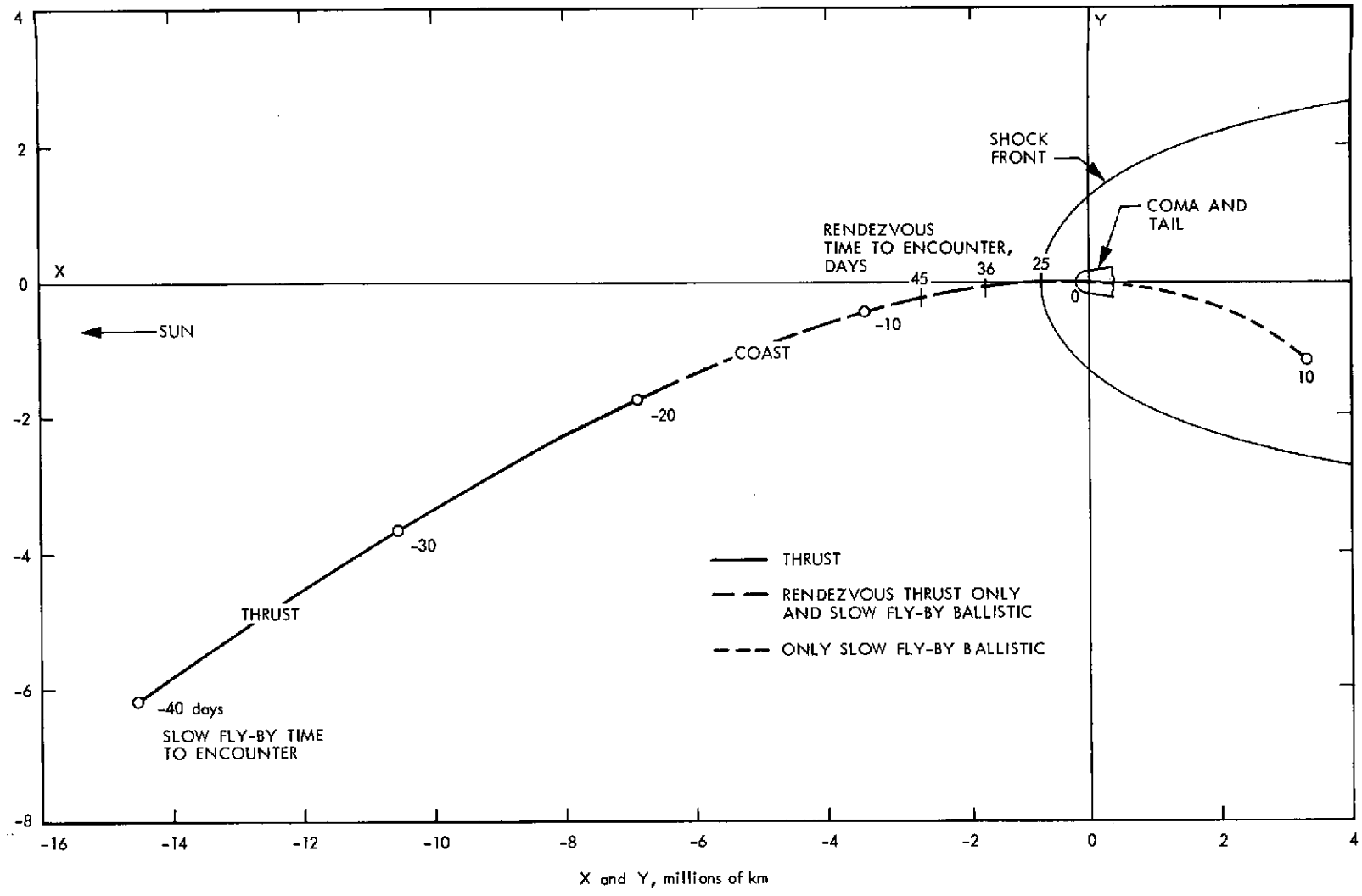

Fig. 4. Trajectories for Encke slow flyby and rendezvous missions in comet-centered coordinates with the comet/Sun line fixed. The numbers below the curve are days from encounter for the slow flyby; those above the curve are days from encounter for the rendezvous

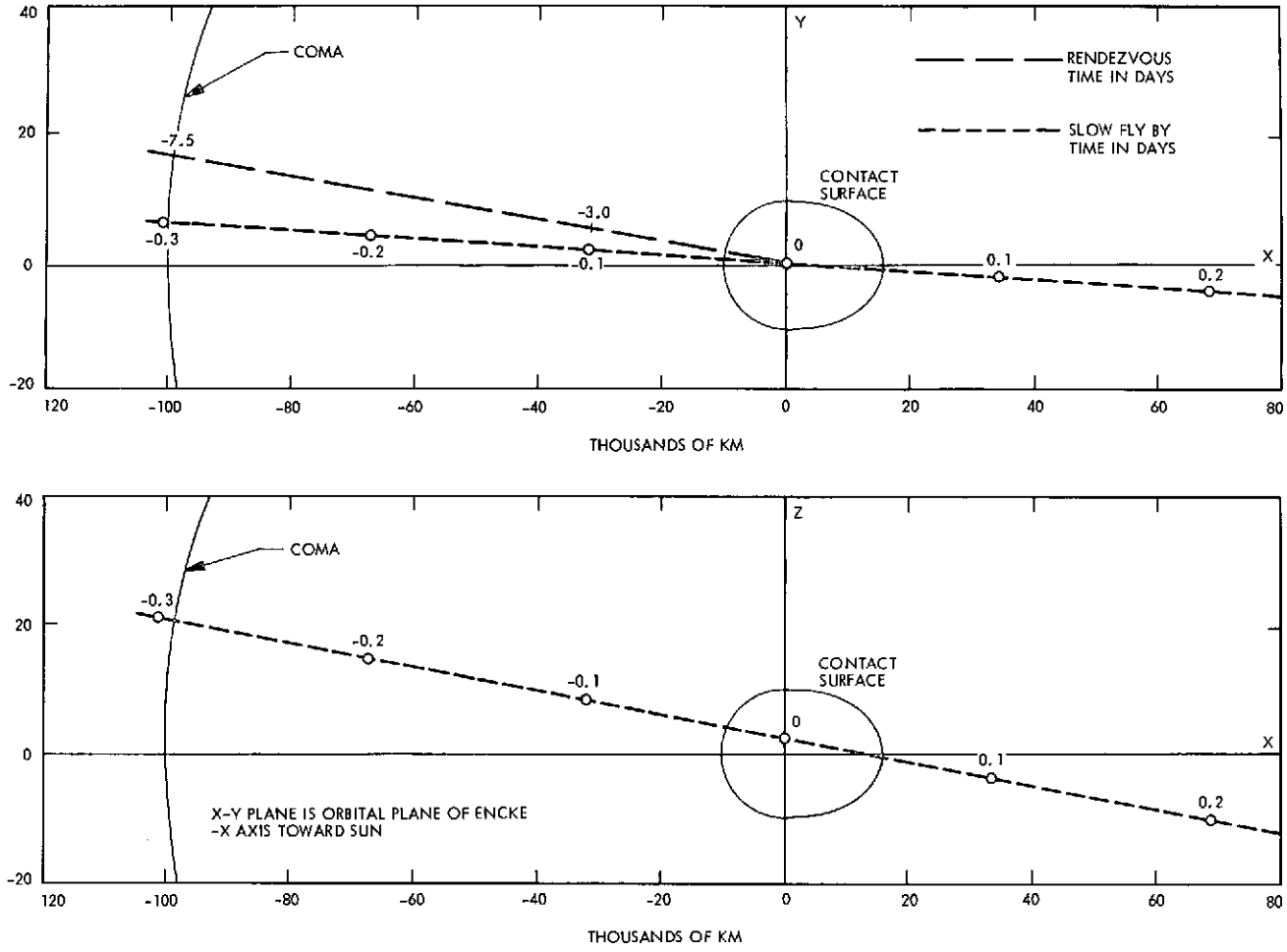

Fig. 5. Near-encounter trajectories for Encke slow flyby and rendezvous missions. The slow flyby trajectory on this scale is all-ballistic, while the rendezvous is mainly thrust periods with short no-thrust times for coma measurement. The top curve is an ecliptic projection; the bottom curve is a projection normal to the ecliptic. Both curves are in comet-centered coordinates with the comet/Sun line fixed

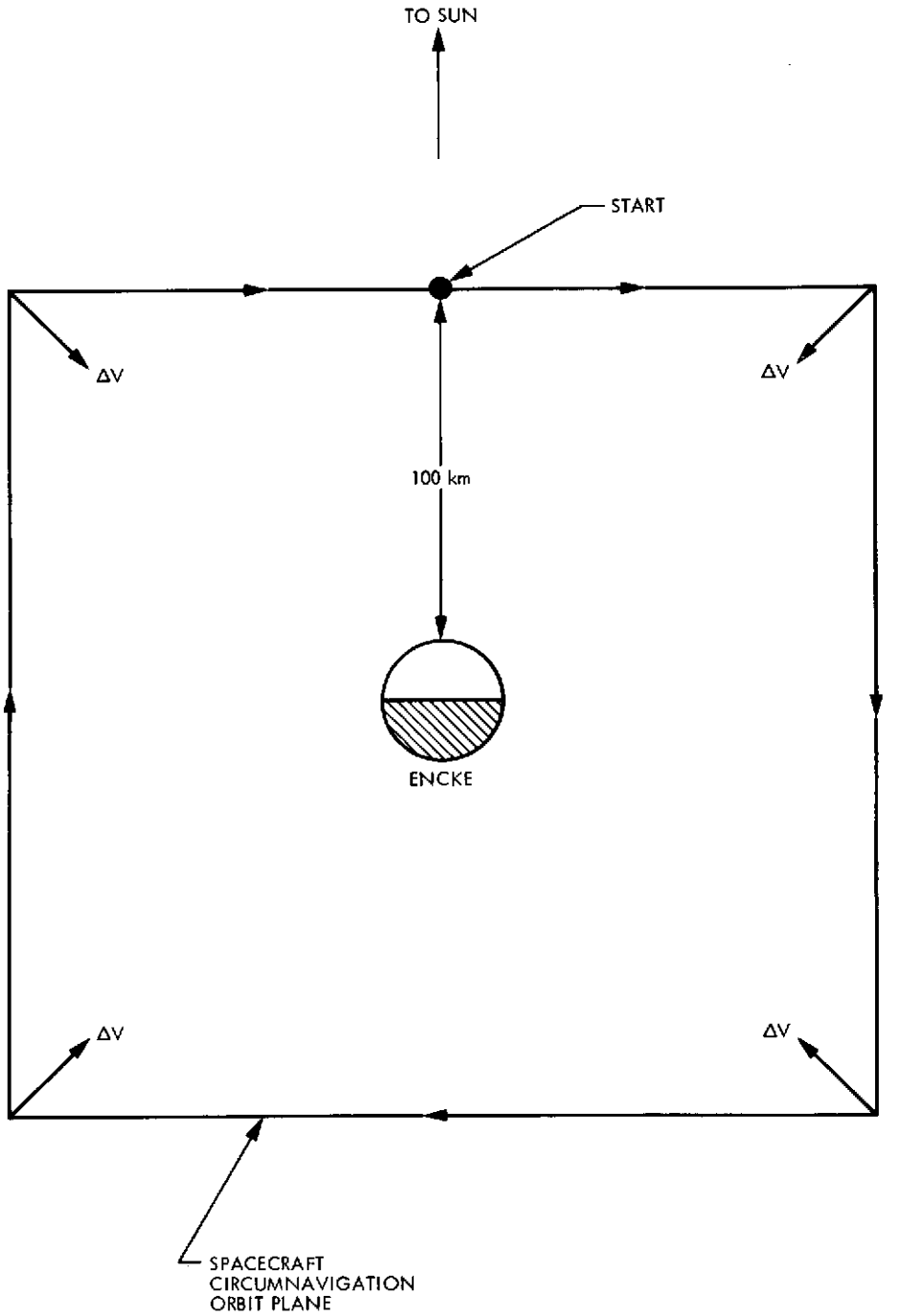

Fig. 6. Comet Encke rendezvous strategy. This path can be lowered to 10-km separation if the meteoroid hazard is small at the 100-km separation shown. Using Δv of 4 m/s will allow reasonably short transit times

spectrometer cannot satisfy their objectives at distances larger then ~50 times the radius of the nucleus.

The model of the science strategy for the slow flyby is presented in Table 3 and for the rendezvous it is presented in Table 4.

C. Summary of Study Results

The environment as currently understood leads to several specific areas of incompatibilities (enumerated below). However, all of these appear to be amenable to solution for the missions studied through additional considerations in design of present systems or through combination of some new methods for compensating or reducing the undesirable effects. Tables 5 through 12 give the compatibility analyses for types of environments of concern to science instruments on a solar electric propulsion space vehicle. The numbers give the relative priorities of both the sources and solutions within each of the eight tables. It is assumed that "typical spacecraft" environments (as defined partially by the design criteria in Appendix A) will be accepted by the instruments, except as specifically stated for specific instruments.

From these tables we see that:

(1) With the thrusters on, both fields and plasma experiments will be affected. With the thrusters off, the effects are significantly reduced provided (a) permeable materials do not lead to large nondipolar magnetic field variations and high multipole distortions if electromagnets are used or if permanent magnets are used that the resultant fields do not require excessive boom lengths, and (b) space vehicle potentials do not reach levels greater than $\sim|2\ V|$.

(2) An indication of thruster arcing is desirable in engineering data telemetered to Earth in order to properly interpret science data during thrusting periods.

(3) Field of view limitations must be considered in payload selection to a greater extent than on smaller non-SEP spacecraft.

(4) Data in support of environmental estimates are needed for a set of thrusters operating under various configurations and loads

Table 3. Abbreviated Encke slow flyby science strategy model

Time	Event and related experiments
E - (60 to 20) days	Begin TV approach guidance photography, secondary science data gathering
E - 20 days	Thrusters off, all instruments on, and calibrations begin (~50 rolls each about 2 perpendicular axes for fields and particles), roll in solar panels to ~10%
E - 6 days	Start primary science data gathering
E - 3 days	Transit shock front at 10^6 km from nucleus, fields and particles
E - 7 hours	Transit visible coma at 10^5 km from nucleus TV, mass spectrometer, Langmuir probe, Sisyphus and UV spectrometer
E - 42 minutes	Transit contact surface, all
E = (perihelion - 30) days	Closest approach to nucleus (1000 ±500 km), all
E + 15 minutes	720 deg roll for fields and particles inside contact surface
E + 1 hour	Transit "center" of tail of Encke at 15,000 km distance
E + 3 days	End primary science data gathering
E + 6 days	Postcalibration (similar to E - 20 days)
E + 10 days	Transit 0.7 au solar distance (design limit of S/V thermal control capability)

Table 4. Abbreviated Encke rendezvous science strategy model

Time	
E - (150 to 0) days	Approach guidance
E - 45 days	Calibration rolls ~0.5-day duration
E - (40 to 0) days	Payload on; brief no-thrust periods
E - 25 days	Encounter shock front at 10^6 km from nucleus
E = (perihelion - 50) days	1000 km from nucleus on sun side with 4m/sec rel. vel.; continue observation of nucleus and coma
E + (1 to 9) days	Begin circumnavigation (see Fig. 6); stationkeeping for 1 day and 1 day for relocation (i.e., average velocity of $\geq$1.6 m/s, 4 m/s delta velocity to change stations), stay in Encke orbital plane
E + (9 to 17) days	Begin circumnavigation in plane normal to first circumnavigation plane; stationkeeping for 1 day and 1 day for relocation
E + 17 days to end of mission	Repeat circumnavigation in Encke orbital plane. If feasible reduce altitude to 10 km

Table 5. Magnetic contamination and potential solutions

Source of contaminant

(1) Thruster electromagnets on, or permanent magnets.

(2) Thruster electromagnets off, remnant magnetism, solar panels, space vehicle currents and materials.

Experiments impacted

(1) Magnetometer, plasma wave.

(2) Langmuir probe, ion mass spectrometer.

(3) All experiments.

Instrument solution

Accept degraded operation during thrusting periods using electromagnets in order to provide a magnetically "clean" environment when electromagnets are off.

Space vehicle solution

(1) Electromagnets off during nonthrusting periods, separation of source of field from instruments (booms).

(2) Dipole pairing and matching arrangements; controlled bucking coils; ringing down electromagnets.

(3) Thruster pole face shaping, magnetic shielding.

Estimate of impact extent

Reasonable boom lengths should provide acceptable levels of magnetic fields; variation in field is expected to be prime determining factor in boom lengths. Use of permanent or electromagnets in thrusters creates critical problem for magnetometer and plasma wave if not controlled.

Remaining concerns

Lack of supporting data on (1) benefits to magnetometer and plasma wave for dipole orientation of thruster magnets, (2) effectiveness of controlled bucking coil, (3) field variations expected within a set of either permanent or electromagnet thrusters precludes quantitative analysis of boom length requirements for the two sensitive instruments.

Table 6. Electrostatic potential contamination and possible solutions

Source of contamination

(1) With thrusters on, the unbalance between electrons and ion charges leaving S/V.

(2) Photoelectric effects charging the S/V positive with respect to the local plasma; coma plasma impinging and, due to higher electron fluxes, charging the S/V negative.

(3) Variations in S/V potential due to conductivity variation of the S/V surfaces.

Experiments impacted

(1) Langmuir probe, ion mass spectrometer.

(2) Plasma probe, plasma wave.

Instrument solutions

(1) Instrument development to handle electrostatic potential variations of the S/V; avoid viewing in directions near S/V surfaces (affects FOV).

(2) Determine S/V potential from in-flight data and factor this into interpretation of results.

Space vehicle solutions

(1) With thrusters on, provide neutralization.

(2) Roll in solar panels; provide extended truss and boom locations for payloads; and/or with thrusters off provide electrostatic control of S/V (i.e., using neutralizer, emission probe, and conducting grids on S/V surfaces).

Estimate of impact extent

With thruster on, possibility of arcing damage to any instrument exists if no neutralization is provided. Although with thrusters off the problems

Table 6 (contd)

are similar for any S/V, they are increased by the S/V size and uncertain coma plasma densities. Both the Langmuir probe and the ion mass spectrometer modeled will begin to compromise their objectives if voltage variations are greater than 2-5 V. The plasma probe and plasma wave will be impacted over a portion of their dynamic ranges. The other instrument should have only negligible effects.

Remaining concerns

Lack of quantitative understanding of space vehicle potential.

Table 7. Conducted electromagnetic contamination and potential solutions

Sources of contamination

(1) Thruster arcing.

(2) Power conditioners (PCs); insufficient isolation; plume.

Experiments impacted

All experiments.

Instrument solution

(1) Increased isolation in instrument; compensation by ground data analysis.

Space vehicle solution

(1) Provide indication of arcing for ground analysis.

(2) Use good design techniques for isolation and cabling; locate instruments away from plume; when possible turn thrusters off; develop quiet thrusters and PCs.

Estimate of impact extent

No problems if design criteria are met but meager data indicate as much as 120 dB isolation may be needed and has not yet been verified as available. Large voltages and currents used on solar electric space vehicle increase the problem over non-SEP spacecraft.

Remaining Concerns

Lack of supporting data on frequency and magnitude of conducted EMI on science data lines in an integrated S/V.

Table 8. Radiated EMI contamination and potential solutions[a]

Sources of contamination

(1) Thruster arcing.

(2) Plume plasma, PC, telemetry subsystem.

Experiments impacted

(1) Fields and plasma, radar.

(2) All.

Instrument solutions

(1) Compensation in ground data analysis for thruster arcing; selection of radar frequencies to avoid telemetry.

(2) None: alters the ambient parameters being measured.

(3) Ground and inflight tests to measure the effects; analytical handling of science data during arcing.

Space vehicle solution

(1) Provide indication of arcing for ground analysis.

(2) Thrusters off; proper isolation of PC; develop quiet thrusters and PCs.

Estimate of impact extent

Probably severe during arcing but if thruster arcing has a small duty cycle and if arcing times are flagged in the engineering data, these can be handled analytically during data reduction; other radiated EMI sources are expected to be only minor concerns if design criteria are met. Large voltages and currents used on solar electric space vehicles increase the problem over non-SEP spacecraft.

Remaining concerns

Absence of supporting data on frequency and intensity of arcs and other EMI sources tends to keep radiated EMI from being discarded as unimportant. PC design as well as solar panel design is not well understood in an integrated S/V.

[a] X-ray and gamma ray interference is in Table 12.

Table 9. Mercury and molybdenum deposition and potential solutions

Sources of contamination

(1) Thruster plume; thruster construction material.

(2) Space vehicle surfaces hit by plume.

Experiments impacted

(1) Optical surfaces; plasma wave instrument.

(2) All experiments.

Instrument solutions

(1) Avoid prolonged viewing in plume hemisphere when thrusting; allow temperature control to increase evaporation.

(2) Provide covers on optics or sensitive nonconducting areas (e.g., boom between probe pairs of plasma E wave detector); provide heating for sensitive regions.

Space vehicle solutions

(1) Thrusters off during view periods.

(2) Provide electrostatic deflection of low-energy ions; plume baffles in certain areas.

Estimate of impact extent

Slight and/or controllable for Hg; probably slight for Mo; highly uncertain especially for Hg on cooled but clean surfaces.

Remaining concerns

Lack of flux and energy data at large angles and distances; absence of data for Mo and other minor plume constituents, including data on energies, flux and sticking as functions of temperature and surface material.

Table 10. Contamination when viewing through plume and potential solutions

Source of contamination

(1) Absorption and scattering of electromagnetic radiation and charged particles by the thrust plume.

(2) Emission lines from the thrust plume.

Experiments impacted

(1) Optical dust detector, UV spectrometer, imaging, radar.

(2) All other experiments.

Instrument solutions

(1) Avoid use of affected emission and absorption wavelength region, (i.e., instrument development), determine inflight the plasma and optical effects of plume and remove by analysis.

(2) Use preflight test program to supplement the understanding of effects and account for them analytically and by instrument design.

(3) Accept degraded data for engineering purposes.

Space vehicle solutions

None.

Estimate of impact extent

Effects limited to specific electromagnetic wavelengths where interference for spectrometers and photometers will degrade the plume portion of the viewing field during thrusting periods. Negligible effect to high ($\geq$1 keV) energy charged particles.

Remaining concerns

Lack of photometric emission and absorption data from the sunlit plume and multiple plumes in the UV, visible, IR and radar wavelengths; lack of plasma wave data on frequency or magnitude, turbulence, interactions with the solar wind or coma, and electromagnetic transmission.

Table 11. Field-of-view limitations and potential solutions

Source of contamination

(1) Space vehicle subtends large solid angle due to its size (longer booms will provide more obstructions for bus-mounted instruments).

(2) Thruster plume degrades viewing in the hemisphere centered around the thrust direction during thrust periods.

Experiments impacted

All experiments.

Instrument solutions

(1) Use increased observation time in rendezvous mission to compensate for reduced FOVs.

(2) Reduce area covered and/or sensitivity.

Space vehicle solutions

(1) Roll-in solar panels, provide extended truss and boom locations for payloads, attitude adjustment of space vehicle.

(2) Limit number of instruments.

Estimate of impact extent

On a Flyby mission the impact is probably significant, with less impact for a rendezvous mission since the ability to adjust the space vehicle attitude allows the FOV to be reduced at the expense of several parameters (e.g., increased available time to obtain (1) areal and phase angle coverage, (2) dependence on nucleus-space vehicle separation distance and on comet distance from sun).

Remaining concerns

Impact caused by changes to mission, payload and/or configuration, ability to roll-in solar panels.

Table 12. Radioisotope contamination and potential solutions

Source of contamination

Trace amounts of Th, U, ^{40}K, Pu, Np, ^{129}I, etc., contained in space vehicle materials (e.g., battery, glasses, Hg) produce background γ rays; de-excitation of chemical elements of S/V (e.g., Si, Al, Mg) produce background X-ray.

Experiments impacted

Gamma ray spectrometer, X-ray spectrometer.

Instrument solutions

Background measurement and subtraction of space vehicle radiation levels; shield low-energy photons by noninterfering material (e.g., W).

Space vehicle solutions

(1) Boom mounting of instruments; control of materials with trace elements of radioisotopes.

(2) Location of radioisotopes far away from the instruments; provide intervening material between instruments and sources in S/V configuration design.

Estimate of impact extent

Similar problem as non-SEP spacecraft but greater impact (due to larger area/mass ratio); critical for the two instruments that adequate control be provided.

Remaining concerns

Absence of information on amounts and location of radioisotopes on space vehicle.

for EMI, magnetic fields, plume deposition and fields of view (FOVs) through the plume.

II. DEFINITION OF INSTRUMENTS AND OBJECTIVES

A. Encke Slow Flyby Payload

The objectives and an abbreviated discussion of the operations of each instrument are given. This payload is described in more detail in Ref. 2. Table 13 is a list of the instruments and objective for the Encke slow flyby mission. Table 14 shows the mass, power, data rate, and field-of-view requirements for the baseline Encke slow flyby payload.

The mass spectrometer is an instrument to measure the neutral and ionic densities as a function of mass for the most likely constituents of the coma region of Encke. The objectives of the experiment are to determine the number density for all mass species in the range of 1 to 100 amu for both the ionic and neutral gases and to determine the component of velocity in the direction of the spacecraft trajectory for the ions detected. These results in conjunction with other fields and particle experiments will help identify coma constituents, parent molecules, pressures, and bulk loss for Encke.

The instrument considered for this experiment is a double focusing magnetic deflection type spectrometer with electric and magnetic analyzers used in tandem (Fig. 7). This instrument, very similar to that proposed for the Venus Pioneer mission, has a sensitivity of 0.1 ion/cm^3 or 100 neutrals/cm^3 with a dynamic range of 10^6 for the mass range of 1-100 amu. In the ionic measurement mode the use of a retarding potential field is used to discriminate against unwanted ions thermalized within the instrument and to determine the ionic ram velocity. The aperture must face in the direction of spacecraft velocity relative to the comet (nearly anti-solar direction) and have an unobstructed field of view. Figure 8 shows the translational energy vs spacecraft velocity with the molecular dissociation energies shown assuming 100% conversion of translational energy to vibrational energy. This points out the scientific basis for small relative velocities in flyby missions. The use of low Z elements in the gas used for the attitude control thrusters will contaminate this mass range and must be avoided.

Table 13. Encke slow flyby instruments and objectives

Instrument	Objectives
Mass spectrometer	Determine mass distribution of ions and neutrals from 1-100 amu in the coma and tail along trajectory.
Imaging	Determine existence of nucleus, size, shape, rotation and features; assist in approach guidance.
Optical particle detector (Sisyphus)	Determine spatial distribution, size distribution and velocity of cometary debries and dust above 1 micron size in the coma and tail.
Magnetometer	Determine magnetic field structure of shock, coma, tail, and comet vicinity in dc to 1-Hz frequency range.
Plasma wave detector	Determine magnetic and electric field variations in the shock, coma, tail, and comet vicinity over frequency range from 1 Hz to 100 kHz.
Plasma probe	Determine ion densities, energies (from 10 eV to 2.5 keV) and flow before the shock front and down to the contact surface in the coma and tail.
Langmuir probe	Determine electron and ion densities, energies (from 0 to 15 eV), and flow in the coma, tail and comet vicinity.
IR radiometer	Determine bond albedo, filling factor, and energy budget over wavelengths 0.3 to 3 μ, 4 to 100 μ, and 5 bands from 6 to 18 μ.
UV spectrometer	Resolve m/e species ambiguities with mass spectrometer; map UV species throughout coma; determine surface composition of nucleus.

Table 14. Encke slow flyby baseline science payload: basic requirements

Instrument	Mass, kg	Power, W	Data rate, bps	FOV
Mass spectrometer	5.3	9	5	±15° along relative (to Encke) velocity vector.
Imaging	20	20	111,000	9 mrad; on scan platform.
Optical particle detector	5	3	6000 peak 1 avg	Four 10° half-angle cones directed 30° from the relative (to Encke) velocity vector toward Encke.
DC magnetometer	2.0	3	200	In situ; but affected by and located away from magnetic field sources of spacecraft.
Plasma wave detector	4.6	5	300	In situ; but affected by and located away from electric and magnetic fields of spacecraft.
Plasma probe	5	6	350	2 60° half-angle cones directed as described in text.
Langmuir probe	2.5	5	200	3 50° half-angle cones directed as described in text.
IR radiometer	9.3	18.5 peak 10.5 avg	290	1 mrad cone boresighted with TV on scan platform.
UV spectrometer	7.8	9	1600	0.25 × 4° boresighted with TV on scan-platform.

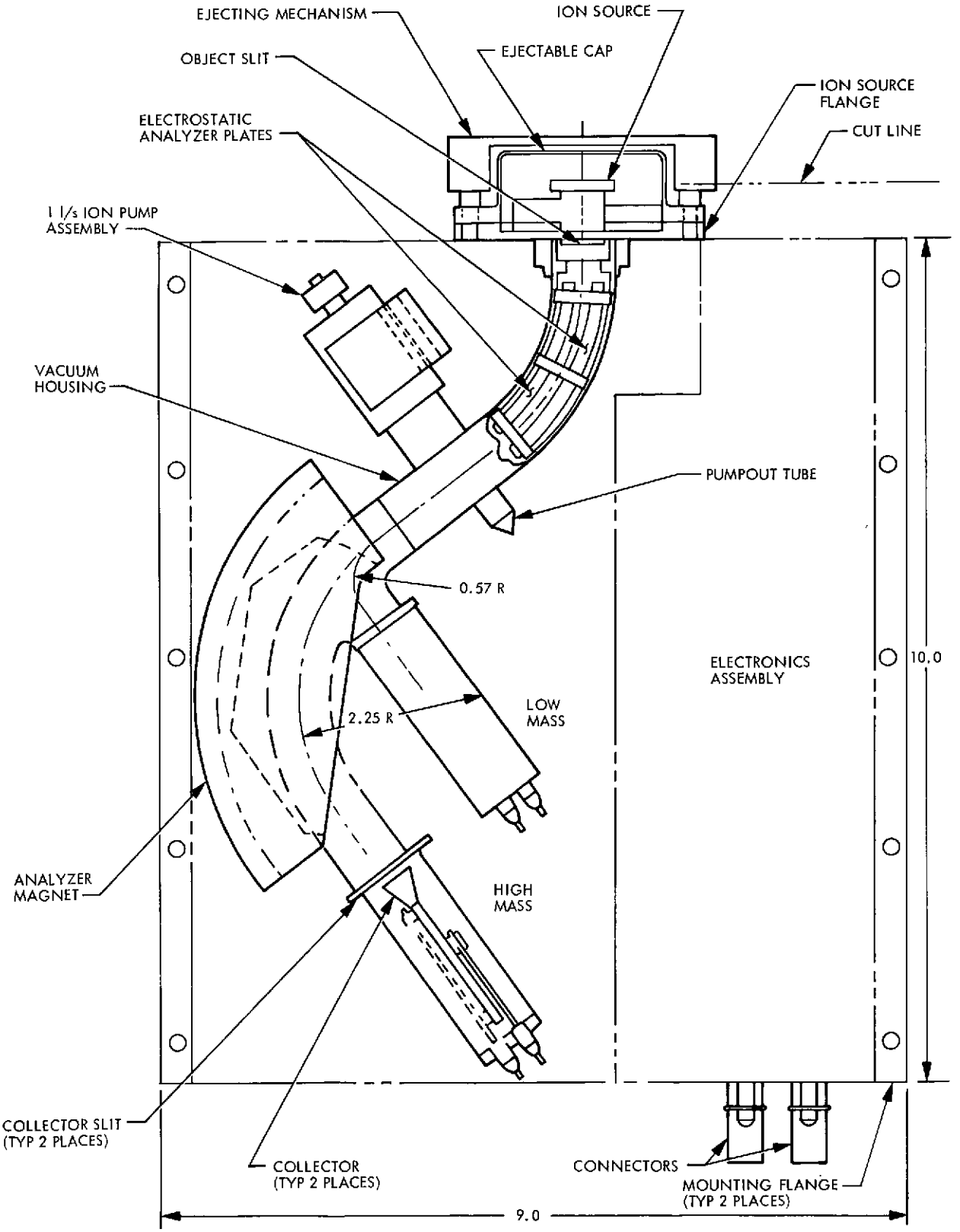

Fig. 7. Schematic of the mass spectrometer. This experiment is to be designed to measure 1 to 100 amu molecules and atoms, both neutrals and ions. Adapted from Ref. 2

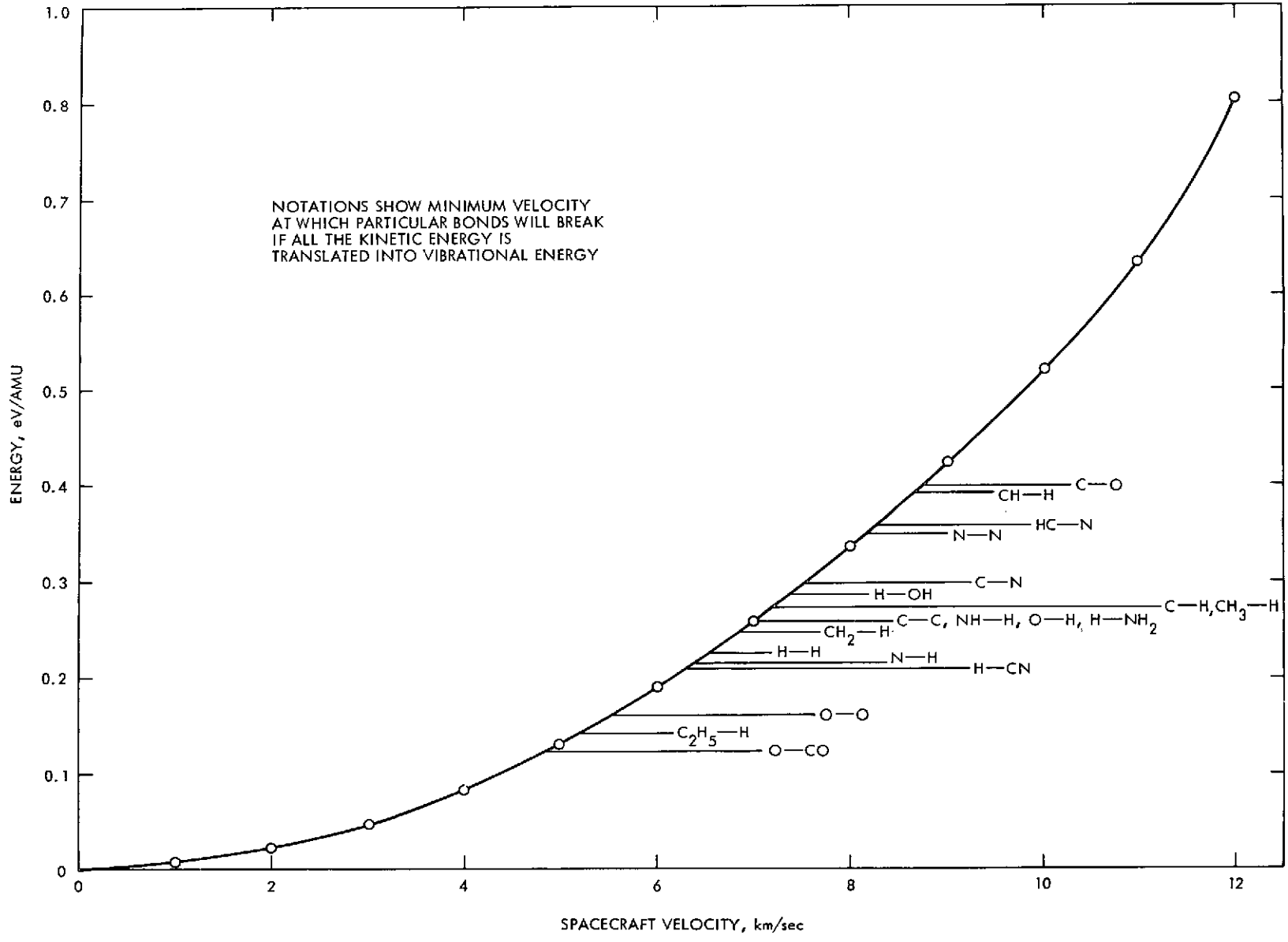

Fig. 8. Spacecraft velocity vs bond energy. Adapted from Ref. 2

The mass spectrometer will measure the ion and neutral mass distributions in the coma starting around 2×10^6 km (E-6 days) from the nucleus and continuing through the coma and tail. Species observed by ground-based astronomy include H, CH, NH, O, NH_2, OH, CN, C_2 and C_3. Parent molecules may include H_2O, N_2, CH_3 and CO_2 among others and ambiguities may arise between CO and N_2 or CH_3 and NH which may be resolved by considering abundances of other species.

The imaging experiment will attempt to confirm the existence of the nucleus if the coma is not opaque. Also imaging will determine size, shape, albedo, and (if features or variable albedos are discernible) rotation rates. In order to reduce costs the MM'71 systems will be used so that the smear assuming 5 μr/sec will be 15 pixels at 10^7 km distances for a 2 minute exposure. Figure 9 shows the approach trajectories considered and Fig. 10 shows the time required for a S/N = 5 at various distances from the nucleus. Time relative to closest approach is also shown. Pictures will be taken starting at approximately E-60 days for approach guidance and for scientific purposes after E-20 days through E + 15 min. The baseline instrument is the MM'71 narrow angle camera. It is anticipated that imaging will be used in the approach guidance phase of comet acquisition provided adequate pointing stability can be provided.

The magnetometer is shown in Fig. 11 and is similar to the Pioneer 10 instrument. The magnetometer is designed to measure the ambient interplanetary magnetic field and the possible changes to it as the space vehicle traverses the coma and tail. Inside the contact surface where the interplanetary magnetic field may be excluded and upper limits can be determined for the magnetic moment of the nucleus. A measurement of 1.0 ± 0.1 γ is needed to satisfy the objectives. At some time inside the contact surface, in the regions possibly shielded from the solar fields, a 720-deg roll is desired to reduce the upper limits of the magnetic field of both the comet and the S/V. The magnetometer will operate through the end of the mission, starting at E-20 days. The sensor is to be located on a boom in order to reduce the effect of the S/V induced magnetic fields.

The plasma wave instrument is shown in Fig. 12 and is similar to the OGO-6 instrument. It is designed to measure electric and magnetic waves in the range of 10 Hz to 100 KHz, with a sensitivity of $10^{-8}\gamma^2$/Hz at 100 Hz

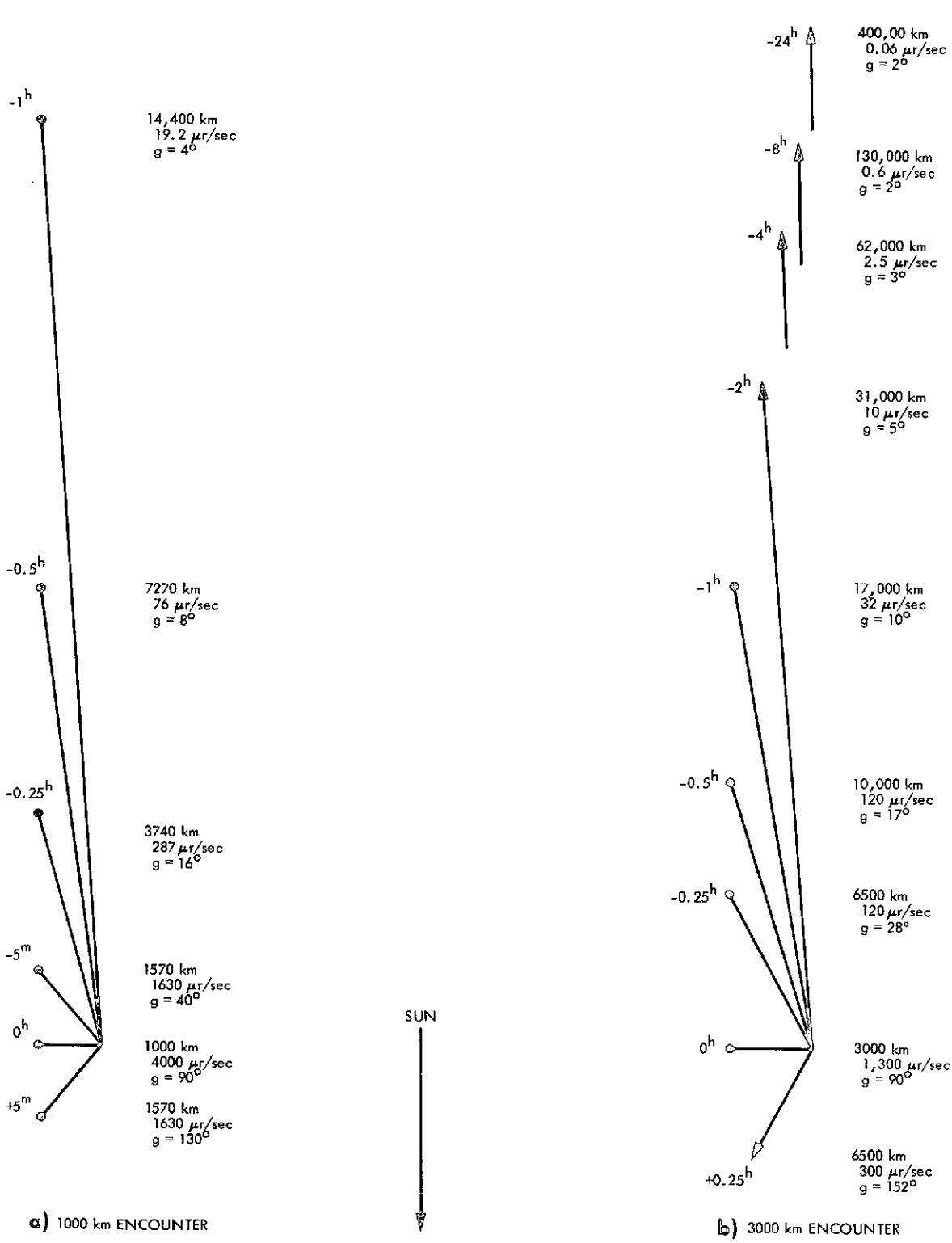

Fig. 9. Imaging and scan platform instrument view data to nucleus for the slow flyby mission. The vectors indicate the view direction. Shown by each are (1) the times relative to encounter in hours or minutes, (2) the separation distance from the nucleus, (3) the angular slew rate needed to point at the nucleus, and (4) the phase angle g of the nucleus. Adapted from Ref. 2

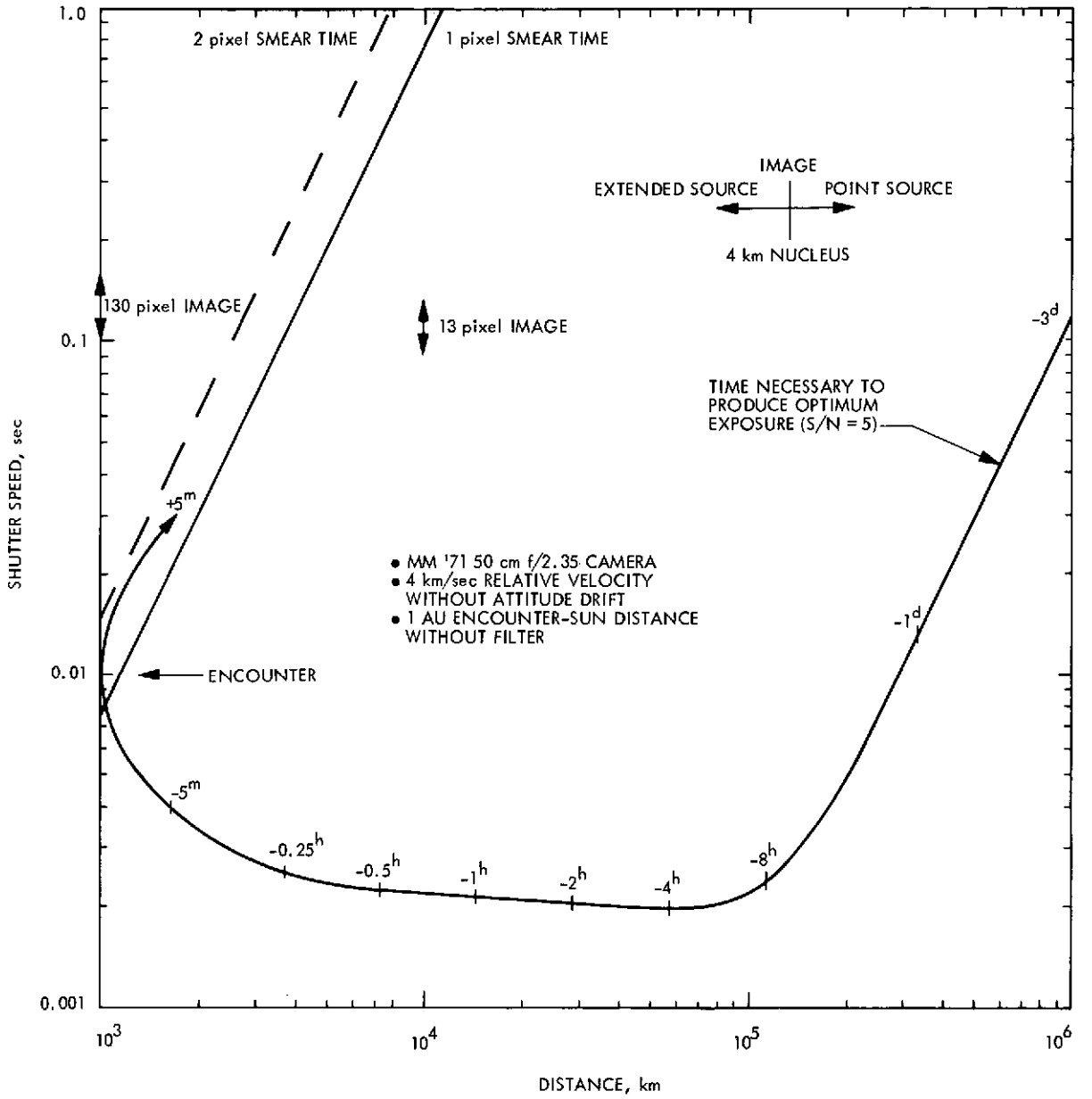

Fig. 10. The time of exposure necessary for imaging to obtain a signal-to-noise ratio of 5.0. Also shown are the times to encounter in the slow flyby. An instrument-to-target pointing stability of ≤5 μrad/s is assumed. Adapted from Ref. 2

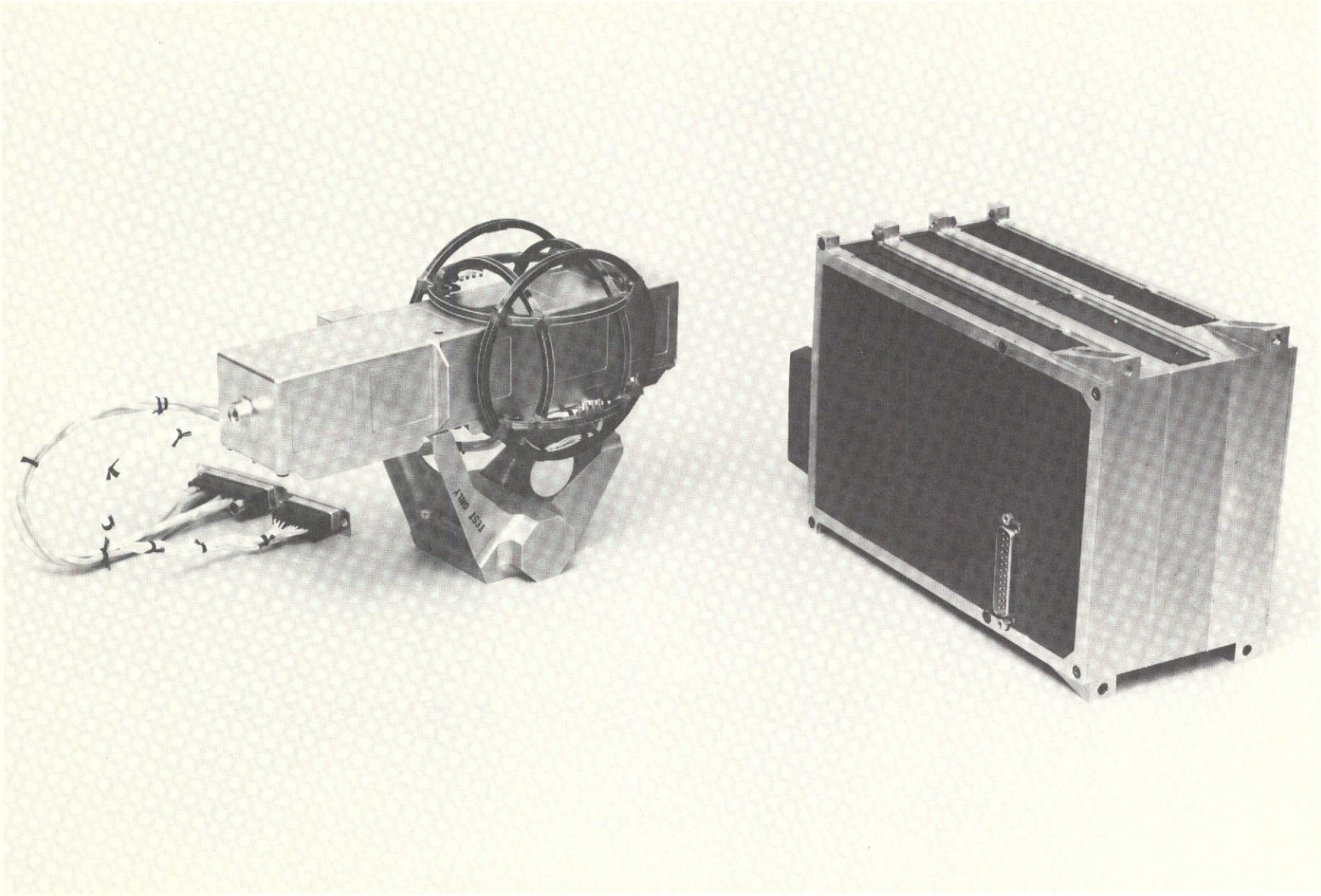

Fig. 11. The magnetometer flown on Pioneer 10 (a vector helium magnetometer). Adapted from Ref. 2

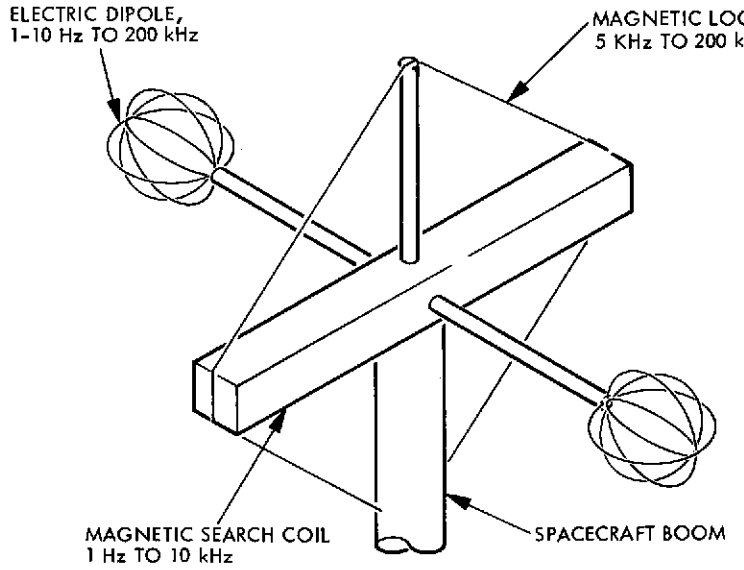

BOOM PACKAGE

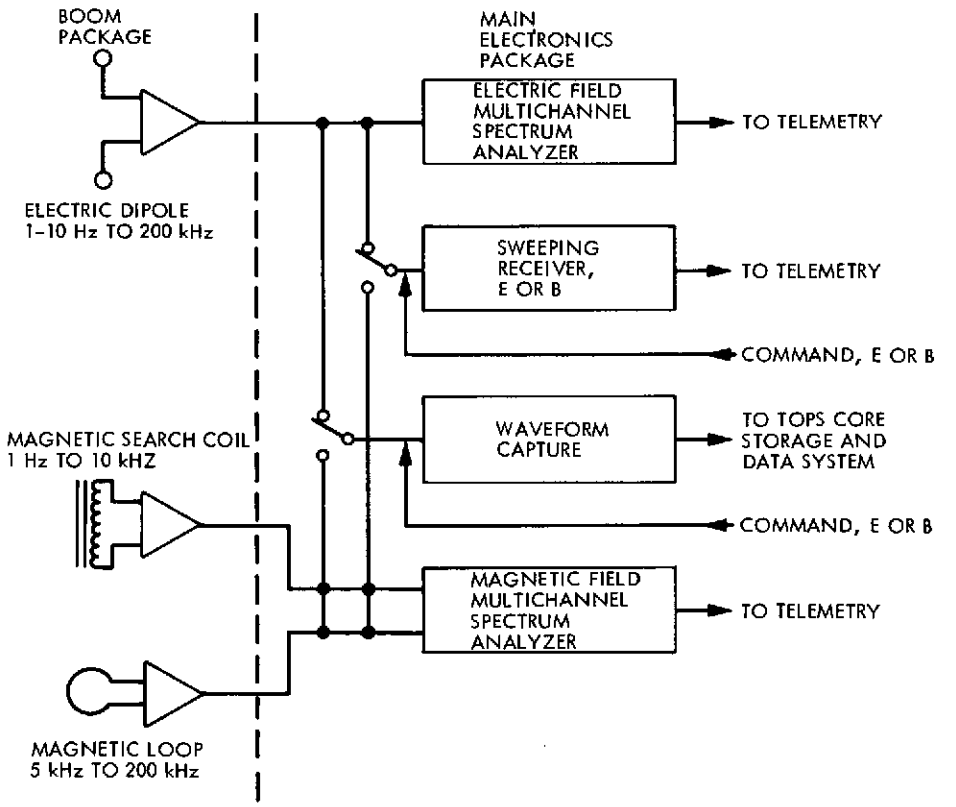

Fig. 12. The plasma wave instrument schematic. The dotted line indicates that items to the left are to be boom-mounted for compatibility with the space vehicle. Adapted from Ref. 2

(assuming a frequency inverse cubed noise requirement). This is consistent with the magnetometer requirement of ±0.1γ from dc to 1 Hz. The plasma wave uses an electric dipole (two conducting spheres separated and connected electrically by an electrometer) and both a search coil and a coil loop in which varying magnetic fields set up a current. Like the magnetometer the plasma wave instrument will measure the structure of the fields and plasma interaction region around Encke from E-20 days throughout the mission. Two models of the interaction region are shown in Figs. 13 and 14 on log polar plots. The models are quite uncertain in their relationship to reality. The set of instruments including the plasma wave, magnetometer, plasma probe and Langmuir probe will be able to model the interaction region around Encke and test it against several possible models. The sensors are to be located on a boom in order to reduce S/V effects.

The Langmuir probe is an instrument to measure the low-energy plasma properties within and near the coma and tail regions of Encke (E-20 days to the end of the mission). The objectives of this experiment are to measure the ion and electron temperatures and densities in the energy range of 0 to 15 eV and determine the anisotropy and spacial distribution of the plasma flow. The results will help determine (with data from the mass spectrometer, magnetometer, plasma wave, and plasma probe experiments) the modes of plasma interaction within the coma, current distribution and bulk charge movement, and existence and location of the postulated contact surface.

The instrument sensor considered for this experiment is a charged particle trap of planar geometry similar to those flown on OGO-6 and IMP-1. A schematic representation of the sensor parts and their relative positions is shown in Fig. 15. The suppressor grid is located above the retarding potential grid, and the suppressor above the collector does not apply for the Langmuir probe. The IMP-1 version is used for this study although it will have to be modernized in its electronics. The retarding potentials used are from about +20 to -20 V. The use of three sensors facing in (1) the antisolar direction (along the S/V velocity vector in Encke-centered coordinates) (2) 60 deg from the S/V velocity vector (antisolar) direction toward the south celestial pole (Encke-centered coordinates) in the plane defined by the Sun, Encke, and spacecraft, and (3) normal at encounter (or near normal) to that plane will enable required measurements to be made for nearly all anticipated conditions within or near the coma.

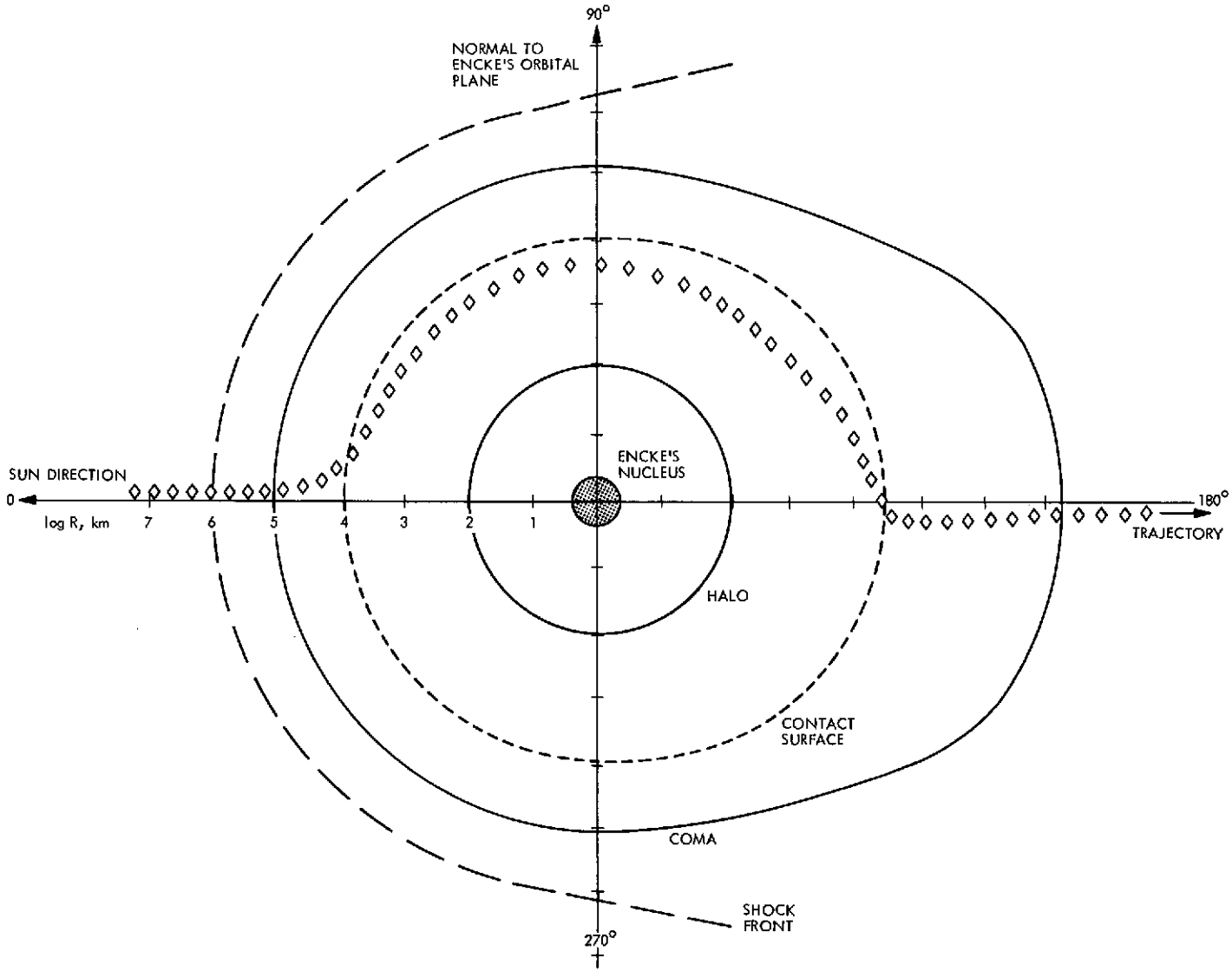

Fig. 13. Log polar plot of the trajectory for the slow flyby showing the postulated interaction region near Encke, including a shock front

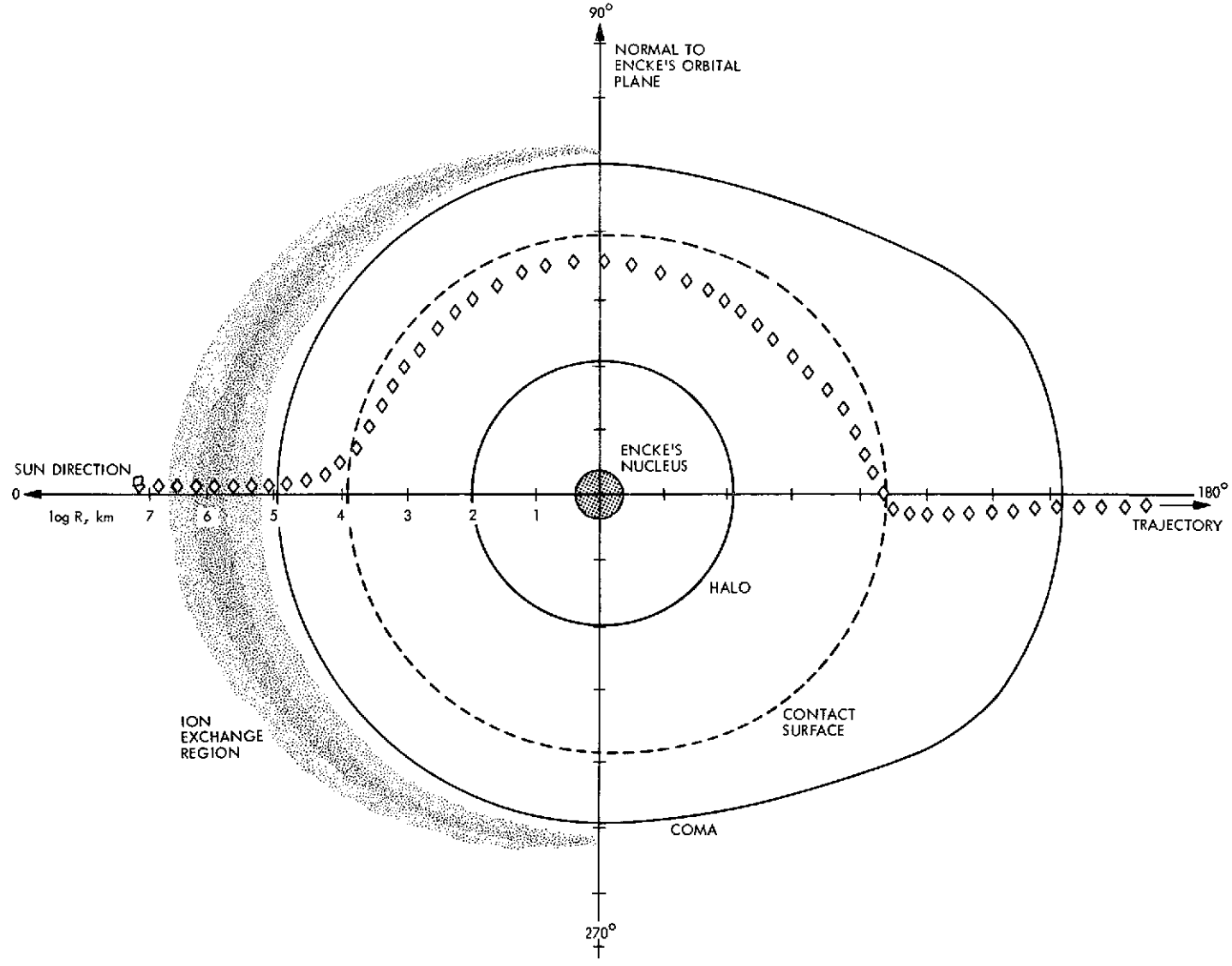

Fig. 14. Log polar plot of the trajectory for the slow flyby showing the interaction region postulated with no shock

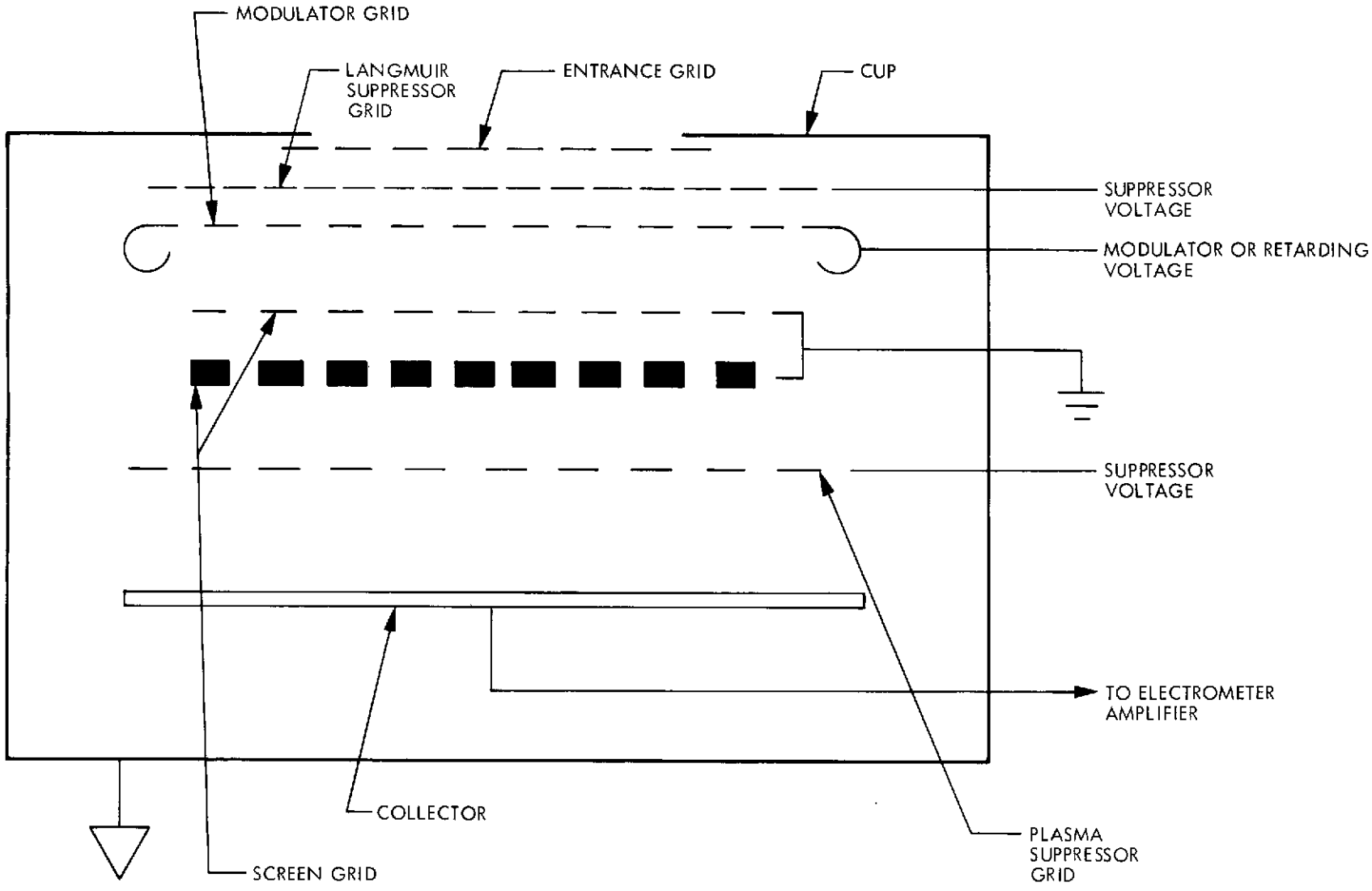

Fig. 15. Schematic of the sensor for both the Langmuir probe and the plasma probe. Only one of the two suppressor grids applies, as is indicated for the two types of instruments. Adapted from Ref. 2

The sensors are to be near (fraction of a meter) the electronics and positioned on the main body so as to have the proper unobstructed viewing field.

The plasma probe is an instrument to measure the solar and cometary plasma properties at and near Encke. The objectives of this experiment are to measure solar and cometary ion density, velocity (including angular flow direction), and temperature both beyond and within the region of interaction with the Encke environment (E-20 days to the end of the mission). These results coupled with the magnetometer results will identify the possible shock front crossing and determine the strength of the interaction. Within the coma the magnitude of the flux is likely to fall below threshold because the direction moves outside the acceptance cone angle or because the speed (ion energy) falls below the spectrometer lower energy window (about 5 to 10 eV). The instrument will be modified from previously flown designs to increase its capability for detecting plasmas under these conditions.

The instrument considered for this experiment is a modulated grid Faraday cup sensor similar to those flown on ALSEP and Explorers 33 and 35. The sensor is schematically similar to that for the Langmuir probe (Fig. 15), having the same functional parts but with the suppressor grid located near the collector (the upper suppressor grid does not apply for the plasma probe). The electronics block diagram for the ALSEP instrument is shown in Fig. 16 and was used for this study. The low-energy window is lowered to ~5 eV (from 75 eV), and the upper window is lowered to 3000 eV (from 9600 eV). This extended energy range will require about 18-20 spectral windows. The angular information is obtained from current measurements of each of three collectors within the cup. The anticipated directions of plasma velocity along the S/V trajectory are from near solar direction (±20 deg) to 60 deg from the Sun toward the south celestial pole in a plane defined by the Sun, Encke, and spacecraft. Since plasma geometry for Faraday cups restricts the acceptance cone to ~±30 deg from aperture normal, two Faraday cups with proper orientation are required. The sensors are to be near (within a fraction of a meter) the electronics and positioned on the main body so as to have the proper unobstructed viewing field.

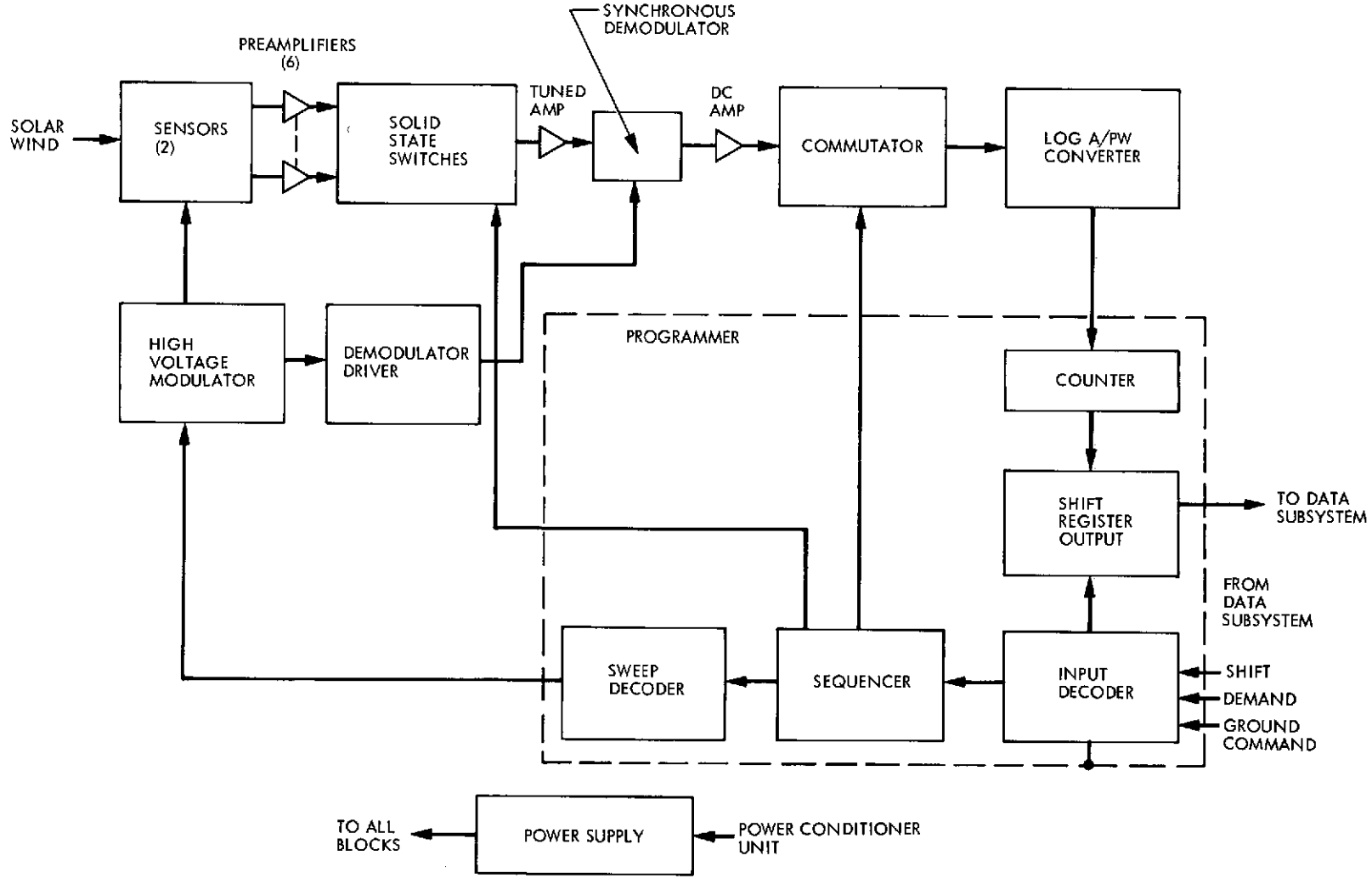

Fig. 16. Block diagram of the plasma probe instrument. Adapted from Ref. 2

The optical particle detector (Sisyphus system) is designed to measure the range, radius, and velocity of dust particles flowing off the comet nucleus. The instrument has a sensitivity of $\geq 10^6$ range/radius. Figure 17 shows a schematic of the sensors used in the Sisyphus system. This is an improvement of the Pioneer 10 instrument. The model used for the dust density is given in Ref. 7. At 1 meter separation from the end of the instrument in a 1.0 au solar light flux and with the coma radiance background the instrument can see ≥1-micron-diameter particles with a 0.2 albedo. The instrument uses four independent parallel telescopes and photomultiplier sensors to measure transit times and intensities through the fields of view. This allows the ranges, velocities, and sizes of the particles to be determined.

The ultraviolet spectrometer is designed to measure light intensity in the spectral range from 1150 to 3500 A. This allows the identification of the same mass/charge ratio species in order to remove ambiguities in the mass spectrometer analysis. In addition, the UV species are mapped throughout the coma as opposed to the local measurements made by the mass spectrometer. Figure 18 is a schematic of the UV spectrometer (the AAFE version). The instrument uses a reflecting grating and channel multipliers to detect various wavelengths.

The infrared thermal mapper is designed to measure seven pass bands (0.3-3, 4-100, 6-8, 9-11, 12-13, 14-15, and 16-18 μ) so that (1) the energy budget of the comet can be measured, (2) solar energy reflected or reemitted vs phase is measured, and (3) a color temperature is obtained. Figure 19 is the schematic of the IRTM similar to that used on Viking.

B. Encke Rendezvous Payload

Table 15 lists the changes in the Encke rendezvous payload from the Encke slow-flyby payload and the new objectives. The objectives of the remaining instruments in Table 13 will be modified to take advantage of (1) the long observation times, (2) the nucleus mapping, and (3) variations of phenomena, (e.g., densities, temperature, etc.) as Encke approaches the Sun. Table 16 shows the mass, power, data rates, and fields of views for the new instruments plus the total mass of the rendezvous payload. If it is assumed that a slow flyby precedes this mission and the payload is modified accordingly, then the UV plasma wave and plasma probe may be less likely candidates for the rendezvous payload set. The gamma ray spectrometer

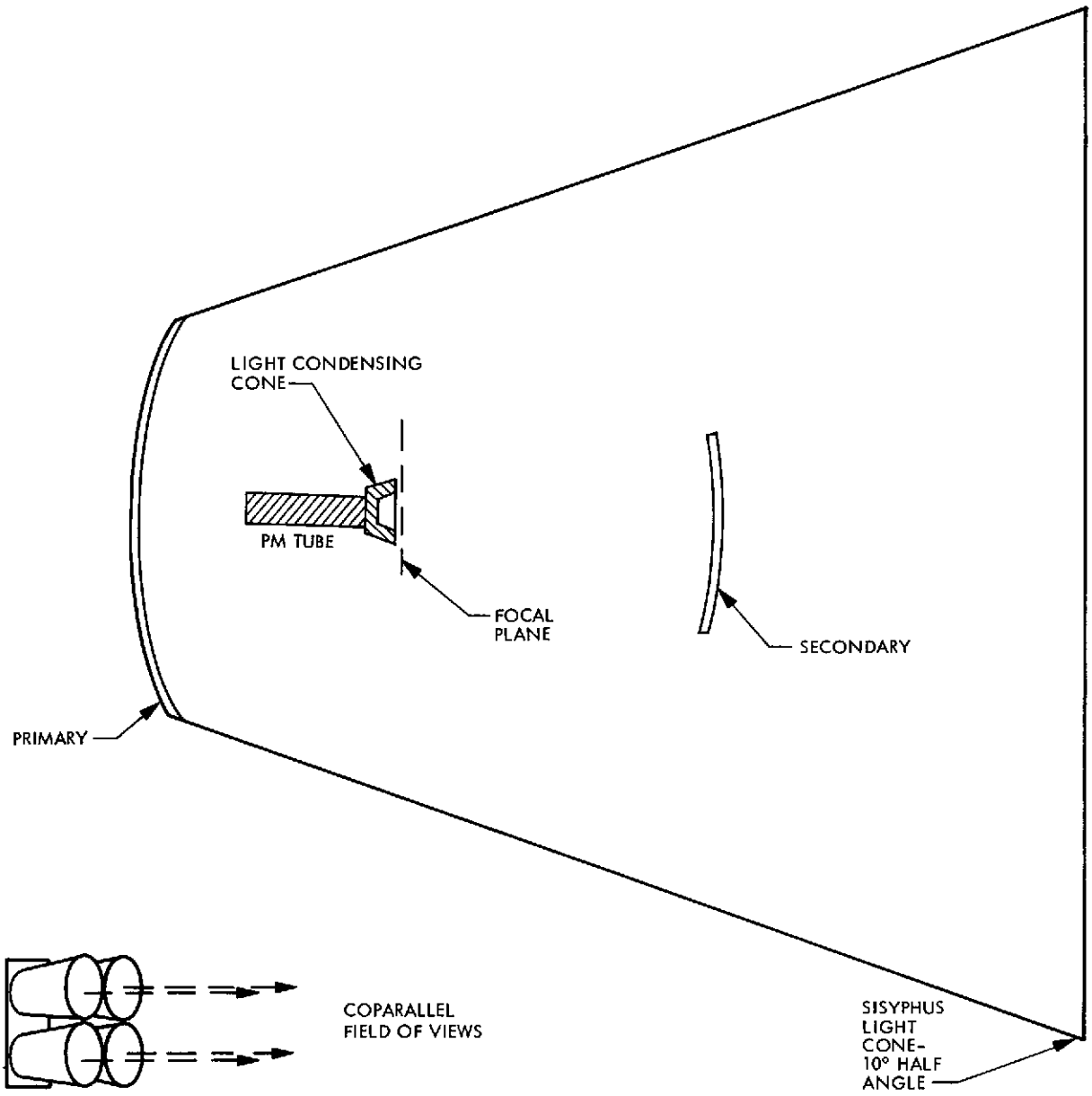

Fig. 17. Schematic of the optical particle detector (Sisyphus) sensor. Adapted from Ref. 2

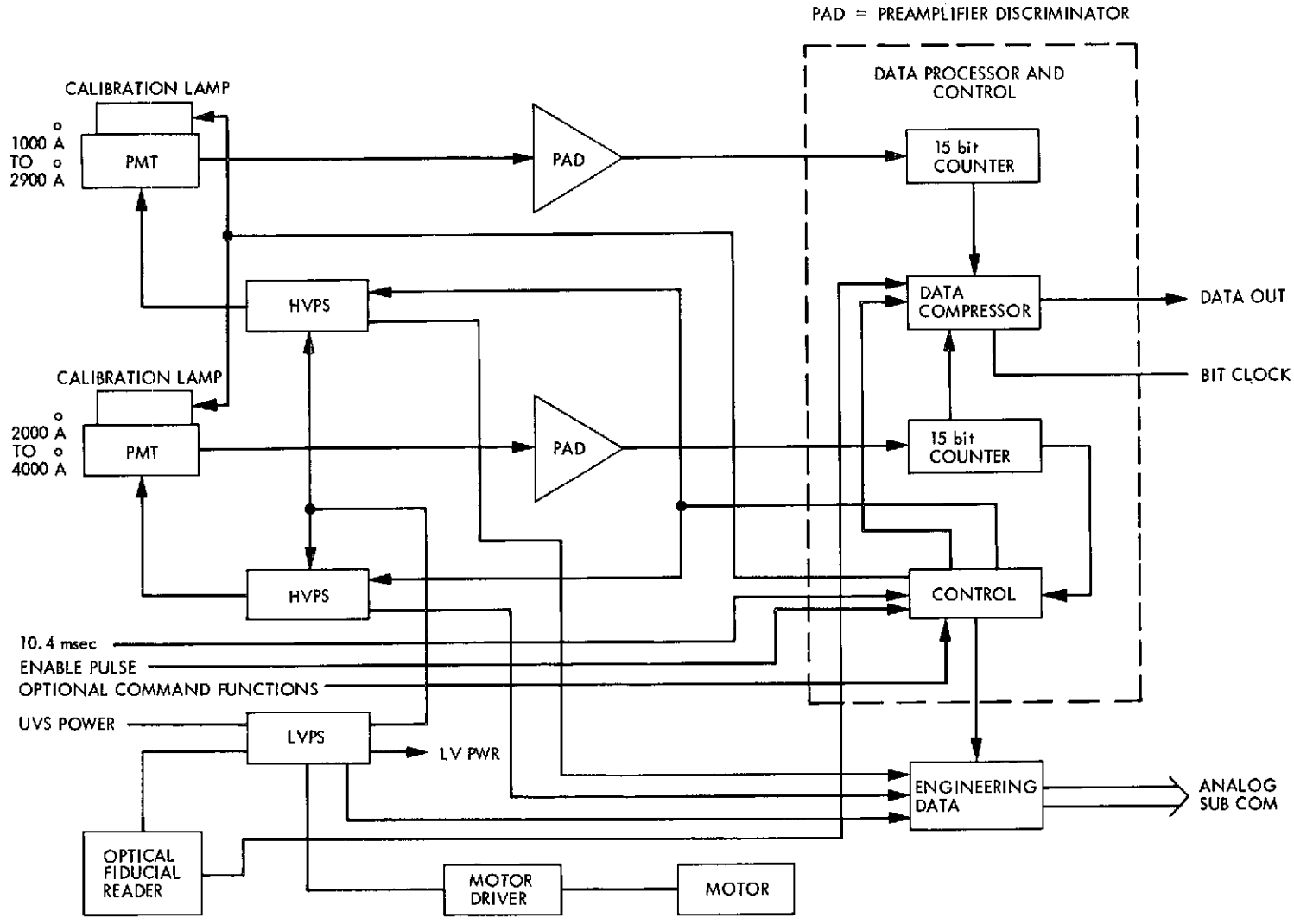

Fig. 18. Block diagram of the AAFE ultraviolet spectrometer. Adapted from Ref. 2

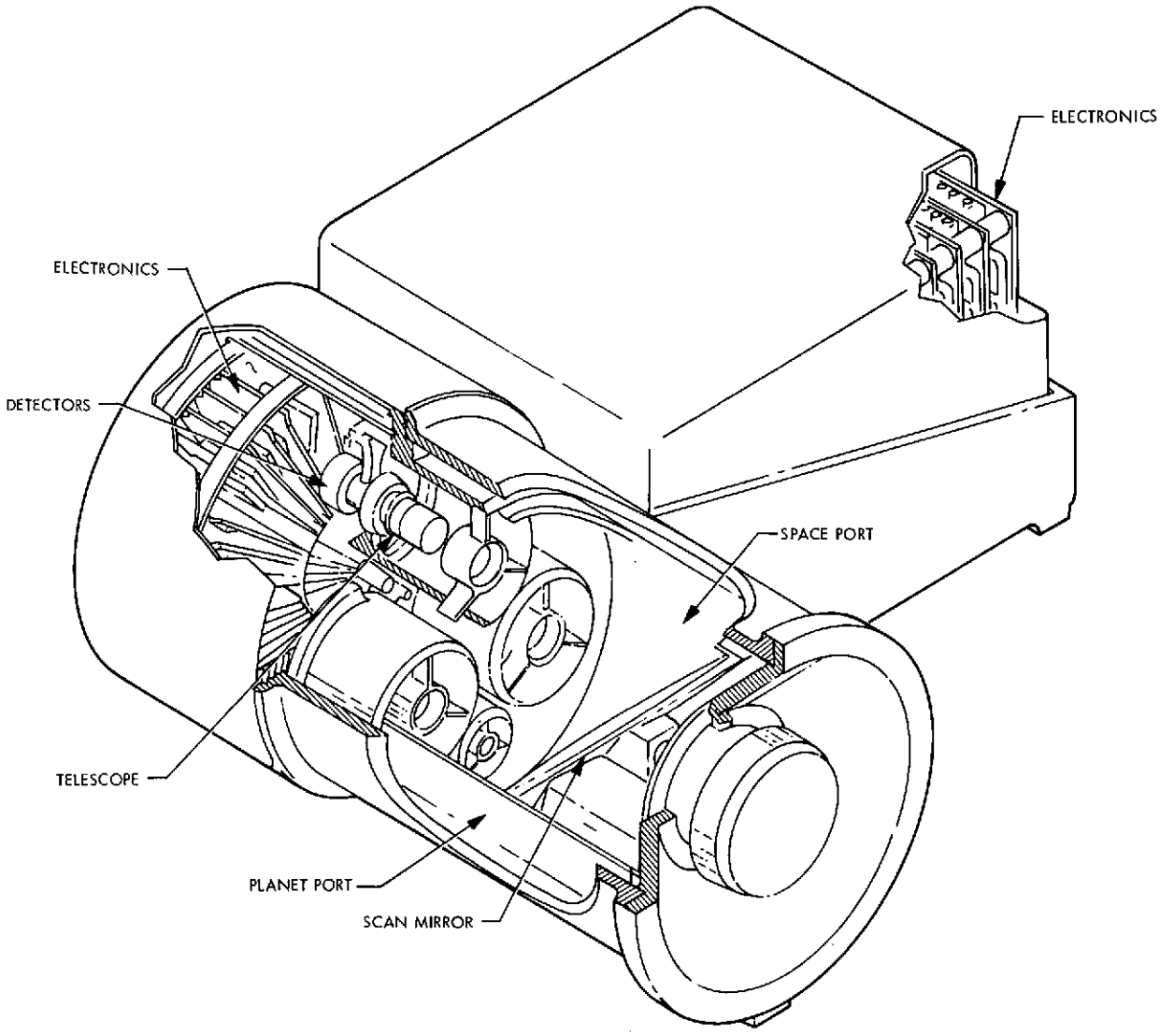

Fig. 19. Schematic of the infrared thermal mapper similar to the Viking instrument. Adapted from Ref. 2

Table 15. Objectives of instruments in the Encke rendezvous payload which are not part of the Encke slow flyby payload[a]

Instrument	Objectives
Radar	To determine conductivity, surface roughness, and range of Encke nucleus through the coma which may be opaque to visible wavelengths.
Gamma ray spectrometer	To observe both the induced and naturally occurring gamma rays (from ~200 keV to ~30 MeV) to determine composition and differentiation of detectable elements.
X-ray spectrometer	To observe X-rays (from ~1 to ~400 keV) to determine composition and differentiation of detectable elements.

[a]The UV plasma wave detector and plasma probe instruments may not be included if the rendezvous mission is preceded by a successful slow flyby mission; others will have mapping, phase variation, and solar separation variation objectives added.

Table 16. Instrument data for Encke rendezvous instruments not included in the slow flyby payload

Instrument	Mass, kg	Power, W	Data rates, bps	FOV
Radar	21	40	10^4	~0.5 mrad (e.g., 226- to 767-m footprint diameter from 1000 km, on scan platform
Gamma ray spectrometer	10	6	≤100	~20° half-angle cone directed at nucleus on boom
X-ray spectrometer	4	5 peak 2 avg	≤100	5 × 5° directed at nucleus, may require boom
Total	~80			

(GRS) and X-ray spectrometer (XRS) both require low altitudes and/or long observation times in order to reasonably determine the chemical composition and the spatial distribution of the composition (Refs. 8 and 9). It appears that observation times of the order of 10^5 seconds will allow resolution of abundances similar to lunar compositions at an altitude of ≤100 km. As the altitude is decreased, the tradeoffs can either be to lower the observation time or to increase the area resolution. Since the XRS and GRS are measuring X-ray and gamma activity respectively, a strict limitation on the trace amounts of K^{40}, Th, U, and other radioisotopes in such areas as solar panels and throughout the entire space vehicle must be observed. For the Apollo GRS a 7.5-m (25-f) retractable boom was used in order to further decrease the contamination by the cosmic ray interactions with the spacecraft and the radioisotopes in the spacecraft, and a similar boom mounting for these missions is assumed here.

Figure 20 is the schematic diagram of the gamma-ray spectrometer used in this study. Several improvements (e.g., mass and power reductions) are possible using intrinsic germanium detectors in place of the Apollo-type scintillators. However, these would require development. The instrument's objective is to measure the gamma-ray flux vs energy over the range of ~200 keV to ~30 MeV; it would have a field of view ≤20 deg half-angle cone directed at the nucleus. At least 20 days of close (≤100 km) observation is desired.

Figure 21 is the schematic diagram of the X-ray spectrometer. It is similar to the proposed instrument for MJS'77. Flight instruments have flown on Apollo missions. This instrument has the ability to measure chemical elements other than those measured by the GRS, providing attenuation in the halo is not large. For a rendezvous of Encke at solar distance ~1 au this should not be a problem. At least 20 days of close (≤100 km) observation is desired. A boom may also be needed for the X-ray spectrometer.

The active radar was selected to represent the next group, since like the laser altimeter, signal attenuation by the plasma and EMI problems are similar. The active radar has the capability to operate through dense atmospheres which are opaque in the visible region. In addition, accurate ranging information is available as are surface and near-surface conductivity

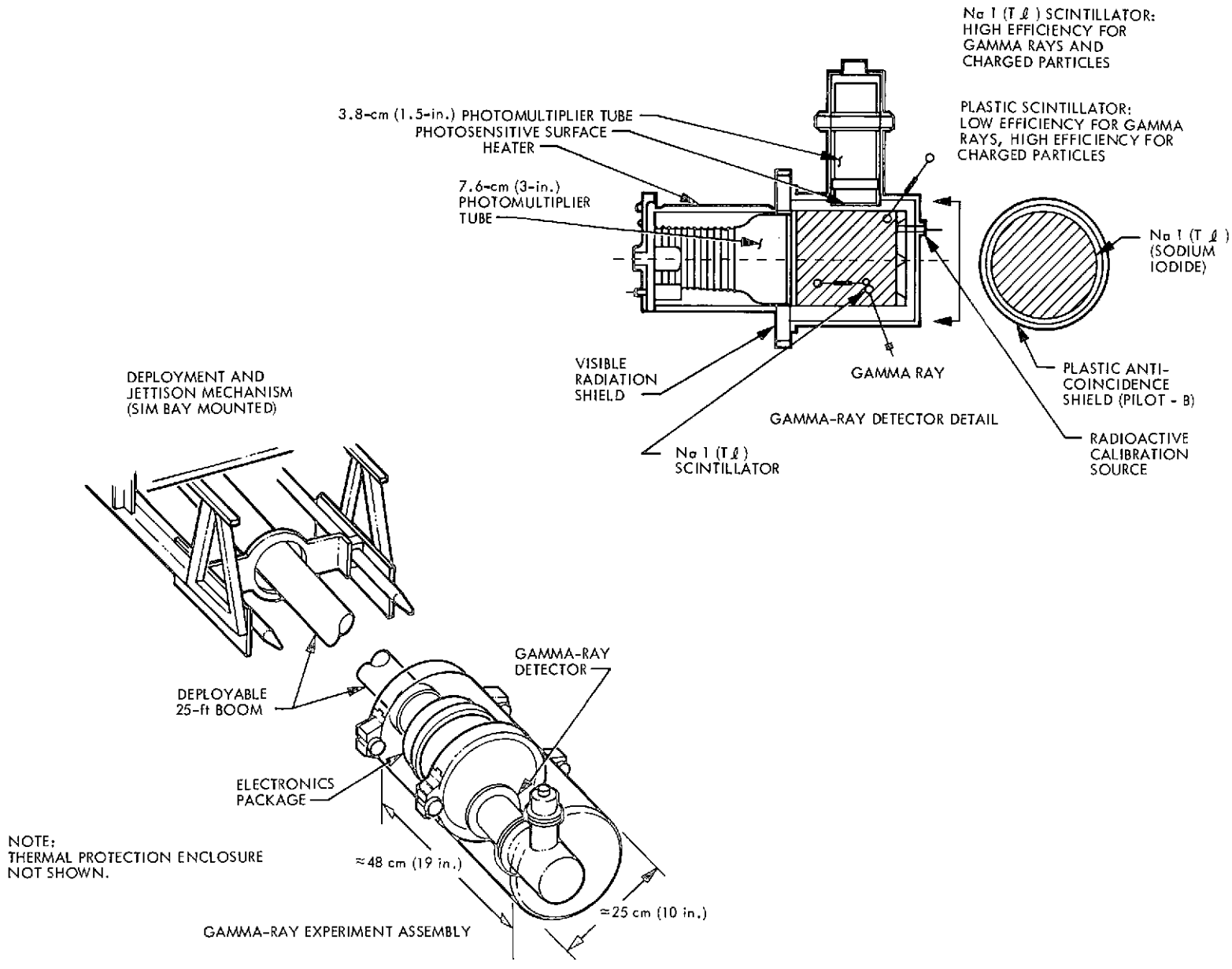

Fig. 20. Schematic of the Apollo 15 and 16 gamma ray spectrometer

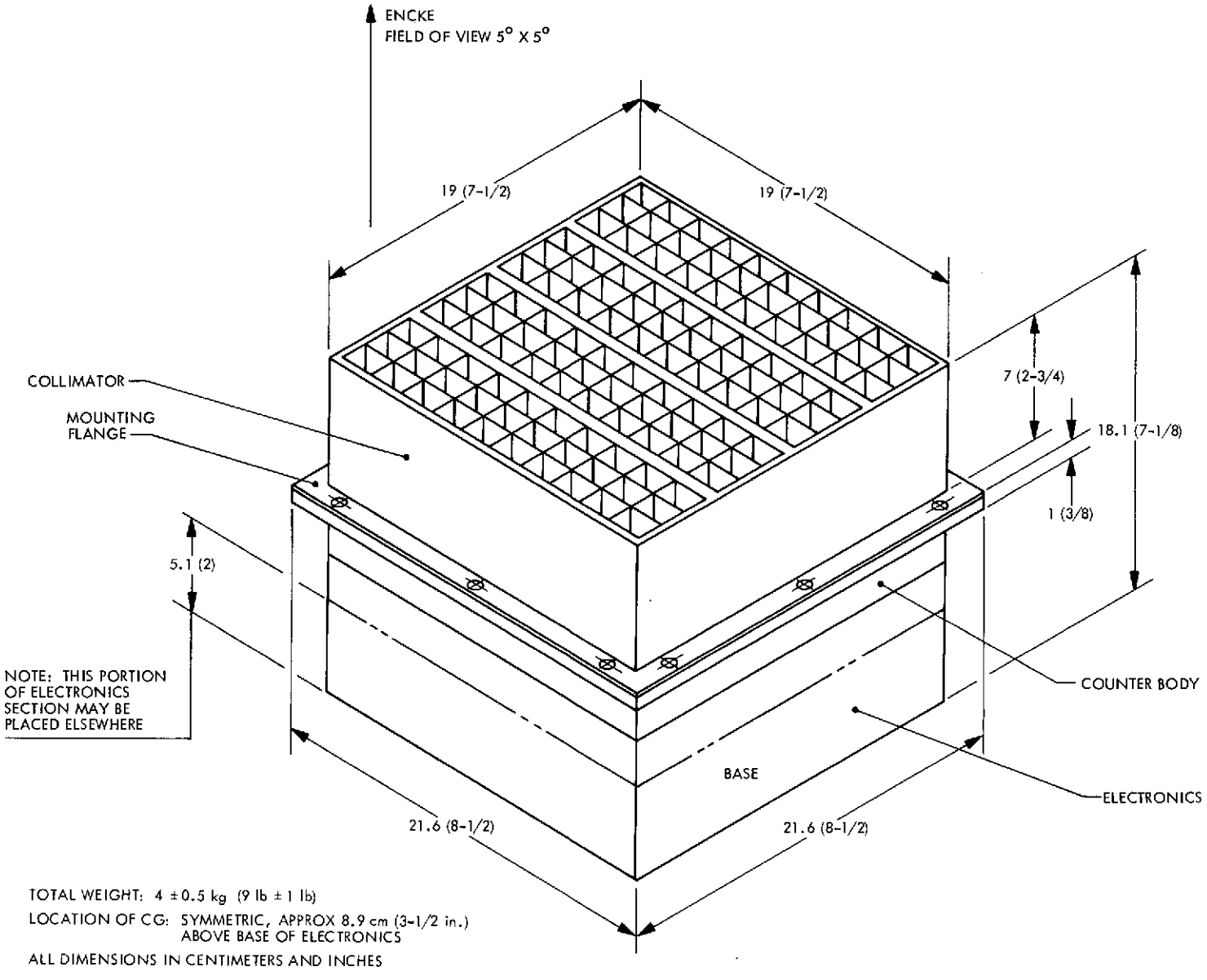

Fig. 21. Schematic of X-ray spectrometer (courtesy of Kevin Hurley)

and structure. Figure 22 is a block diagram of an imaging radar instrument which shows some of the functional areas of active radar instruments.

The remaining instruments are assumed to be the same as for the slow flyby payload. Although this may oversubscribe the payload in mass, power, etc., the actual payload is expected to be chosen from this group based on information obtained from the slow flyby, which precedes the rendezvous. The instruments used in the rendezvous will now have their objectives enlarged to determine the finer details of the nucleus and vicinity. For example, (1) the imaging camera may be able to provide resolution of any features greater than a few meters in diameter and will map the Sun side of the nucleus; (2) the magnetometer will be able to detect surface magnetic field variations $\gtrsim 2000$ gamma at 100 km and $\gtrsim 2\gamma$ at 10 km from a 2-km-radius nucleus.

C. Other Classes of Instruments, Non-Encke Payloads

Table 17 shows (1) the list of additional instruments considered, (2) several groupings of instruments with similar compatibility problems, and (3) the ones selected from each group for consideration to provide more generality to the study. Table 18 shows the objectives of the selected instruments. Table 19 shows the mass, power, data rate, and FOV needs of these instruments. The alpha scattering and X-ray fluorescence instruments use solid-state detectors (proportional counters can also be used to detect X-rays) to determine compositional analysis of a sample. These instruments typically are part of a lander payload. However, they have been suggested for orbiters, atmospheric skimmers, and probes. Prototypes are available for lander-type operations using sample compactors to present a uniform sample surface. Cryogenic gas and dust sampling has been mentioned but nothing significant has been developed. Figure 23 is a schematic diagram of the alpha scattering technique. Figure 24 shows a comparison of combined alpha/X-ray analyzer vs conventional chemical analyses for an andesite sample.

Instruments in the next group (Table 17) measure high energy ($\gtrsim 1$ keV) electromagnetic radiation with solid-state detectors (for the X-ray experiment a proportional counter may be used). The HSR/GSR is a cryogenically cooled instrument which is extremely massive. The X-ray

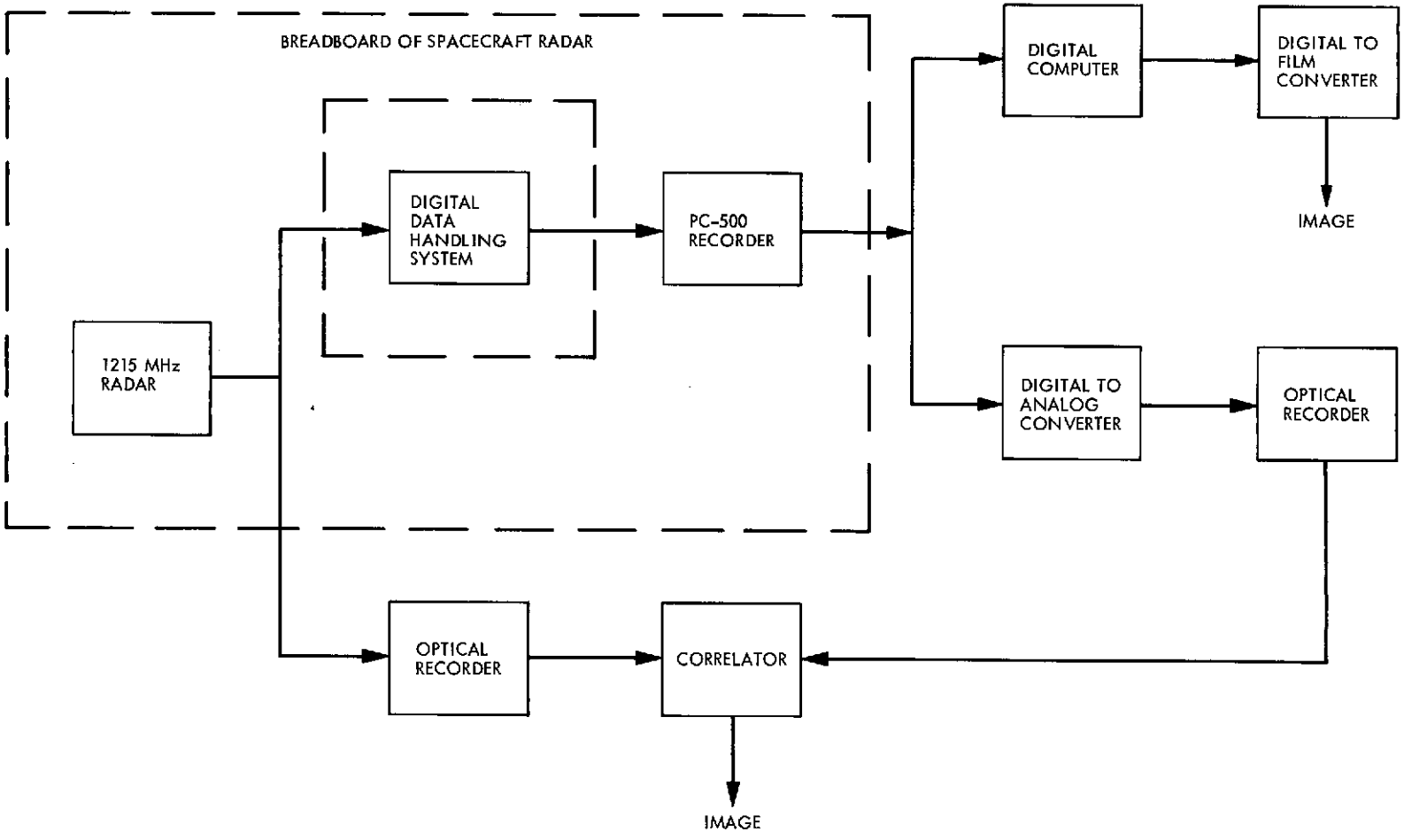

Fig. 22. Block diagram of imaging radar instrument. This is a bistatic radar system

Table 17. Science instruments not part of the Encke payloads

Instruments considered	Representative instruments
Alpha scattering X-ray fluorescence	Alpha scattering
X-ray diffractometer High spectral resolution gamma ray spectrometer	Represented by gamma ray spectrometer and X-ray spectrometer
Cosmic ray detectors Charged particle telescope Low-energy charged particles	Charged particle telescope
Imaging radar Laser altimeter Topside sounder	Represented by imaging radar
Photopolarimeter	Photopolarimeter
IR spectrometer UV photometer	Represented by UV spectrometer and IR radiometer
Meteoroid detector (pressure cells)	(assumed compatible)

Table 18. Objectives of instruments not on or represented in the Encke payloads

Instrument	Objectives
Alpha scattering	Elemental analysis of collected sample
Charged particle telescope	Charged particle energy (~100 keV to 100 MeV/nucleon), spatial, flux, atomic number distributions
Photopolarimeter	Measure absolute photometry and polarimetry

Table 19. Physical data for non-Encke payload instruments

Instrument	Mass, kg	Power, W	Data rates, bps	FOV
Alpha scattering	~7	~7	~3 K	In situ collection placed inside as prepared sample. Sample collection field of view ~2π strad
Charged particle telescope	~4	~5	$\lesssim$2 K	32° half-angle cone somewhat west of the antisolar direction in the ecliptic plane
Photopolarimeter	2	1	200	4° full angle boresighted with TV, periodic alignment with Sisyphus

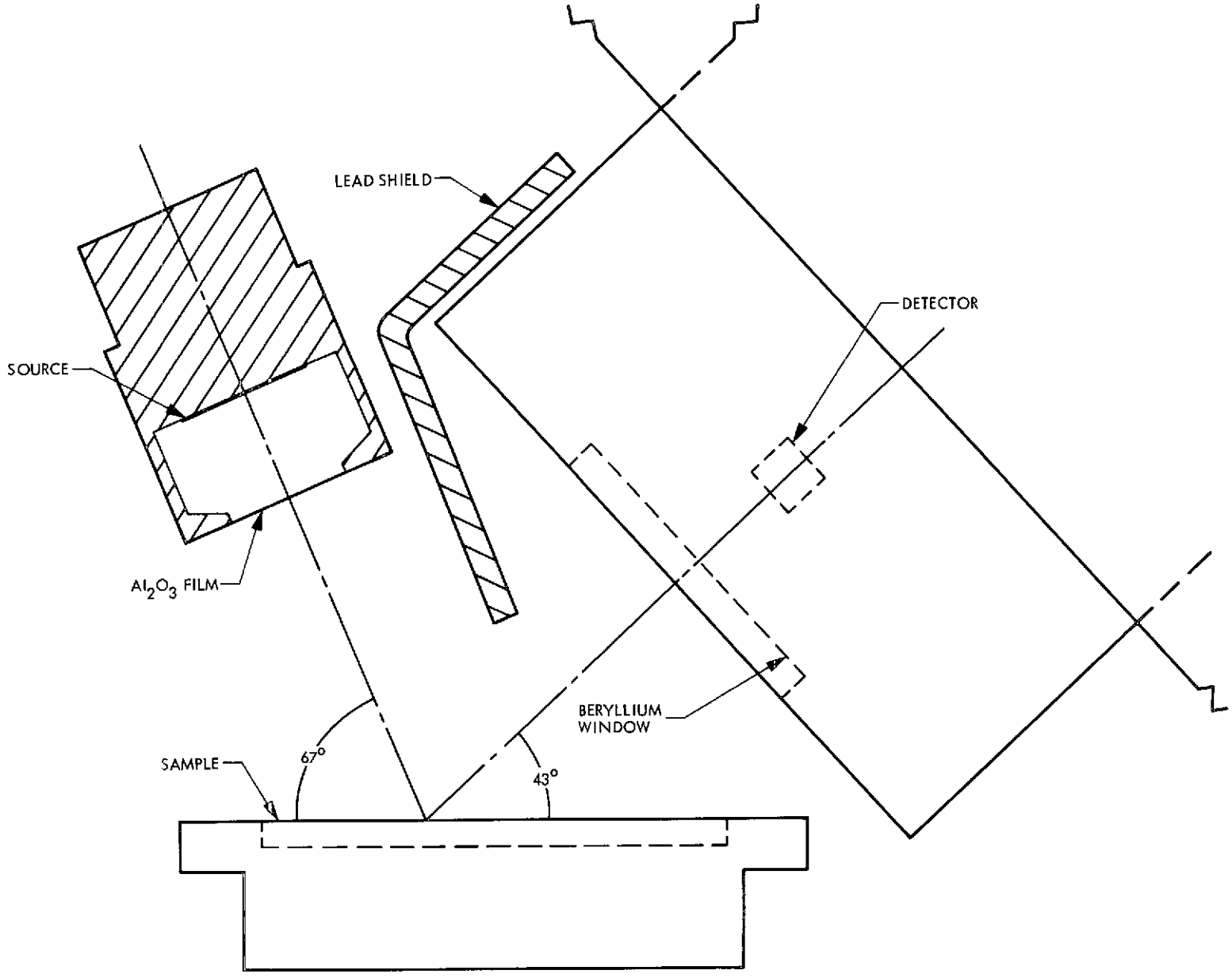

Fig. 23. Technique of alpha scattering from a prepared sample

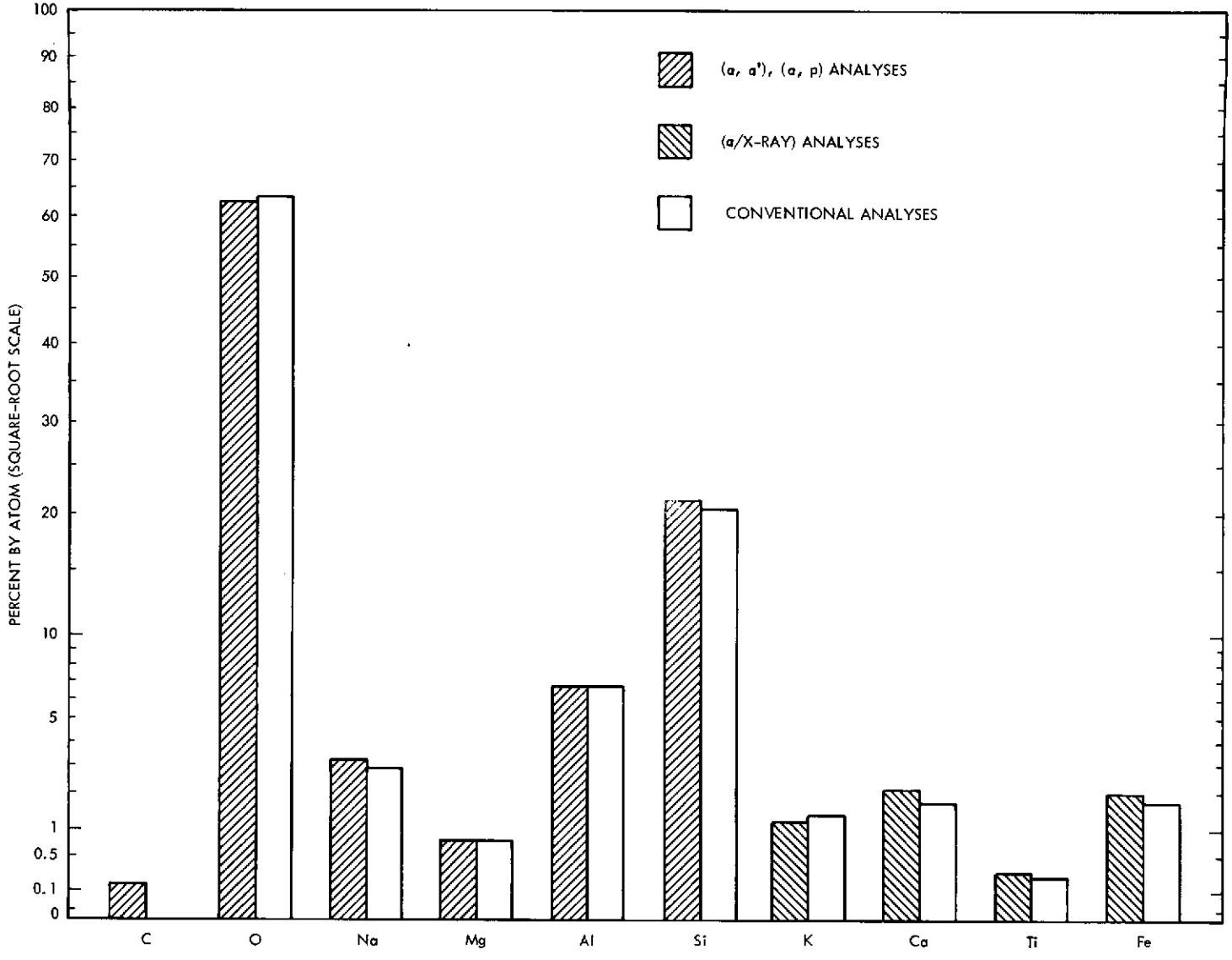

Fig. 24. A comparison of the conventional chemical techniques with the combined alpha scattering (for the light and intermediate elements) and alpha/X-ray (for the heavier elements) analyses

diffractometer is fairly similar to the X-ray spectrometer in terms of integration problems. Both can be represented by the X-ray spectrometer (XRS) for the group's compatibility considerations.

The energetic (≥10 keV) charged particle instruments are represented by the charged particle telescope (CPT) shown schematically in Fig. 25. Figure 26 shows the range of energies and particle types measured by the CPT. The CPT measures the isotopic distribution, the energy distribution, temporal distribution, spatial distribution, flux levels, and flux directions of charged particles. From this data models can be made of the original and intervening media.

The photopolarimeter is similar to the proposal for MJS'77 and will be able to obtain absolute photometry to ±0.3%, using a calibrated optical system and photomultiplier sensor with a series of filters.

The photometer, radiometer and spectrometer instruments covering the UV to IR wavelengths are assumed to have their compatibility concerns represented by the Encke slow flyby payload instruments measuring the same wavelength photons.

The meteoroid detector uses a penetration/pressure cell technique to measure energy and size for objectives similar to the optical particle detector. The instrument is assumed compatible with the SEP space vehicle if EMI problems are solved for other instruments.

Each of the instruments not part of the Encke payload is integrated into the space vehicle assuming that particular instrument comprises the entire SEP space vehicle payload.

III. ENVIRONMENT DESIRED FOR SCIENCE

A. Magnetic and Electrostatic Requirements

The most serious dc to 1-Hz magnetic constraints on the S/V in both Encke payload sets are due to the requirements of the dc magnetometer: 1 ±0.1 γ at the magnetometer sensor location. Most requirements are about 10^4 gamma for the other instruments as indicated in Table 20 except for the plasma wave experiment which is matched to the magnetometer by a (frequency) extrapolation to ~0.5 Hz. This implies approximately a 10 γ sensitivity to dc magnetic fields.

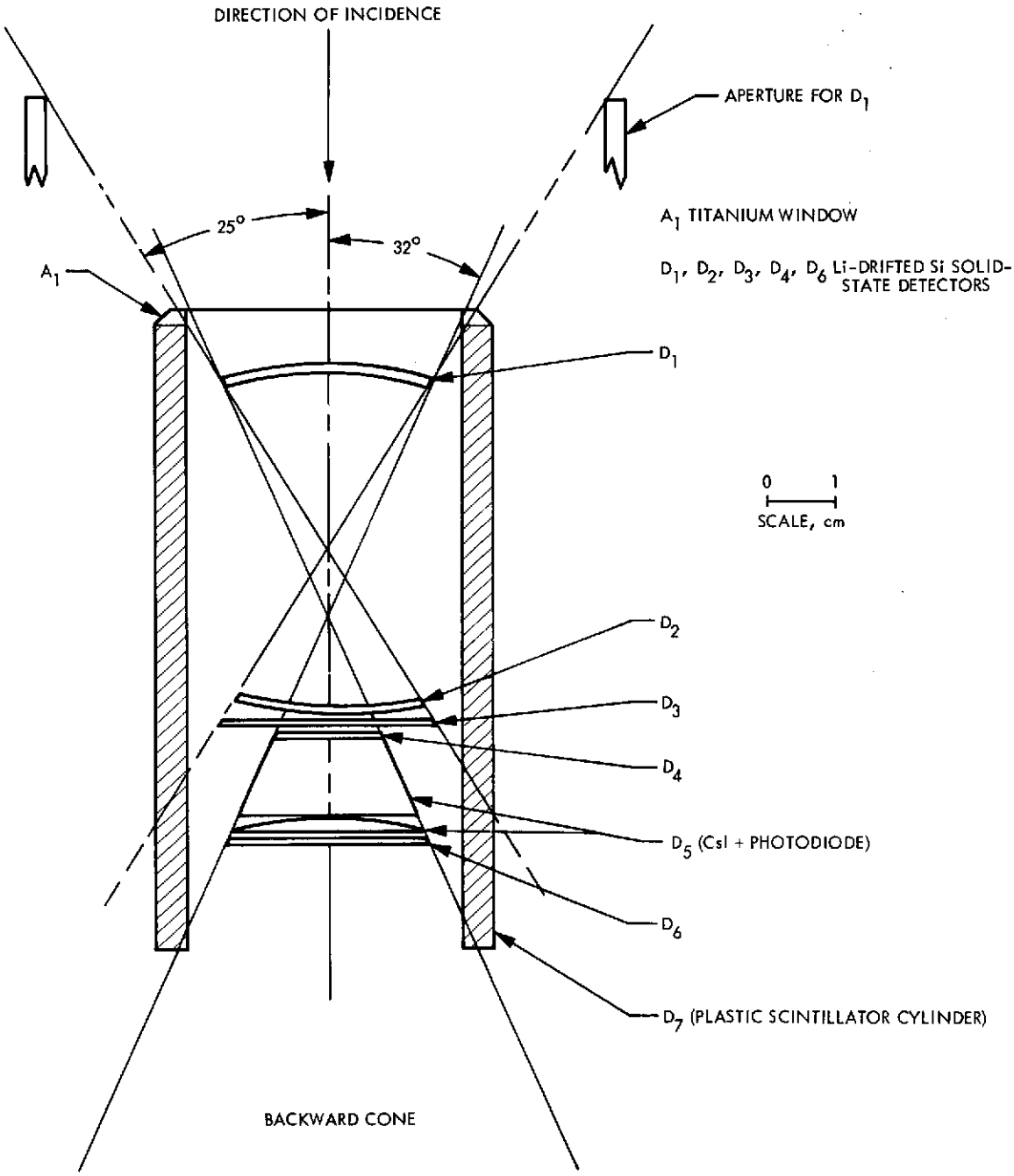

Fig. 25. Schematic of the University of Chicago charged particle telescope sensor

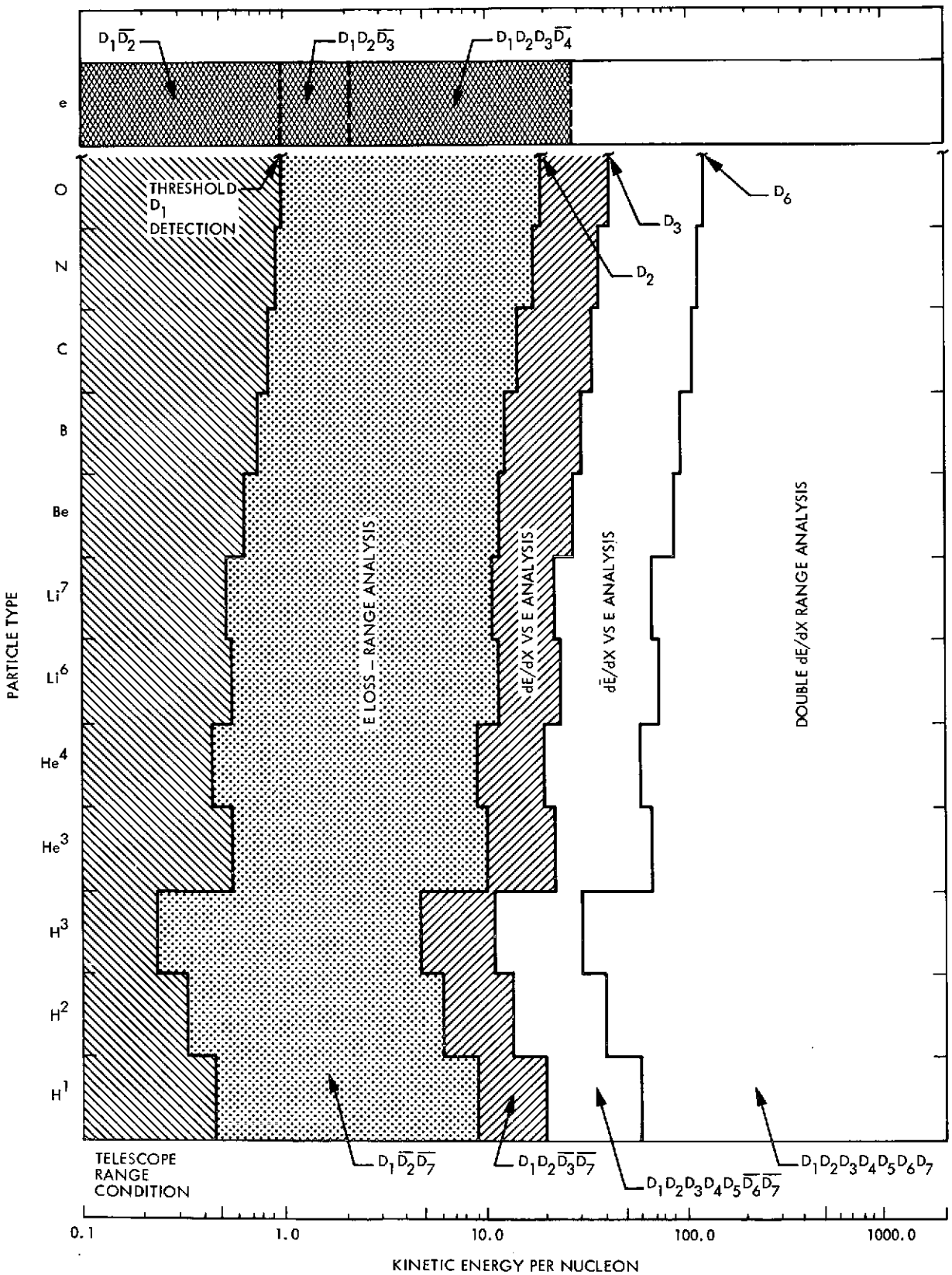

Fig. 26. Energy vs particle type histogram for the charged particle telescope. The various coincidence situations are indicated

Table 20. DC magnetic field requirements

Instrument	B(γ) at sensor
Mass spectrometer	3100
Imaging	10^4
Optical particle detector	10^4
Magnetometer	1 ± 0.1
Plasma wave	10
Plasma probe	6×10^4
Langmuir probe	3100
UV spectrometer[a]	10^5
IR radiometer[a]	10^5
Alpha scattering	10^5
Gamma-ray spectrometer	10^4
Charged particle telescope[a]	10^4
Radar[a]	10^5
Photopolarimeter[a]	10^4

Note: The B(γ) value assumes the magnetic dipole is 1 meter from the sensor.

[a]These values are estimated by analogy to other instruments and may be revised.

B. Radiated EMI

The plasma wave instrument requires a radiated noise-level environment which as mentioned above is consistent with the magnetometer's static-level requirement (Refs. 10 and 11). If we assume an inverse cubed frequency dependence which matches the magnetometer stability requirement near 0.5 Hz and use the noise sensitive shape passing through $10^{-8}\gamma^2$/Hz at 100 Hz, then we obtain the graph in Fig. 27, which gives the requirement over the 1-Hz to 200-kHz range.

The plasma probe places rather high limits on S/V-produced magnetic fields. For the frequency range of 0 to about 2 kHz, the distance-integrated magnetic field over the ion traversal path for a 5 eV proton to the cup collector must be smaller than 33,000 γ-meters (corresponding to a dipole field strength of $5.6 \times 10^5 \gamma$-m^3 at 3 meters distance). The electric fields for these frequencies must be small enough so that the potential along the path shall be less than 5 V in addition to the usual small (e.g., ~5 V) basic space vehicle potential (Ref. 12). At higher frequencies the limits are even higher.

The Langmuir probe requires lower limits on these same fields, since this instrument measures the ions and electrons at lower energies. The integrated magnetic field over the charged particle path for a 2 eV electron must be less than 1560 γ-meters for frequencies less than 2 kHz (corresponding to a dipole strength of 7×10^4 γ-m^3 at 3 meters distance). The electric field must produce potentials less than 2 V along the charged particle trajectory. For this experiment, the basic S/V electrostatic potential is important, and as has often happened, the electron-ion measurement at these low energies may be strongly influenced by the S/V potential.

The mass spectrometer places limits on the magnetic and electric fields when it is in the ionic measurement mode. These limits are like those of the Langmuir probe for frequencies up to a few Hertz. Beyond about 10 Hz the limits are a factor of 2 higher than that of the Langmuir probe. In the neutral gas measurement mode, the field limits for the mass spectrometer are higher (~5000 γ and volts per meter).

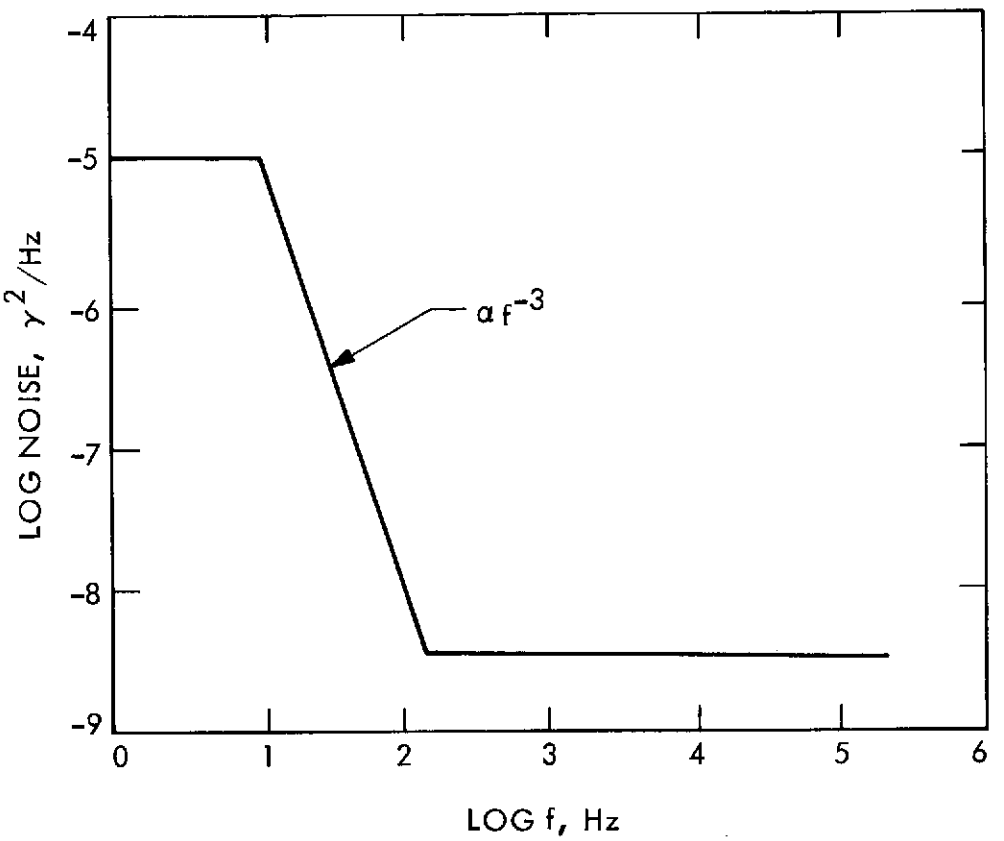

Fig. 27. Maximum radiated electromagnetic interference acceptable to the plasma wave instrument. The inverse frequency cubed region is from 10 to 160 Hz

The vector helium magnetometer uses a signal with a frequency in the range 27 to 108 MHz to excite the helium atoms. In this frequency range it must have $\leq 10^{-5}$ W/cm^2 internal to the housing. If we assume a 50-dB attenuation by the housing (this requires care in avoiding leaks in the housing at seams and feedthroughs), then this means a limit of ≤ 1 W/cm^2 is placed on the S/V by the magnetometer in the range 27 to 108 MHz. If only a 20-dB attenuation is available, the limit is $\leq 10^{-3}$ W/cm^2.

A typical value for an acceptable level for the X-ray spectrometer is ≤ 0.1 photons/cm^2-s at the sensor for 0.1 keV $\leq E_{photon} \leq$ 0.5 MeV. The EMI levels must be lowered at least to the MJS levels (Appendix A) to prevent data degradation. The FOV is to be directed at the nucleus.

Limits on the remaining instruments are either not restrictive or not yet determined. For the ones not yet determined it is expected that the

limits will not be as severe as those presented above. Table 21 gives the maximum radiated and conducted EMI levels that are acceptable for the instruments in order to meet the stated objectives.

X-ray and gamma-ray radiation is present in all space vehicles due to trace amounts of radioisotopes and ambient radiation (e.g., cosmic rays and solar flares) impinging on the space vehicle material (Ref. 13) and we have included it as an EMI source. Gamma ray and X-ray photons are of concern only for the X-ray spectrometer and gamma ray spectrometer for usual amounts of radioisotopes. For the gamma ray spectrometer, maximum acceptable flux is ≤1 photon/cm^2-s at the sensor for photon energies between 0.1 MeV and 5 MeV. For the X-ray spectrometer, the maximum acceptable flux level is ≤0.1 photon/cm^2-s at the sensor for photon energies between 0.1 keV and 0.5 MeV.

C. Conducted EMI

Instrument response to unwanted voltage and/or current signals on interface connectors can have several levels of severity. The highest allowable level is that where the ability to survive extremely noisy environments of several volts or several hundred milliamperes is demonstrable Ref. 14). A design safety factor of several hundred percent usually exists. As the duty cycle for this type noise is extremely low, there is no permanent loss of instrument functioning, and occasional "data drops" or bit errors are the only adverse effects.

A lower level of noise by conducted EMI exists wherein an instrument subassembly should operate with essentially no spurious effects. This is about one order of magnitude lower (e.g., the smaller of 0.3 V and 30 mA). This level of noise can be applied to any external point, including interface connections, with no adverse effects in performance.

All instruments require reasonably clean signal lines inside their electronic packages. This can be made somewhat quantitative by assuming that after the sensor and amplifiers the signal is analyzed using 10 V, which is digitized into 500 parts or 20-mV steps. Thus if a ±10% requirement is placed on this, a ±2-mV noise limit is needed. Some instruments such as the cosmic ray detector use 4096 digital steps and others such as imaging only 64.

Table 21. Maximum acceptable EMI levels for science instrument operation

Instrument	Radiated EMI	Conducted EMI[a]
Mass spectrometer	$<$(2 V and 2×10^3 γ - m) along ion trajectory (0 - to 5 Hz); (10-2 kHz) is 4×10^3 γ m	1 mV[b]
Imaging	ND	100 μV[b]
Optical particle detector	ND	1 mV[b]
Magnetometer	$\lesssim 10^{-9}$ W/m^2 (27 to 108 MHz)	10 μV
Plasma wave	$<10^{-8}\gamma^2$/Hz at 100 Hz (see Fig. 27)	10 μV
Plasma probe	$<$(5 V and $3.3 \times 10^4\gamma$-m) along FOV 0 to 2 kHz	10 mV[b]
Langmuir probe	$<$(2 V and $1.6 \times 10^3\gamma$-m) along FOV 0 to 2 kHz	1 mV[b]
UV spectrometer	ND	10 μV[b]
IR radiometer	ND	10 μV[b]
Alpha scattering	ND	10 μV[b]
Radar	ND	100 μV[b]
Gamma ray spectrometer	$\lesssim$1 photon/cm^2-s(0.1 MeV $\lesssim E\gamma \lesssim$ 5 MeV)	1 mV
X-ray spectrometer	$\lesssim$0.1 photon/cm^2-s(0.1 keV $\lesssim E\gamma \lesssim$ 0.5 MeV)	1 mV
Charged particle telescope	ND	10 μV[b]
Photopolarimeter	ND	100 μV[b]

ND = not determined. These are expected to be significantly less restrictive than those listed.

[a]Internal to instrument housing. Digital signals (after analog processing) can typically tolerate 0.3-V noise.

[b]These values are estimated by analogy to other instruments and may be revised.

Interference prior to the analog amplifier chain is even more sensitive (e.g., ~1 μV), and a considerable fraction of the design effort for sensors, detectors, and/or preamplifiers is associated with this protection.

Table 21 includes estimated levels for satisfactory instrument operation within the electronics package. The listed radiated EMI values are external to the spacecraft and within the field of view of the sensors, where its influence may affect detector operation or the environment being measured.

Although for power lines both rise time and overshoot limits are appropriate, without voltage levels, frequencies, and wave shapes for the electronics of the instruments and their interfaces any requirements appear to be premature.

For preliminary planning the following values taken from the quiet signal line design criteria (Appendix A) may be useful for the digital data lines for all instruments:

Rise times ≤10 V/μs
Noise level ≤1.0 V
Z ≤ 500Ω

For the magnetometer on Pioneer 10 the preamp is not placed on the boom with the sensor. Thus the analog signal line from the sensor to the preamp must be shielded such that the noise is ≤10 μV. An alternative is that the preamp be located on the boom. Then this noise limit for a 6-m cable on the signal line may be raised to ≤150 mV meter. This electronics location, which implies attitude control considerations, etc., which are beyond the scope of this report, are traded off against the cost to provide electromagnetic compatibility. Other instruments may also require a trade-off analysis if detectors are required to be placed more remotely from their electronics packages than indicated.

D. Solar Panel Effects on Field-of-View and In Situ Measurements

The instruments all require unobstructed fields of view (FOV) and are in competition with each other and the space vehicle subsystems such as telemetry, power, and propulsion for available space (see Tables 14 and 17).

The competition for FOV is similar for every spacecraft. However, the increased solar panel size and the use of thrusters on SEP space vehicles reduces the available unobstructed FOV even more.

The magnetometer does not have a FOV in the optical sense. Since it is measuring the local magnetic field in situ, however, any nearby perturbation in 4π steradians can alter the field at the sensor location. Currents on any S/V produce magnetic fields which are superimposed on the natural ambient fields. Roll maneuvers about two axes allow for subtraction of these fields, leaving an uncertainty which must be small compared to the ambient field if the ambient field is to be measured. Ambient fields can be further distorted if significant amounts of permeable material are placed on the space vehicle, since more of the ambient field lines are drawn into this material. Thus, if large strips of magnetic conducting metal such as Covar are used in solar panels, potential problems exist from (1) magnetic fields produced by solar panel currents and (2) ambient fields distorted by the magnetic material.

The plasma wave instrument measures in situ parameters of electromagnetic waves and plasma oscillations. Both types of phenomenon can be distorted by the space vehicle. In fact, data from Ref. 10 indicates variations in solar panel output due to rotation of IMP-7 dominate the plasma wave data. Portions of the view angle within a Debye wavelength (~1 m) of the solar panels should be minimized.

The plasma probe, Langmuir probe, and mass spectrometer all require an unobstructed view of the incoming particles and an additional 10 to 20 deg from their FOV limits where no large obstruction or space vehicle fields strong enough to alter electron and/or ion velocity vectors may be present.

The plasma probe has two sensor cups, whose acceptance cone is (a) approximately sunward and (b) 40 deg toward the south celestial pole from the Sun in a plane defined by the Sun, Encke, and S/V at encounter. The half-cone angle for each is 60 deg.

The Langmuir probe has three sensors with half-cone angles of 50 deg centered in (a) S/V velocity direction in Encke-centered coordinates at encounter (antisolar), (b) 140 deg from the Sun line (toward the south

celestial pole) in the plane defined by the Sun, Encke, and the S/V at encounter and (c) 60 to 90 deg from the Sun perpendicular to that plane defined by (a) and (b).

The mass spectrometer has a 15-deg half-angle cone centered on the S/V velocity direction in Encke-centered coordinates.

The imaging camera, UV spectrometer, and IR radiometer are all to have co-parallel FOVs which are directed at the coma and/or nucleus during encounter. This requires a scan platform with one or two degrees of motion. These instruments must not be permitted to look within 20 deg of the Sun or spacecraft reflected Sunlight. The imaging camera has a 1.1×1.4 deg FOV which must be unobstructed to the nucleus from E-60 days to E-20 days for approach guidance purposes and from E-20 days to E + 15 min for science imaging purposes.

The UV spectrometer is boresighted with the TV on the scan platform, has a $(1/4\text{-deg})^2$ FOV and is operated during the E-20 to E + 3 day time period.

The IR radiometer is boresighted with the TV on the scan platform and has a 1-mrad half-angle cone (or a ~0.11-deg full-cone angle).

The optical particle detector has four parallel 10 deg half-angle-cone FOVs which must be unobstructed. It is highly desirable to avoid structure in the hemisphere centered around the FOV in order to avoid light scattering into the light cone.

The alpha scattering instrument must not be exposed to dust and gases escaping from the space vehicle, particularly by elements which are expected to be observed in the ambient environment. A limit of $\leq 1\%$ of the expected density collected in the sample is reasonable at this time. It is expected that there will not be a compatibility problem in this area.

The charged particle telescope has a 32-deg half-angle cone FOV, the gamma ray spectrometer has a ~20 deg half-angle cone FOV, and the X-ray spectrometer has a 5×5 deg FOV. These instruments will see an increased background due to high-energy radiation interactions in materials near the instruments and trace radioisotope radiation. The angles to the solar panels will require additional shielding (i.e., weight and volume) or separation (boom structure) in order to compensate for the problem of increased material with respect to, say, a Mariner-class S/V. Counting rates >10% of the

expected ambient rates create a problem which must be considered on a mission by mission basis using trace element composition and location knowledge. Neither the active radar nor the photopolarimeter has been analyzed for solar panel incompatibilities.

E. Field of View, Through the Plume

Viewing through the plume can create two general types of problems for science. First the signal to be measured can be distorted in its passage through the plume. Second, the background or noise can be altered by reflected, scattered or emitted signals from the plume (Ref. 15). Figure 28 shows a typical geometry situation for viewing through the plume.

The plasma probe will be observing ions in the 10-eV to 2.5-keV region, which may be distorted in energy and direction by passage through the plume. The basic energy offset is caused by the electrostatic potential of the S/V and is controlled by the neutralizer (Ref. 14). (Interactions with the Hg ions in the plume by the solar wind particles, for example, are negligible because of the large mean free paths.) The direction distortion may be caused by inhomogeneities in densities and electric fields within the plume. Significant angular deviations will occur for ions or electrons below a 50- to 150-eV energy limit. This limit depends upon the details of the neutralizer charges, the thruster configuration, and charged particle paths within the plume.

Obviously this sort of effect is largest only where the thrust plume is in anti-plasma-flow direction. At times when the thrust direction is far from the anti-plasma-flow direction (i.e., greater than 60 deg and outside the basic field of view of the sensor), essentially none of the collected ions have been near the plume. Thus the remaining distortions are caused by the greatly reduced fringing plasma (see Figs. 2 and 3) from the thrusters and neutralizers. Under these conditions it is only conjecture at this time as to the extent of limitations which thrusting places on the plasma probe operation and ability to measure solar wind or coma plasma parameters.

The Langmuir probe detects lower-energy ions and electrons, so that interactions with the plume will be more degrading. It is assured that no determinations about the ambient plasma characteristics can be made when the plasma traverses the plume. At other viewing angles the interaction

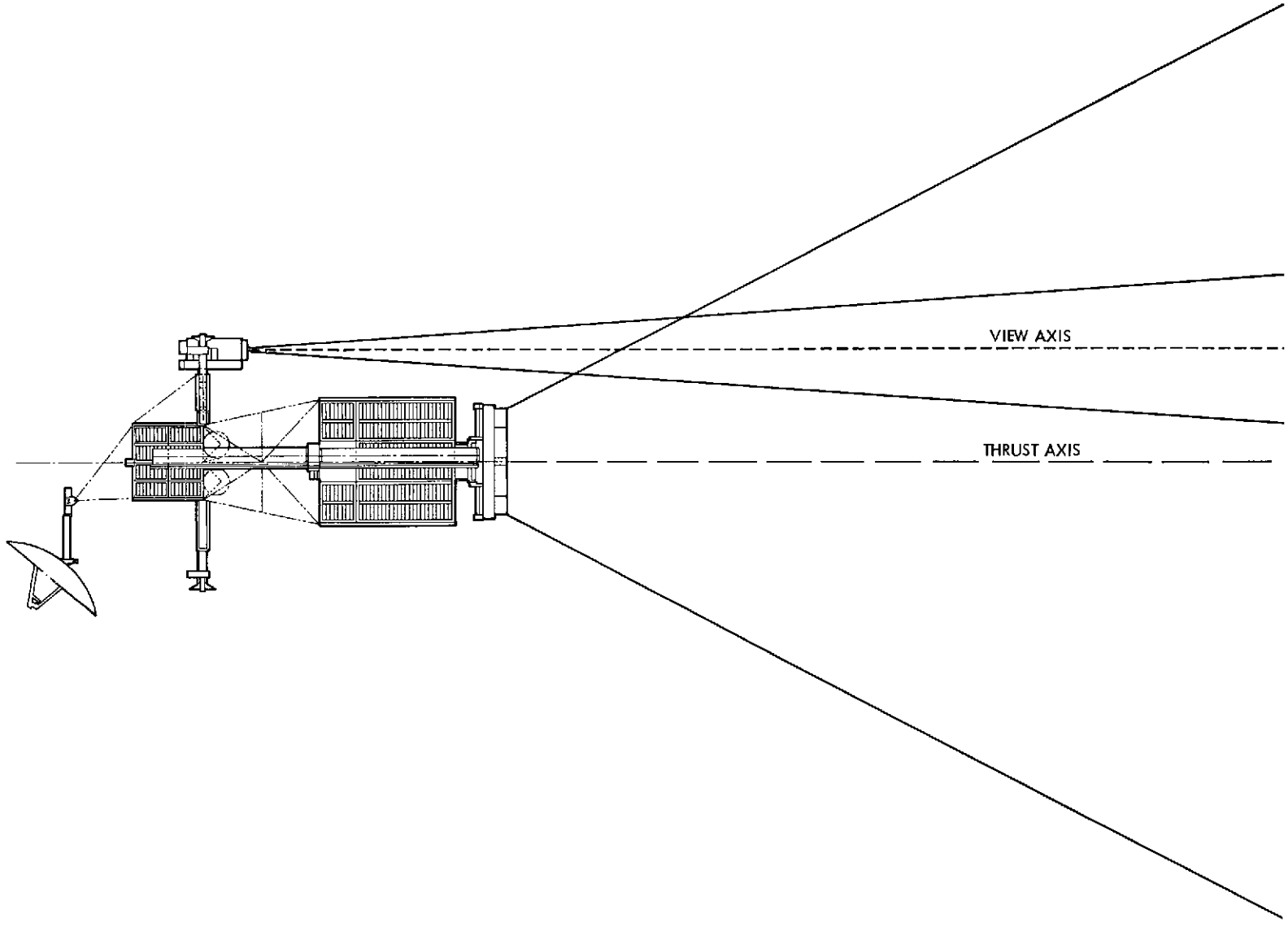

Fig. 28. Schematic of science instrument viewing parallel to the thrust axis of a SEP space vehicle. The potential interference column density is calculated in Appendix B

with the ambient plasma is still likely to be large and, furthermore, the flux of charged particles from the thrusters and neutralizers at the sensor may be larger than the flux from the ambient plasma itself. This experiment, therefore, requires time-sharing with thrusting since meaningful science data is not expected during thrust periods. However, experiment activation during thrusting times will not be damaging to the instrument and in fact may be valuable in understanding plume-plasma interaction and neutralizer effects as well as certain thruster-operation parameters.

The optical type instruments have a potential problem when viewing through the plume (Ref. 15). Calculations have shown that the total irradiance is quite small over the visible and UV regions. However, Appendix B indicates the intensity is a marginal problem for the wavelengths near Hg and Mo emission lines. Specifically the UV spectrometer has a threshold sensitivity of $\sim 10^{11}$ atoms/cm^2 and the plume will have $\sim 4 \times 10^{11}$ atoms/cm^2 for the FOV parallel to the thruster axis and looking back over the space vehicle bus 1.5 meters off the thruster axis. The above concern is probably applicable to the photopolarimeter, although data from an experiment viewing a sunlit plume is not yet available. Imaging, optical particle detector, and IR radiometer are not expected to have a significant problem although again experimental data is needed to compare calculated coma irradiance levels at various distances with the level due to the plume. Also the IR radiometer problem is extremely complex since the plume is not in thermal equilibrium. This infrared irradiance calculation requires an effort beyond the scope of the present effort.

The active radar has not yet been considered and data will be added later as telemetry studies develop the effects expected. The alpha scattering instrument will not be affected by the plume since it is not designed to view through it. The cosmic ray telescope, X-ray spectrometer, and gamma ray spectrometer will have their energy spectra altered as the particles and photons traverse the plume. However, for a column density of Hg of 5×10^{12} atoms/cm^2 (i.e. 1.67×10^{-9} gm/cm^2), the effect is negligible.

Although fields instruments are not normally thought of as having fields of view, the effects on their in situ measurements by the plume are discussed below.

For the magnetometer the plume may trap the ambient magnetic field and distort it such that no meaningful magnetic measurement can be made in or near the plume. In addition, the magnetic fields produced by the plume currents will be superimposed on the ambient fields. Since a boom is needed due to permanent or electromagnet fields, any field distortions from the plume will also be reduced by the separation. However, quantitative data is not available on the magnetic effects of the plume or the S/V. The magnetometer data is seriously degraded with S/V contaminant levels greater than $1 \pm 0.1\ \gamma$ at its location.

The plasma wave instrument will detect the turbulences created in the plume and its interaction with the solar wind. This will completely dominate measurements in the plume and is expected to distort the plasma wave effects for a significant region surrounding the plume. The plasma wave needs to have noise below that indicated in Fig. 27. A boom located on the opposite side of the S/V from the thrusters is expected to reduce the impact of the plume on the plasma wave to an acceptable level.

F. Deposition of Hg and Mo

Figure 29 shows the effects of deposition vs temperature where absorbed monolayers already exist (Ref. 4). The deposition of the initial monolyaer is not considered, since the physics and chemistry of the process are not well understood. However, three things are apparent. First, the original monolayer takes longer to be deposited. Second, for normal (around 20°C) and elevated temperatures there is no deposition problem for Hg. Third, more data is needed, particularly for molybdenum, on (1) flux levels vs angle and distance and (2) deposition rates vs flux, temperature, and material.

For cryogenically cooled devices such as IR sensors (~100 to 150°K) the problem may be significant. Here we do not expect the deposition to harm the instrument electrically, but the thermal control system may be altered by an altered emissivity.

The thermal control problem as affected by deposition effects on absorption, emission, and reflection is obviously of general concern to all instruments (Ref. 4) and we recommend some consideration be given to this area.

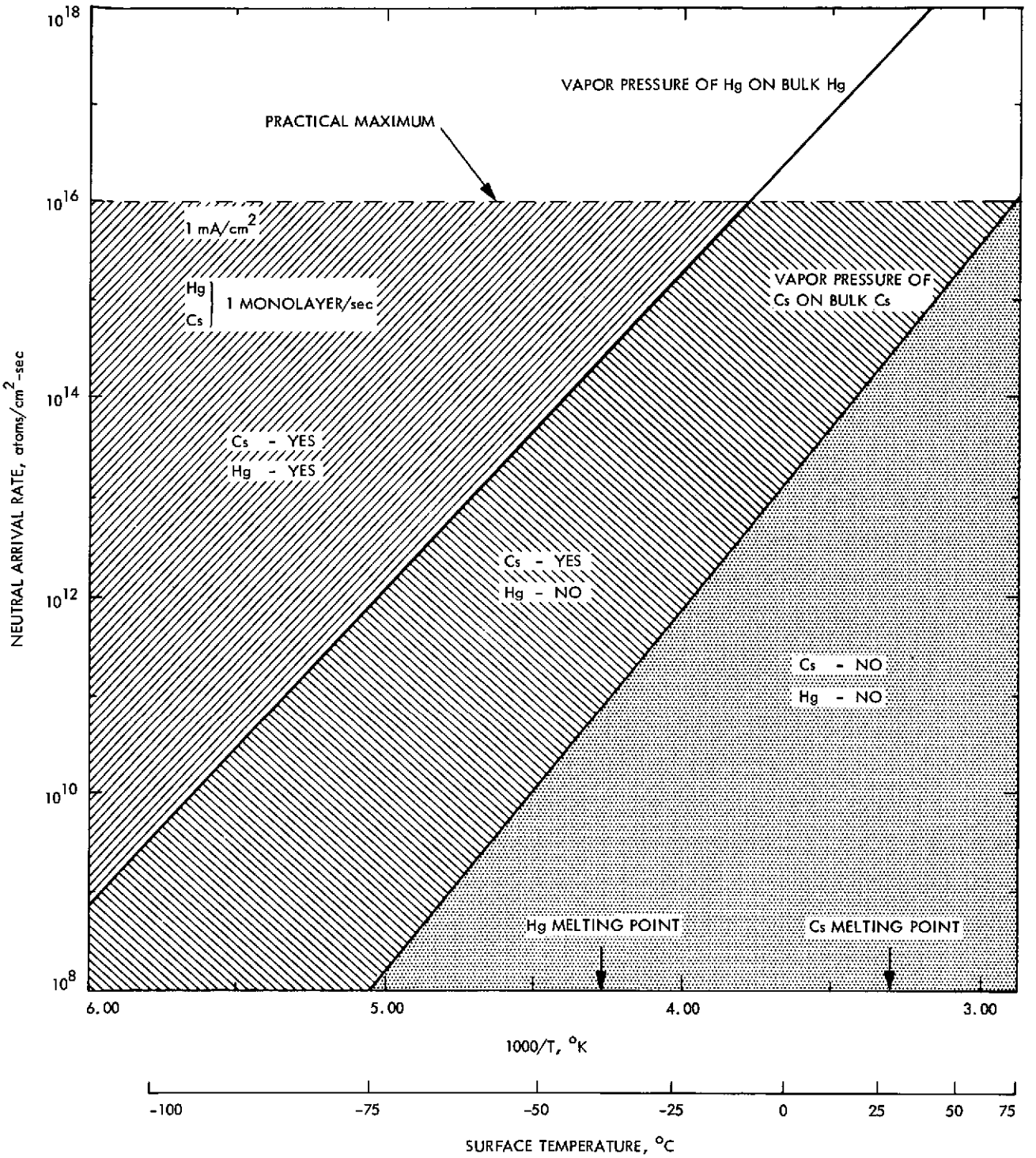

Fig. 29. Mercury and cesium deposition rate vs temperature. This shows that except for very cold surfaces Mercury is not a potential problem

Electrically, the plasma wave instrument cannot have the dipole antenna altered by depositions of a metal on the dielectric rod isolating the two spheres. Since the instrument measures the electrostatic potential between two points and divides by the separation distance to get the field, any change in the isolation of the two points is critical.

The deposition on optical coatings and elements only becomes critical when it affects transmission and reflection of the wavelengths of interest. If the criteria for uniform deposition on cooled optical surfaces are met, then Ref. 14 indicates that 20% reflectance would be affected by about 20 Å (2 nm) thickness or 7 monolayers.

IV. COMPATIBILITY CONCERNS FOR SCIENCE IN THE PRESENTLY UNDERSTOOD ENVIRONMENT

A. Definition of SEP Space Vehicle Environment

Appendix A shows the SEPSIT Environment Design Criteria (EDC) and some data on the presently understood EMI environment from the power conditioning unit. The EDC does not cover some environmental problems such as the comet Encke coma environment (Ref. 7), the plume deposition environment (Refs. 4, 6, and 11), and the radioisotope levels. Other problems which are covered are considered equivalent to non-SEP S/V environments. In addition, for the compatibility of science on a SEP space vehicle the available fields of view must be considered (Fig. 1). Table 2 listed some of the variations between the EDC and the presently understood environment.

For the environments covered in EDC there will be no overwhelming incompatibility at the levels shown. Other compatibility areas have been considered, and four areas plus conclusions are summarized here; (1) the deposition problems are either acceptable or marginal, (2) the comet's environment is to be measured and thus, for science, by definition, is not considered to be a problem, (3) vibration levels are dependent on the mechanical designs and are not yet defined, and (4) the fields of view do appear to be a problem since the instruments and other subsystems appear to require location in the -X axis region (Fig. 1) of the space vehicle where they see each other and/or the solar panels.

This generally optimistic picture is clouded somewhat by the EMI data (see Appendix A and Table 2), which is taken here as the currently understood environment.

All the instruments are subject to the considerable EMI problem. Presently this appears to be as high as ±1 V if there is no isolation. Although the amount of isolation is not well defined, it should reduce the level of noise considerably. Noise levels at the sensors are assumed to vary from a few microvolts to a few volts (see Appendix A). This is quite unacceptable for any instrument where the required accuracies range from 10^{-2} (1%) to 10^{-4} (0.01%) unless careful attention is paid to shielding and isolating techniques.

The EMI design criteria used by Viking are adequate for the instruments considered in this study since there will be additional isolation in the instruments. Although EMI is not considered an insurmountable problem, until supporting data is in hand it will remain a concern for compatibility (e.g., Ref. 16). In particular, an indication of thruster arcing times appears to be a useful piece of data to telemeter during science data gathering periods in order to remove contaminated science data.

Unknown mechanical and compositional designs preclude quantitative analysis of X-ray or gamma ray contamination from trace radioisotopes. However, a level of 0.1 ppm of 10^6 yr halflife isotope in a 1000 kg mass is equivalent to 1 photon/cm^2-s at a separation distance of 10 m if self-shielding is neglected. At this point no additional contaminants are allowed.

Unknown vibrational levels may become a problem involving tradeoffs between (1) mass needed in the truss and boom structures to meet the requirements of Appendix A and (2) fields of view and background needs of the instruments.

The plume impingement levels shown in Figs. 2 and 3 when compared with the available deposition data given in Ref. 4 do not appear to be a problem for most instruments. There are some concerns which are discussed below for each instrument.

Field-of-view problems appear to be significant for the Encke slow flyby payload. Compromises of the fields of view for some instruments are possible but still the solar panels, antenna, booms, etc., appear in many

of the FOVs. For the rendezvous mission, viewing through the plume does not appear to be a severe problem, although there are marginal problems for UV instruments, visible to IR photometers, and spectrometers in certain bands of wavelengths (see Appendix B).

The types of instruments most sensitive to the SEP S/V environment are those measuring the fields of low-energy ($\leq$10 keV) charged particles. The remaining problems such as EMI and viewing through the plume are shared to some extent by certain nonscience subsystems (e.g., telemetry and star tracking systems).

B. Specific Instrument Compatibility Concerns

The special compatibility problems during operation of each instrument in the SEP space vehicle environment are given below and are summarized in Table 22.

The mass spectrometer will probably detect wake effects (see Ref. 10) in the ion mode due to the solar panels depleting the low-energy ions in the coma and may possibly be sensitive to a shock front located on the order of few meters from the space vehicle. If hydrazine or any low-atomic-weight propellants are used in attitude control, they will severely contaminate the mass spectrometer data in these amu regions. Similarly, outgassing from the extremely large surface area of the SEP space vehicle will cause potentially severe background problems unless the experiments wait until the outgassing rates are acceptable. This is not likely a problem for Encke missions, since long times (months) elapse prior to prime science observation periods.

The imaging instrument will be turned on prior to E-60 days in order to perform approach guidance to the comet starting at that time. But even for a full 60 days of exposure (as indicated by Refs. 4-6) and supported by information in Section III) there is no deposition problem expected. The interference from emission lines and scattered light is seen to be at worst a marginal problem which can be handled by proper instrument design if data is made available on emission line intensities in sunlight (even at 2×10^7 km, e.g., extrapolating the photometric model from 1.75×10^5 km to 2×10^7 km by $1/R^2$; i.e., 10^2 photons/cm^2-sec, from Appendix B. The magnetic field and deposition environments appear from Table 22 not to be

Table 22. Compatibility of science instruments on a SEP space vehicle

Instrument	Magnetic field at sensors (ac or dc)	EMI		Plume deposition	FOV and in situ distortions
		Conducted	Radiated		
Mass spectrometer	<3100 γ	DCL	DCL	Not serious	Ions distorted by plume, S/V, thrusters
Imaging	$<10^4$ γ should not cause a problem	DCL	ND	Probably not serious	Must not view S/V and thruster; on scan platform
Optical particle detector	$<10^4$ γ should not cause a problem	DCL	ND	Not serious	Avoid reflected light into shadow cone; do not view plume
Magnetometer	<1 γ requires ≥6-m boom, magnetic cleanliness program	DCL	DCL	Not serious	Magnetic field distorted by solar panels, thrusters, plume, S/V currents
Plasma wave	Fig. 27 requires ≥8-m boom	DCL	DCL	Probably not serious	Plasma waves distorted by plume, thrusters, solar panels
Plasma probe	$<6\times10^4$ γ should not cause a problem	DCL	DCL	Not serious	Plasma distorted below 150 eV by thrusting; must avoid solar panels, S/V structure, plume;
Langmuir probe	<3100 γ; requires ≥2 m from thrusters if other sources are small	DCL	DCL	Not serious	Plasma distorted by thrusting; must avoid thruster, S/V structure
UV spectrometer	$<10^5$ γ	DCL	ND	Probably not serious	Must not view S/V; thrust plume bands in UV a marginal problem
IR radiometer	$<10^5$ γ	DCL	ND	Cryogenic surfaces may be a problem	Must not view S/V; plume IR not known
Alpha scattering	$<10^5$ γ	DCL	ND	Not serious	Not serious
Gamma ray spectrometer	$<10^4$ γ should not cause a problem	DCL	<1 γ/cm^2-s at instrument over 0.1 MeV ≤Eγ≤5 MEV	Not serious	FOV must not be near S/V; requires ~8-m boom
Charged particle	$<10^4$ γ should not cause a problem	DCL	ND	Not serious	Must not view S/V
Imaging radar	$<10^5$ γ no problem	DCL	ND	Not serious	Must not view S/V
Photopolarimeter	$<10^4$ γ should not cause a problem	DCL	ND	Probably not serious	Must not view S/V; plume marginal problem
X-ray spectrometer	$<10^4$ γ should not cause a problem	DCL	<0.1 photon/cm^2-s at instrument over 0.1 keV ≤E photon ≤0.5 MeV	Not serious	Must not be near S/V (~8-m boom); tracks nucleus

Note: All instruments need an indication of thruster arcing times occurring during data taking periods.

DCL = design criteria level (see Fig. A-8). These levels are acceptable. Data is needed supporting the attainment of these levels.

ND = not determined.

of more concern to imaging for SEP than for any other S/V type. The EMI problem requires the electromagnetic levels to be at least as low as the MJS'77 or Viking levels (i.e., SEPSIT design criteria) for the imaging instrument to avoid a loss in the light level sensitivity. This loss would not only be detrimental to the imaging science objectives but would also severely impact approach guidance capability.

The optical particle detector is not expected to have any problems if the EMI design criteria and FOV requirement can be satisfied. In the case of FOV, even multiply scattered solar light from various S/V surfaces getting into the light cones of this instrument is unacceptable, and S/V structure cannot be allowed in the FOV or even extend far into the hemisphere centered on the FOV.

The magnetometer requires a 6 meter boom (i.e., 8-meter separation from thrusters) in order to provide a field $\leq 1 \pm 0.1\,\gamma$ at the sensor location using the data in Appendix A. The boom length assumes that there are no significant field sources other than the magnets for the thrusters. Since the fields to be studied are estimated to be $\leq 20\gamma$, even a small variance from $1\,\gamma$ will significantly affect the capability of the magnetometer (e.g., a rise to $5\,\gamma$ represents a factor of 5 loss of dynamic range and a 99% loss of data). The solar panels will create a wake effect which may trap the field lines and distort them. Space vehicle currents or permeable materials in the PCU, solar panels, etc., will add to the field distortion. EMI (narrow band) at the assumed level will dominate the signal, alter the environment, and seriously limit any measurements. However, EMI will not be a problem if the design criteria are met. Deposition is not a serious problem. The mass spectrometer may be required to be magnetically shielded to be compatible with the magnetometer.

The plasma wave instrument data cannot be guaranteed to be scientifically meaningful with the thrusters on. This instrument is also highly sensitive to EMI, especially in the frequency range 10 Hz to 200 kHz. For this reason, an $\geq$8-m boom is required to provide an acceptable sensor location even assuming the EDC levels. For the currently understood levels the EMI will dominate the signal, alter the environment, and thus seriously limit any measurements. Reference 10 addresses some of the concerns for a plasma wave device (these are associated with wake effects of the space vehicle plus photoelectrons from space vehicle surfaces). Variations

in the magnetic fields will be affected by the amount of soft metal on the space vehicle. Since temperature and vibration alter the permeability of the electromagnetic poles when the electromagnets are off to a greater extent than a saturated permanent magnet, the possible decrease in boom lengths due to reduced field strengths may be negated by the increase in variability unless the electromagnets are rung down with decreasing voltages and currents. This must be supported by magnetic field strength and variation data vs temperature and vibration (see Appendix C) for electromagnetics and permanent magnets (assuming the permanent magnets can survive the operating temperatures). If the level of EMI is at or below the EMC design criteria, no problems are expected.

The plasma probe instrument will probably have its useful energy range restricted to above 50 to 150 eV during thrusting periods (see Section III-E). The conducted EMI as depicted in Table A-13 of Appendix A shows 2 V peak-to-peak at interface connectors. This is larger than the design of the instrument will tolerate on a continuous basis by about a factor of 3. The shielding of the electronics package and sensors further requires lower conducted EMI than the currently understood levels (or some instrument redesign). For this instrument too, design criteria levels appear to be acceptable on all but the internal digital data lines where instrument provided isolation is needed.

The radiated EMI during thrusting causes the above plasma energy restriction when the field of view includes the plume. This view condition does not occur for the Encke missions since it will occur only before aphelion, which would impact cruise science or during rendezvous maneuvers when observations can be suspended. Distortions and restrictions during other thrusting periods are problematical. Radiated EMI when not thrusting appears to marginally affect operations, but the description in Appendix A is not precise enough to make a complete evaluation. In general, we feel this interference is about an order of magnitude above the threshold for degradation of operation.

The field-of-view requirements (see Section II) are likely to be partially compromised to meet the total mission requirements. The tradeoffs between optimal sensor position and fulfillment of FOV requirements have not been evaluated or demonstrated for the configuration in Fig. 1.

The Langmuir probe has similar problems but is more sensitive to S/V environmental interference. Radiated EMI is serious while thrusting, but the relative importance of it and charged particle flux (deposition) from the thruster plume plasma cannot be made on an abstract basis without experimental data. While direct measurement of ambient plasma parameters is not likely to be achieved while thrusting, useful information about thruster operation and plasma-plume interactions may be obtained as described in Section III-E. The slow flyby and the rendezvous (by time-sharing) missions will be in a no-thrusting condition when this instrument is likely to make positive measurements of Encke and its environment. Thus, compatibility with the S/V for non-thrusting periods will be discussed.

The conducted EMI and field-of-view considerations have the same degree of problems as the plasma probe instrument, and those comments apply. When the thrusters are powered down, it seems likely that radiated EMI from the PCs and solar panels will be less than the 2-V peak-to-peak limit required in the frequency range from 1 Hz to 10 kHz. Effects on low-energy particles are likely for this mission as has been true of all space missions, but active control of the S/V electrostatic potential by means of a neutralizer should be a very beneficial asset. Since S/V electrostatic potential may be controlled and significantly lower than previous spacecraft, an effort should be made to keep all EMI as low as possible so that the science resolution may realize this potential new limiting factor.

The UV spectrometer also will not have EMI problems for levels at or below the EMC design criteria. Potential FOV problems exist for viewing through the plume at specific wavelengths (see Appendix B). The ratio of expected to sensitivity levels is $4 \times 10^{\pm 1}$ when viewing parallel to the plume. Deposition is expected to be an order of magnitude less than the problem level of ~2 nM. However, the estimated deposition depth is uncertain. The FOV from the scan platform must not be obstructed by S/V structures from E-6 days through E + 3 days for the Encke slow flyby (ESF) mission.

The IR radiometer also will not have an EMI problem, if EMC levels or lower are provided. The infrared radiance from the plume is not currently known. It is in a nonequilibrium condition and is expected to radiate in an exponentially decreasing fashion from the thrust plane with

a large (km?) decay length. The FOV from the scan platform should not be obstructed by S/V structure. Again, nucleus viewing for the ESF from E-6 to E + 3 days is required. The low temperature (100 to 150 K) used for some IR optics and sensors may create a deposition problem even for Hg. Data on this is not available at the angles and distances of interest.

The alpha scattering instrument is not part of the Encke slow flyby or rendezvous mission payloads for this study. Thus the compatibility considerations do not consider other instruments in the payload (i.e., FOV problems reduced) or a specific mission (i.e., objectives only typical). In general, the acceptable magnetic field levels are quite high (e.g., $10^5 \pm 10^4 \gamma$). The EMI problems will be negligible at or below the design criteria levels. There are no incompatibilities identified at this time.

The gamma ray spectrometer requires a boom long enough to lower the S/V-induced background to <10% of the expected levels from the surface of the planet, comet, etc., in the trajectory from which they are being observed. A typical length is ~8 m. Control of trace elements on the space vehicle such as thorium, uranium, and potassium (only isotope with an amu of 40) is important in order to provide $\leq 1\ \gamma/cm^2$-s with energy (0.1 MeV $\leq E\gamma \leq$ 5 MeV) at the instrument. The EMI levels should not be a concern at the design criteria levels.

The charged particle telescope requires EMI levels no higher than the design criteria for signal stability of 10^{-4}. The FOV must not be obstructed by S/V structure.

The active radar and photopolarimeter will not be degraded by the design criteria EMI levels. S/V structure cannot be in the fields of view. Plume viewing may attenuate the radar signal and produce interfering emission and absorption lines for photometry. Plume effect data is needed to resolve the last item.

The fields and particles instruments (especially the magnetometer) would benefit from a roll maneuver inside the contact surface. It appears that rolling about various axes at 1 deg/s may require long periods of time to attain and remove the angular velocity. Rolling about the Y-axis may require as long as 500 s in order to attain an angular velocity of 1 deg/s. Rolling

about the X- or Z-axes may require 5000 s for acceleration and deceleration. If other orientation requirements preclude the Y-axis roll, then the maneuver will not be possible for the slow flyby mission since 10,000 seconds (5000 s each to add and remove the angular velocity) is too long to assure that the S/V is still inside the contact surface.

Pointing stability is an area of compatibility concern which as yet has not been well studied in terms of science requirements. A preliminary estimate (Ref. 2) indicates that during the approach guidance phase of the slow flyby a ±5 μrad/s stability is needed to resolve Encke as early as E-60 days. This appears to be quite difficult for the large SEP space vehicle. At E-20 days in the slow flyby a stability of ±20 μrad/s is required. For the rendezvous, it is expected that ±20 μrad/s will be acceptable during the entire mission.

Science measurements are currently designed to end before ~0.7 au (but no earlier than E + 3 days) due to thermal control problems. Deposition effects on the thermal control problems for the instruments are not yet understood, but could have significant implications on the actual thermal degradation point on the trajectory.

V. POSSIBLE MEANS TO ATTAIN COMPATIBILITY AND SUGGESTED TRADEOFF STUDY TASKS

This section describes the avenues to attain compatibility being considered by the Science Compatibility Team and the recommendations for further activities. The validity of attempting to suggest solutions prior to fully understanding the problems is certainly suspect. However, since an iterative procedure is required to integrate a payload, information feedback at an early time is essential.

The EMI (conducted and radiated) problems are quite severe as shown by the available data unless isolation is better than ~120 dB. Determined efforts by representatives of the nonscience areas appear necessary to meet the Environmental Design Criteria which will satisfy the science instrument requirements. If individual EMI isolation systems are required to be fitted to each instrument, the instrument mass will be increased and the design, at

least in the power supply sections, will require modification which will lead to repackaging, retesting, etc. The tradeoff here (and in the following) should be to place the responsibility and resources for the implementation of EMI requirements in the project areas in such a manner as to make the cost level of the mission and the capabilities of the SEP space vehicle compatible with both NASA resources and the science community needs.

Lack of environmental data for radioisotopes on the S/V precludes a quantitative analysis of interference. The gamma ray spectrometer and the X-ray spectrometer both require, however, a very low ($\leq$1 photon/cm^2-s with 0.1 keV $\leq E_{photon} \leq$30 MeV) flux from the space vehicle. This puts limits on potassium, uranium, and thorium in S/V materials such as glass, batteries, etc., which vary with relative location and intervening material on the space vehicle.

In the case of magnetic fields from the thrusters, dipole orientation and bucking coil techniques discussed in Appendix B must be developed in tradeoff studies supported by experimental data. The magnetic field requirements can be met in principle if sufficient project effort can be directed toward solving the problems. Magnetometer and plasma wave instrument require low-level contaminant fields, and the actual acceptable level depends on its stability. If the field at the sensor could be guaranteed to be absolutely stable with all three components known in advance to $\pm 0.1\ \gamma$, a field at the magnetometer as high as $\approx 10\ \gamma$ in all three components might be acceptable. Unfortunately, no such field stability can be expected, much less guaranteed to the user. At the same time, magnetometer data good to $1\ \gamma \pm 0.1\ \gamma$ is considered of great importance to the missions under consideration.

We suggest that under these circumstances, a strong effort is needed to develop some strategies to accommodate the magnetometer and plasma wave requirements. These strategies should then be examined for feasibility and cost prior to assessing the tradeoff of degrading the magnetometer data. In fact, we believe that the strategy outlined in Appendix C plus a ring down of electromagnets (Ref. 17) meets both the feasibility and cost requirements.

Plume deposition of Hg appears to be at worst a marginal problem based on extrapolation of available data. However, additional study is needed for the thermal control problem. Techniques such as warming the outer lens of the camera, cycle heating IR devices, and shadow shielding sensitive regions are being considered. Molybdenum deposition rate data is not available.

Field-of-view problems are complicated by (1) requirement to separate instrument from thruster area, (2) the thrust plume, and (3) the large size of the S/V (e.g., large solar panels). Essentially all instruments must be located as far away from the thrusters as possible, producing a clustering at one end of the S/V. This means that the science instruments will tend to get in each others' fields of view and compromises will be required to a greater extent than for smaller, non-SEP space vehicles.

Optical instruments which view through the plume will have a marginal problem at or near some emission lines. Instrument design will have to account for these possibilities, and unless supporting experimental data is provided, excessive conservatism may be required in the design. For the Encke slow flyby mission the thrusters must be turned off prior to the shock front encounter (see Figs. 4 and 13) estimated inside 2×10^6 km (e.g., by E-6 days). An even earlier turnoff of thrusters is desirable. Avoidance of low Z elements for attitude control propellant is required for the Encke mission. A high Z noble gas (e.g., xenon) would be acceptable.

For the large solar panels, some FOV compromises may be made, but a significant improvement would be to roll in some of the solar panels to the point where the space vehicle power needs were just met for the slow flyby mission. This would be particularly useful when the thrusters were off near Encke and during roll maneuvers. For the rendezvous mission, confidence in multiple deployment would play a greater part in exercising this option.

There is a considerable amount of work yet to be done in the compatibility study area. At the same time there is a lack of available S/V data needed in many areas. Areas where empirical data is needed include (1) plume deposition as a function of large angles and on clean surfaces, particularly for Mo_2, (2) emission and absorption data in the UV, visible and IR regions from the thrust plume, (3) plume effects on radar signals and transmission in S/X bands, (4) EMI levels for frequencies from dc to ~20 GHz,

(5) magnetic dipole orientation and ring down techniques for thruster sets, and (6) α/ϵ changes due to plume deposition. Simultaneously, design trade-off studies in these areas must continue.

APPENDIX A

SEPSIT ENVIRONMENTAL DESIGN CRITERIA AND SOME AVAILABLE PERTINENT DATA

I. ENVIRONMENTAL DESIGN CRITERIA FOR SEPSIT

A. Scope

This document specifies environmental design criteria for use in the Solar Electric Propulsion System Integration Technology (SEPSIT) study. The requirements contained herein reflect typical 3-σ environments and/or design qualification test levels unless otherwise defined. The intent is to provide "typical" spacecraft design criteria, and only for selected environments has mission-pecular information been generated. In particular, Encke comet environments are not contained in this document. The basis for mission-independent criteria is existing information drawn from the Viking Orbiter or Mariner Jupiter-Saturn (MJS) programs.

The source information for most of the content of this document is provided in Refs. 1, 18, and 19.

1. Purpose. The environmental design criteria contained in this document provide a basis for design of space vehicle subsystems and supporting data for space vehicle and mission design tradeoff analyses with emphasis on information supporting the thrust subsystem technology development. Where hardware is developed in consonance with these requirements, the design will be considered flight-qualifiable within the bounds of the guidelines or assumptions stated below.

2. Basis of environmental criteria. The following paragraphs identify the source of the criteria contained in this document and major assumptions made.

a. Handling/shipping/storage requirements. The stated criteria are typical Mariner or Viking requirements and similar to typical Mil. Spec. requirements.

b. Launch environment. The Titan III D/Centaur launch vehicle has been assumed and applicable levels taken from the Viking Orbiter program. These levels are generally considered to be compatible with Space Shuttle applications.

c. Thermal environments. Stated requirements represent typical Mariner or Viking requirements for thermally controlled assemblies. It is noted that the Encke mission offers significant thermal control challenge (solar distances ranging from 3.5 to 0.34 au). Until thermal control design is further developed, additional thermal requirements are to be determined.

d. Meteoroids. A mission-dependent estimate of meteoroid fluence has been generated assuming the meteoroid model of NASA SP-8038 (Meteoroid Environment Model - 1970) and the nominal Encke rendezvous 1980 trajectory. Early Pioneer data suggests the asteroidal meteoroid model is conservative.

e. Solar flare protons. A mission-dependent estimate using the nominal Encke rendezvous 1980 trajectory has been developed.

f. Magnetic fields and electromagnetic compatibility. Precise requirements are very dependent on mission and science payload. Values included herein are taken from Viking Orbiter or MJS as applicable and provided as SEPSIT guidelines.

3. Definitions. The following terminology is intended to be consistent with that adopted for SEPSIT.

Space Vehicle:	Combined spacecraft and SEP module.
Spacecraft:	Science instruments and Viking-type spacecraft assemblies grouped into a spacecraft system.
SEP module:	The solar electric propulsion module made up of the thrust subsystem and propulsion support subsystems including the rollout solar arrays.
Subsystem:	By example: the power subsystem.
Assembly:	An element of a subsystem which is replaceable as a spare (e.g., an electronics bay).

B. SEPSIT Environmental Design Criteria

1. Transportation vibration.

a. Assemblies. Assemblies in shipping containers shall be capable of withstanding sinusoidal vibration of the container in any axis at the levels in Table A-1.

b. Subsystems and the space vehicle system. Transportation vibration of the entire vehicle or major subsystems (e.g., the thrust subsystem) shall be constrained such that induced loads do not exceed launch phase conditions.

2. Transportation and handling shock.

a. Assemblies. Shipping containers shall isolate shock on assemblies such that they will survive container drops on any corner, edge, or surface from the heights specified in Table A-2.

In addition, assemblies shall be capable of withstanding bench handling shocks in the unpackaged configuration (or in handling fixture, if applicable) induced by drops described in Table A-3.

3. Ground handling temperatures. The space vehicle system, subsystems, and assemblies shall be capable of withstanding temperatures specified in Table A-4 during ground handling operations at local ambient pressure. The "uncontrolled environment" levels apply only to items which may be afforded no environmental protection at some time during ground handling operations.

4. Moisture, fungus, and corrosion resistance. The design of the spacecraft, subsystems, and assemblies shall include adequate protection from damage or malfunction attributable to moisture, fungus, and corrosion. In lieu of spacecraft design penalties, adequate environmental control, handling, and operations procedures shall provide the required protection.

5. Humidity. The space vehicle, subsystems, and assemblies shall be designed to be compatible with the Earth atmospheric humidity environment presented in Table A-5. The "uncontrolled environment" levels apply only to items which may be afforded no environmental protection at some time during ground handling operations.

Table A-1. Acceleration levels for transportation vibration

Frequency, Hz	Acceleration level, g pk
2.5 to 35	1.3
35 to 48	3.0
48 to 500	5.0

Table A-2. Drop heights for transportation shock (in shipping container)

Total mass of assembly and container,		Drop height,	
kg	(lb)	cm	(in.)
0 - 9.1	(0 - 20)	107	(42)
9.1 - 22.7	(20 - 50)	91	(36)
22.7 - 113.6	(50 - 250)	76	(30)
113.6 - 227.3	(250 - 500)	61	(24)
≥227.3	(≥500)	46	(18)

Table A-3. Handling shock (unpackaged)

Drop configuration
Impact surface: solid hardware bench top, or equivalent.
Drop 1: With one edge used as a pivot, assembly is tilted up until any one of the following positions is achieved, then released. (a) Opposite edge is 4 in. (10 cm) from bench top. (b) Face on which it is dropped is at a 45-deg angle to the bench top. (c) Item is lifted to just below the point of perfect balance.
Drop 2: Assembly is positioned 1 in. (2.5 cm) above bench top with face on which it is dropped parallel to bench top, then released.

Table A-4. Ground handling temperatures

Uncontrolled environment			Controlled environment		
Low	High	Transient	Low	High	Transient
-40°C	70°C	15°C/hr	0°C	40°C	5°C/hr

Table A-5. Humidity characteristics

Relative humidity, %	Temperature range, °C
Controlled environment, 40 - 70	0 to 40
Uncontrolled environment, 0 - 100	-40 to 70

6. Explosive atmospheres. An explosive atmosphere is defined to be an atmosphere capable of being ignited and possessing physical characteristics of pressure, temperature, and autoignition temperature falling within the ranges given in Table A-6. The space vehicle, subsystems, and assemblies shall be designed so that when operation in any explosive atmosphere is required, ignition will not result.

7. Static and dynamic loads.

a. Space vehicle system and major subsystems (e.g., the thrust subsystem). The space vehicle system shall be capable of withstanding launch loads equivalent to the following (the Titan III C/Centaur launch vehicle has been assumed):

Static acceleration: The static acceleration levels are given in Table A-7.

Transient vibration: The space vehicle system shall be capable of withstanding launch vehicle induced transient vibration equivalent to the sinusoidal vibration levels of Fig. A-1. These levels should be interpreted as occurring on primary structure near the space vehicle separation plane (i.e., on primary structure of the thrust subsystem).

Acoustic field: The launch acoustic design requirement is given in Table A-8. The design shall be capable of withstanding this environment for 5 min.

Pyrotechnic shock: The pyrotechnic shock environment is dependent on the type of pyrotechnic devices present on the space vehicle and the proximity to such devices. The environments for several device types are defined in Fig. A-2. The attenuation with distance from the source may be estimated using the curves of Fig. A-3.

b. Assemblies (e.g., electronic assemblies and power conditioner assemblies).

Static acceleration: The static acceleration levels are given in Table A-7.

Sinusoidal vibration: Assemblies shall be capable of withstanding sinusoidal vibration applied to their mounting points in any direction at the levels given in Table A-9.

Table A-6. Range of explosive atmosphere physical characteristics

Explosive atmosphere physical characteristics	Range
Pressure, nT	133 to 1067
Temperature, ^{o}C	15 to 55
Autoignition temperature, ^{o}C	350 to 750

Table A-7. Static acceleration levels (launch)

Direction	Acceleration, g	Duration, min
Thrust axis	+6, -2	5
Any lateral axis	±2	5

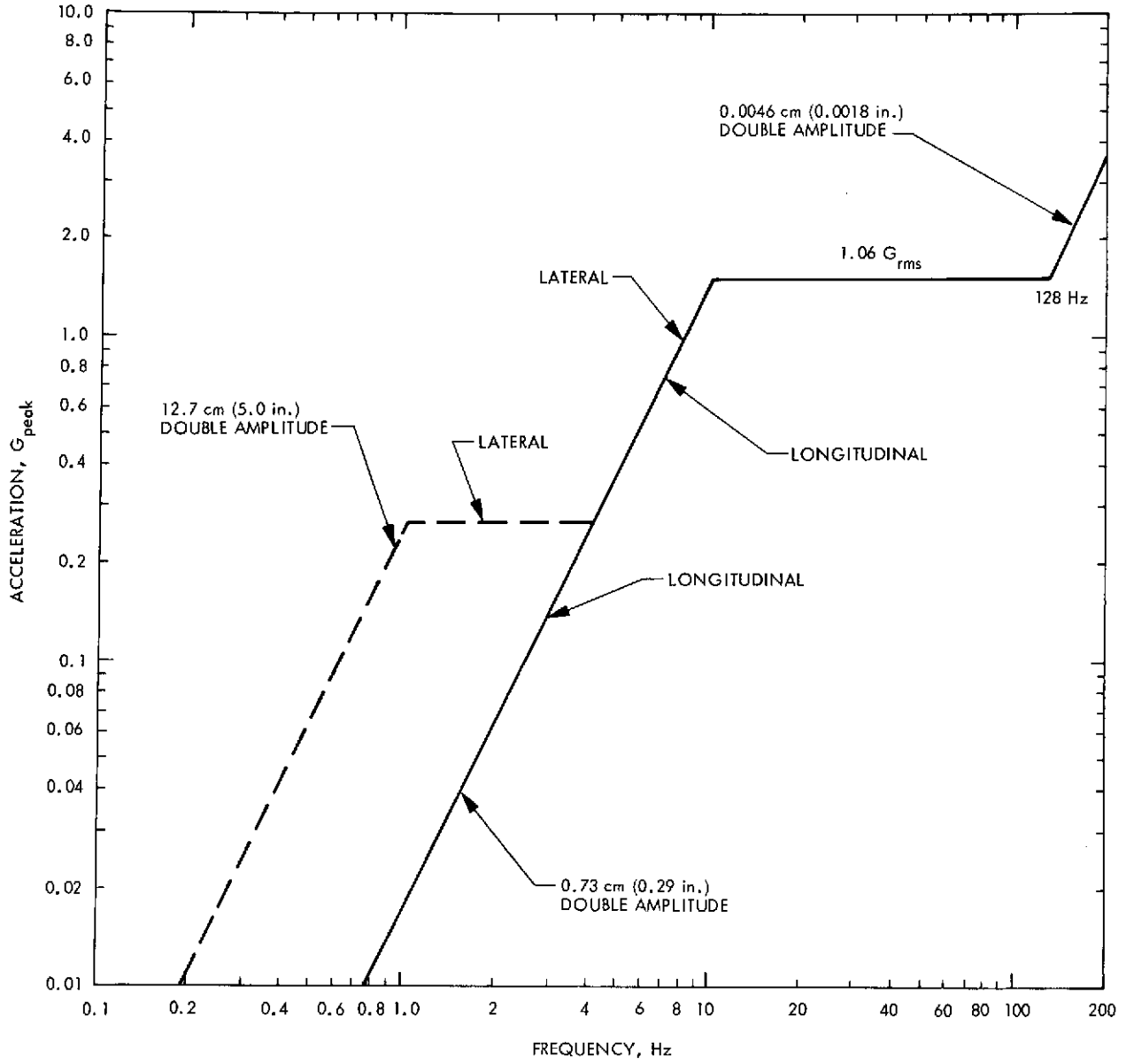

Fig. A-1. Space vehicle sinusoidal vibration environment

Table A-8. Launch acoustic field levels

1/3 octave band center frequency, Hz	Sound pressure level in 1/3 octave bands, dB re 2×10^{-4} dynes/cm^2
50	133.5
63	134
80	134.5
100	135
125	137
160	139
200	140
250	140.5
315	140
400	138.5
500	137
630	136
800	135
1,000	134
1,250	133
1,600	132
2,000	131
2,500	130
3,150	129
4,000	128
5,000	127
6,300	126
8,000	125
10,000	124
Overall	149

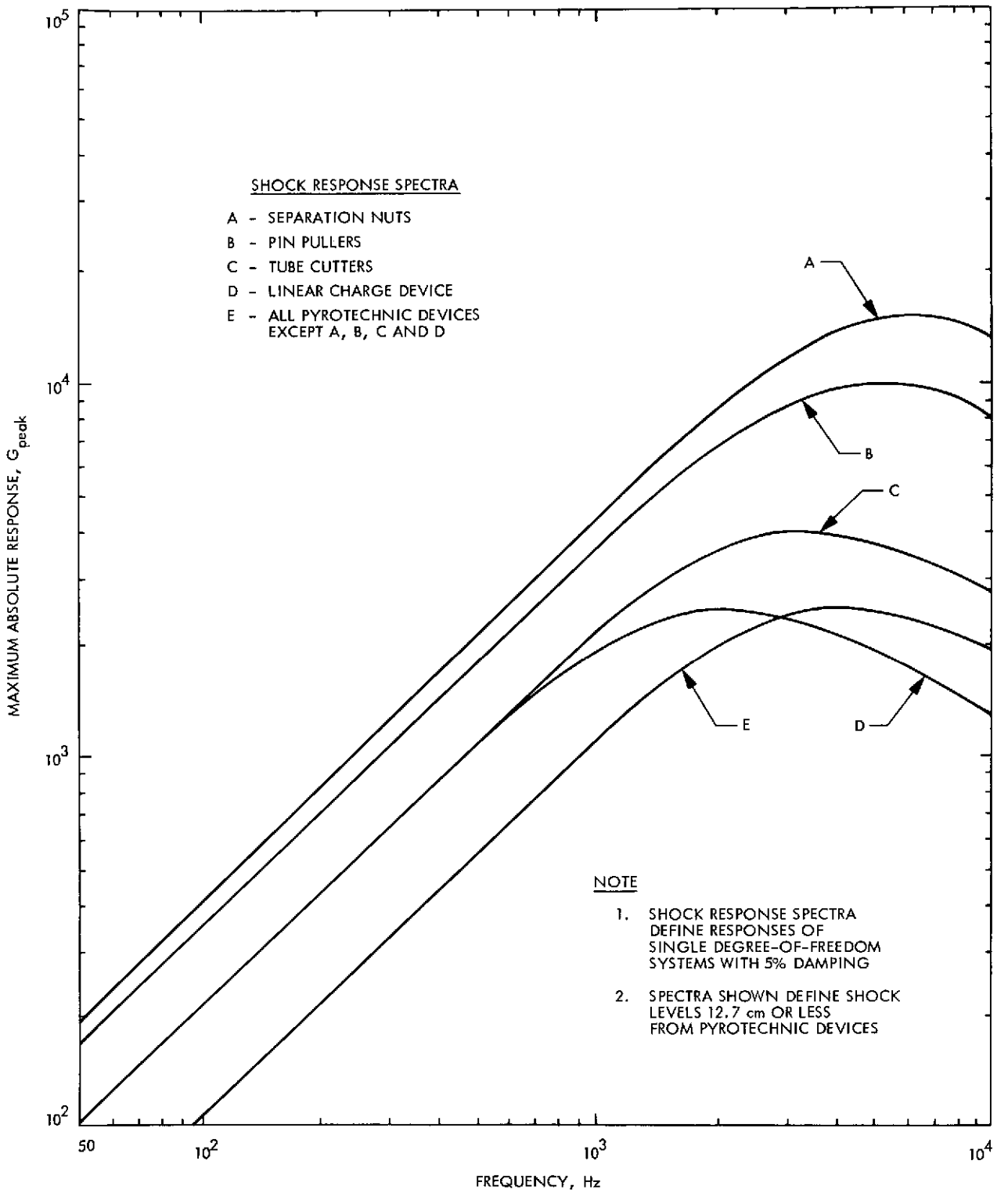

Fig. A-2. Pyrotechnic shock response spectra

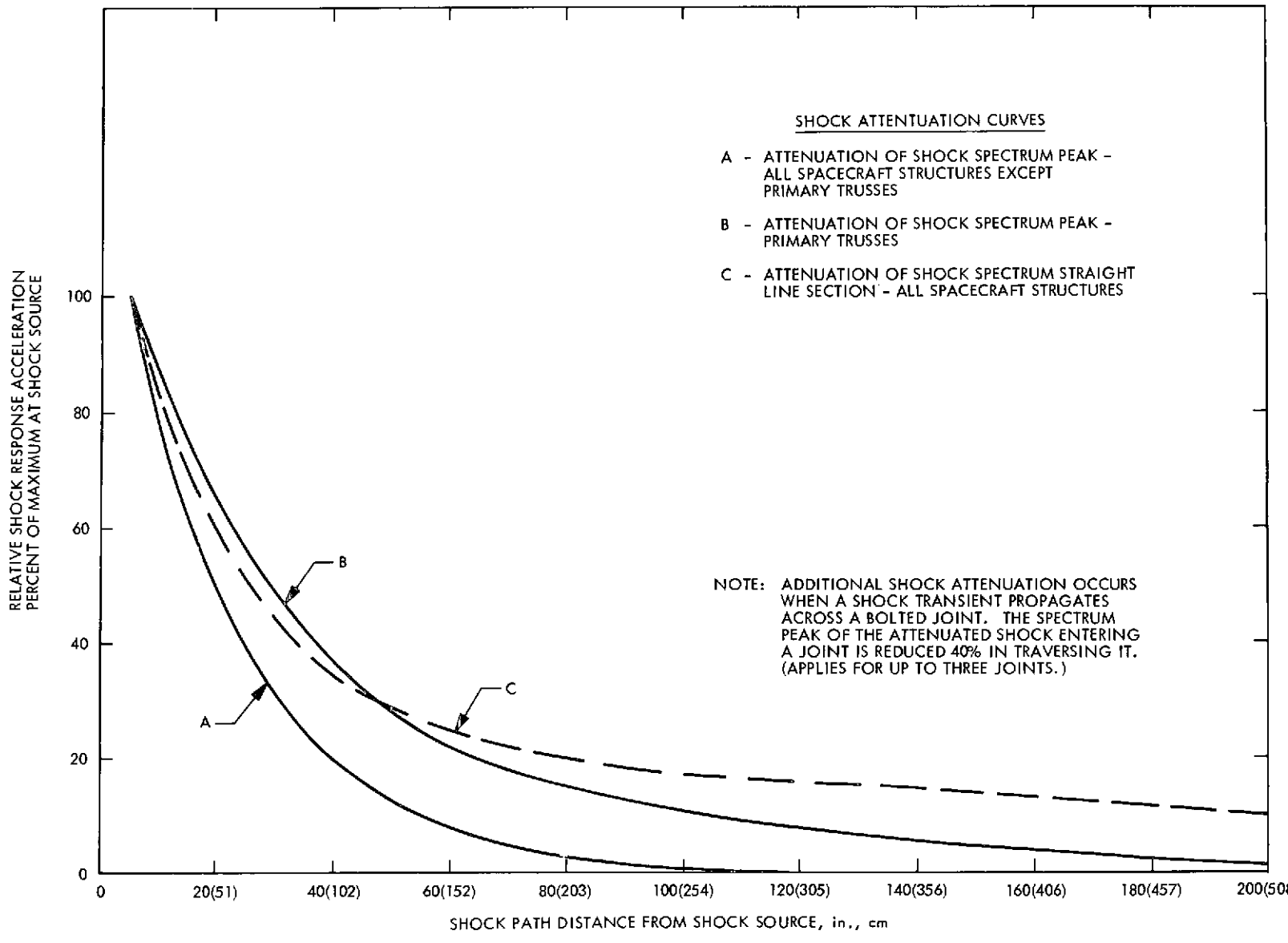

Fig. A-3. Structural attenuation of pyrotechnic shock spectra

Table A-9. Sinusoidal vibration levels for assemblies

Frequency, Hz	Amplitude
5 - 10	1 cm (0.4 in.) double amplitude
10 - 40	1.5 g rms
40 - 100	5.5 g rms
100 - 1000	4.5 g rms

Random vibration: Assemblies shall be capable of withstanding random vibration applied to their mounting points in any direction. The random vibration level and spectral shape is given in Fig. A-4. The vibration should be considered to have a Gaussian amplitude distribution with no peaks greater than three sigma.

Acoustic field: Assemblies having large surface-to-weight ratios (e.g., solar arrays and antennas) must consider the acoustic field as a design constraint. Levels are as defined in Table A-8. The design shall be capable of withstanding this environment for 5 min.

Pyrotechnic shock: See Figs. A-2 and A-3.

8. Launch pressure decay. The space vehicle will experience atmospheric pressure decay during launch. Design conditions for pressure decay in the space vehicle compartment are bounded by the following:

The pressure drops from 10^5 Nm^{-2} (1 bar) to 6.89×10^3 Nm^{-2} in less than 75 s.

The maximum pressure decay rate is 6.66×10^3 Nm^{-2}/s for a 3-s period.

9. Corona. High-voltage flight equipment is designed and fabricated so as to prevent or be immune to the formation of corona or arc discharges during exposure to critical pressure regions (typically 6.66×10^3 Nm^{-2} to 6.66×10^{-2} Nm^{-2}. Detailed design guides are contained in DM 505139A, "High Voltage Electronic Packaging, Flight Equipment," a JPL design specification.

10. Temperature. The design requirement for subsystems and assemblies is dependent on the system thermal control design. The Encke mission is sufficiently unique (solar distances range from 0.34 to 3.5 au) that temperature requirements and thermal control requirements are not well defined. Temperature ranges at least as severe as Viking Orbiter and Mariner Jupiter-Saturn should be assumed. These are summarized in Table A-10.

11. Thermal-vacuum

a. Thermal radiation. The design value of the solar constant at 1 au is 135.3 ± 2.1 mW cm^{-2}. This value varies as R^{-2} (R = distance from

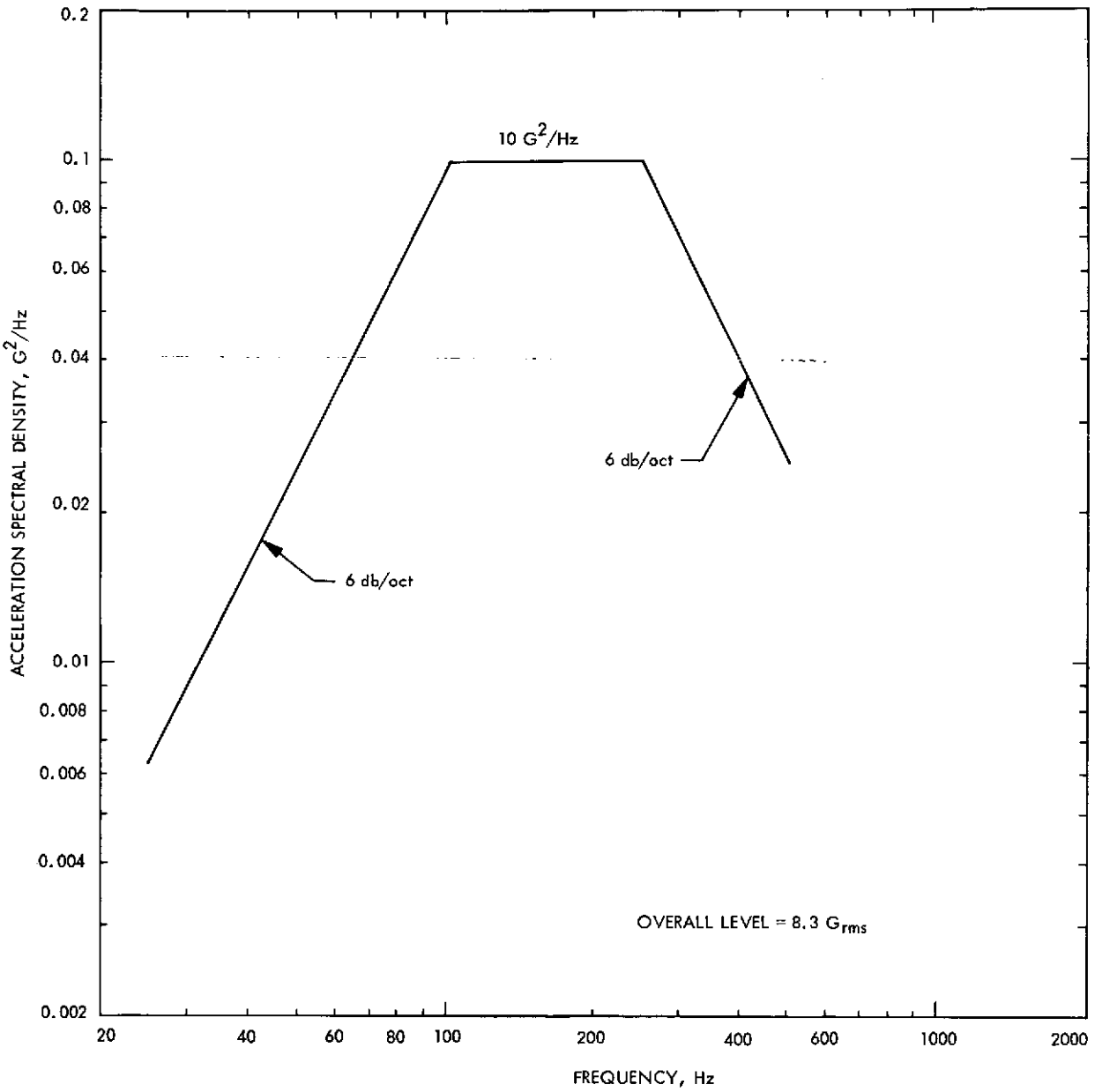

Fig. A-4. Assembly random vibration spectrum

Table A-10. Design temperature range

Assembly	Design temperature, °C Low	High
Electronics mounted in space vehicle primary structure	-30	85
All others	TBD	

Sun in astronomical units). The percentage of the solar constant occurring at wavelengths less than λ (μ) (in microns) is given in Table A-11.

Interplanetary space is equivalent to a black body with an effective radiating temperature of 4 K. (Note: The values in this paragraph are environmental estimates and contain no design margins.)

b. Ambient pressure. The space vehicle, subsystems, and assemblies shall be designed to withstand pressures ranging from 1 atmosphere ($\sim 10^{5}$ Nm^{-2} to 10^{-12} Nm^{-2}).

c. Radiation pressure. The space vehicle, subsystems, and assemblies will experience a radiation pressure on sunlit surfaces. For flat surfaces facing the Sun at 1 au this pressure is between 4.5×10^{-6} Nm^{-2} and 9×10^{-6} Nm^{-2}, depending on surface properties (4.5×10^{-6} for surface with zero reflectivity and 9×10^{-6} for surface which reflects totally and specularly). This pressure varies as R^{-2} (R in au).

12. Interplanetary meteoroids. Meteoroid fluences for the nominal Encke rendezvous 1980 mission have been developed from the meteoroid model given in NASA SP-8038, "Meteoroid Environment Model," 1970. Figure A-5 shows the accumulation of meteoroid fluence (particles per M^2) with time along the Encke trajectory for all particles having mass $>10^{-6}$ grams. Figure A-6 shows the variation of fluence with mass.

Impact probabilities may be calculated assuming a Poisson distribution:

$$P(O) = \exp(-FA)$$

where

$P(O)$ = probability of no impact

F = fluence, m^{-2}

A = surface area, m^2

For cometary particles the flux may be considered omnidirectional. For asteroidal particles surfaces within ±60 deg of the antisolar direction may experience a higher flux by a factor of 3 while on the outbound trajectory segment, and surfaces within ±60 deg of the solar direction may experience a higher flux by a factor of 3 while on the inbound trajectory segment.

Table A-11. Integral solar constant data

λ, μ	P, %	λ, μ	P, %	λ, μ	P, %
0.0850	1.3×10^{-4}	0.36	5.53	0.67	46.0
0.0900	1.4×10^{-4}	0.365	5.95	0.68	46.7
0.0950	1.5×10^{-4}	0.37	6.42	0.69	47.8
0.1000	1.7×10^{-4}	0.375	6.90	0.70	48.8
0.1050	1.8×10^{-4}	0.38	7.35	0.71	49.8
0.1100	1.8×10^{-4}	0.385	7.78	0.72	50.8
0.1150	1.9×10^{-4}	0.39	8.19	0.73	51.8
0.1200	2.0×10^{-4}	0.395	8.60	0.74	52.7
0.1250	6.0×10^{-4}	0.40	9.08	0.75	53.7
0.1300	6.2×10^{-4}	0.405	9.70	0.80	57.9
0.1350	6.3×10^{-4}	0.41	10.3	0.85	61.7
0.1400	6.4×10^{-4}	0.415	11.0	0.90	65.1
0.1450	6.7×10^{-4}	0.42	11.7	0.95	68.1
0.1500	7.0×10^{-4}	0.425	12.4	1.0	70.9
0.1550	8.0×10^{-4}	0.43	13.0	1.1	75.7
0.1600	1.0×10^{-3}	0.435	13.7	1.2	79.6
0.1650	1.2×10^{-3}	0.44	14.4	1.3	82.9
0.1700	1.8×10^{-3}	0.445	15.1	1.4	85.5
0.1750	2.1×10^{-3}	0.45	15.9	1.5	87.6
0.1800	3.2×10^{-3}	0.455	16.7	1.6	89.4
0.1850	4.9×10^{-3}	0.46	17.5	1.7	90.83
0.1900	7.0×10^{-3}	0.465	18.2	1.8	92.03
0.1950	1.1×10^{-2}	0.47	19.0	1.9	93.02
0.2000	1.5×10^{-2}	0.475	19.8	2.0	93.87
0.2050	2.0×10^{-2}	0.48	20.6	2.1	94.58
0.2100	3.0×10^{-2}	0.485	21.3	2.2	95.20
0.2150	4.0×10^{-2}	0.49	22.0	2.3	95.71
0.22	0.06	0.495	22.8	2.4	96.18
0.225	0.08	0.50	23.5	2.5	96.37
0.23	0.11	0.505	24.2	2.6	96.90
0.235	0.14	0.51	24.9	2.7	97.21
0.24	0.16	0.515	25.6	2.8	97.47
0.245	0.18	0.52	26.3	2.9	97.72
0.25	0.21	0.525	26.9	3.0	97.90
0.255	0.25	0.53	27.6	3.1	98.08
0.26	0.29	0.535	28.3	3.2	98.24
0.265	0.35	0.54	29.0	3.3	98.39
0.27	0.42	0.545	29.8	3.4	98.52
0.275	0.51	0.55	30.5	3.5	98.63
0.28	0.59	0.555	31.2	3.6	98.74
0.285	0.70	0.56	31.8	3.7	98.83
0.29	0.85	0.565	32.5	3.8	98.91
0.295	1.06	0.57	33.2	3.9	98.99
0.30	1.30	0.575	33.9	4.0	99.05
0.305	1.50	0.58	34.5	4.1	99.13
0.31	1.66	0.585	35.2	4.2	99.18
0.315	2.03	0.59	35.9	4.3	99.23
0.32	2.32	0.595	36.5	4.4	99.29
0.325	2.66	0.60	37.2	4.5	99.33
0.33	3.08	0.61	38.4	4.6	99.38
0.335	3.46	0.62	39.7	4.7	99.41
0.34	3.86	0.63	40.9	4.8	99.45
0.345	4.27	0.64	42.1	4.9	99.48
0.35	4.69	0.65	43.3	5.0	99.51
0.355	5.10	0.66	44.5	6.0	99.74
				7.0	99.86

λ, μ is wavelength; P is the percentage of the solar constant associated with wavelengths shorter than λ, μ.

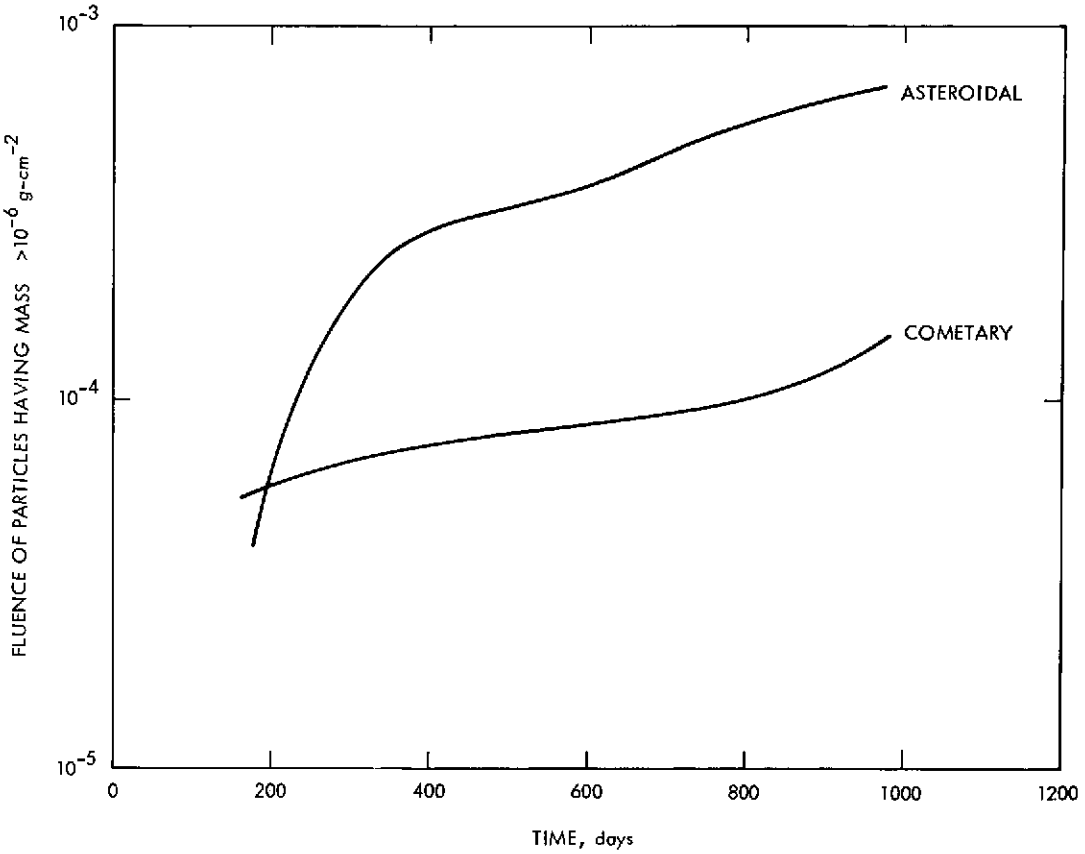

Fig. A-5. Meteoroid fluence

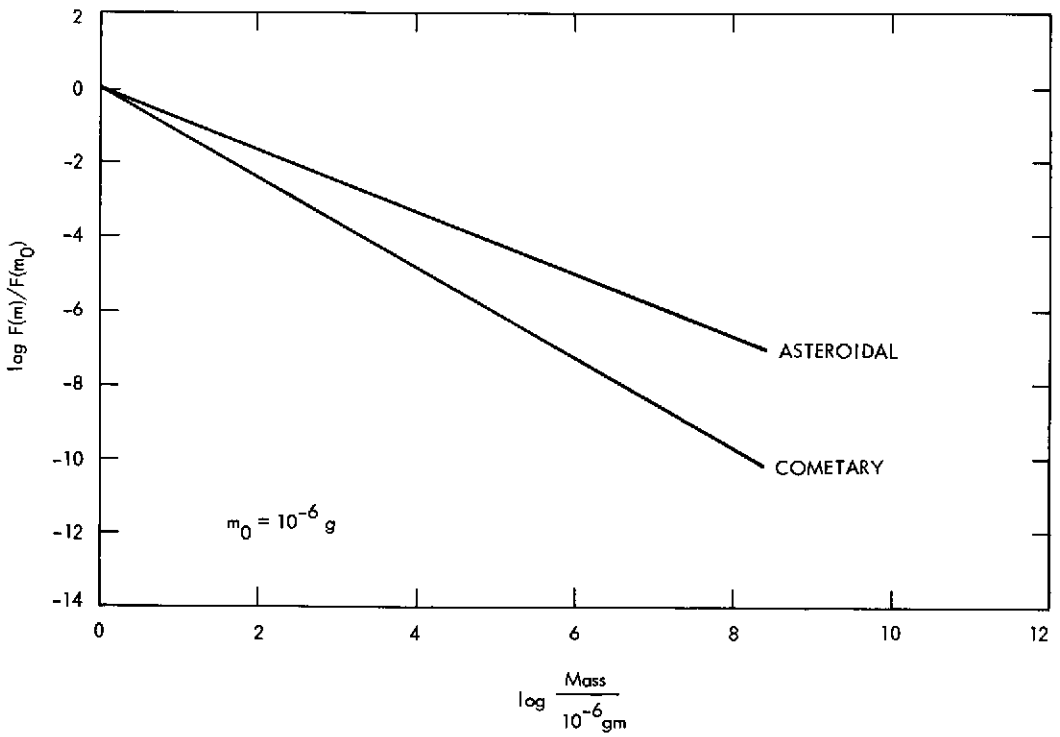

Fig. A-6. Meteoroid fluence vs mass

Particle density and relative velocity are estimated as:

	Cometary meteoroids	Asteroidal meteoroids
Mass density, gm/cm^3	0.5	3.5
Mean relative velocity, km/s	20	12

13. Solar wind. At the Earth's orbit (i.e., 1 au from the Sun, in the ecliptic plane, and near the Sun's equatorial plane) the solar wind parameters listed in Table A-12 (first column) are at least as large as the "quiet" values shown. Frequently, these parameters are larger than the "quiet" values, but they have not been observed to exceed the "maximum disturbed" values shown. The composition of the solar wind includes, in addition to protons and electrons (as in Table A-12), alpha particles which share the proton flow and temperature but have only 0.05 times the proton concentration and flux (a "quiet" value; the "maximum disturbed" value is 0.16), and heavier nuclei at even smaller concentrations and fluxes. The direction of the solar wind flow is approximately radially outward from the Sun and is limited to within about 10 deg of this direction. The "energy density" entries in Table A-12 indicate the order of dominance of the kinetic properties of the particles; the solar wind flow carries the interplanetary magnetic field along with it. The major features of the solar wind have been qualitatively explained by theoretical considerations which predict that the dependence on distance R from the Sun should follow the proportionalities shown in Table A-12 for the region specified by $0.3 \leq R \leq 30$ au, independent of latitude and longitude.

14. Solar flare protons. The solar flare proton environment has been estimated for the SEPSIT study mission, the Encke rendezvous (1980), using the nominal trajectory. The curves of Fig. A-7 define probabilities of encountering fluences of solar flare protons having kinetic energies greater than 30 MeV. Fluences of protons having energies greater than 10 or 100 MeV may be derived by multiplying the Fig. A-7 fluence values by:

7.81 for 10 MeV

0.105 for 100 MeV

The environment is independent of direction of incidence.

Table A-12. Summary of solar wind properties

Quantity	Quiet values[a] at 1 au	Maximum disturbed values[a] at 1 au	Radial dependence[b]
Proton concentration, cm^{-3}	8	120	R^{-2}
Proton flow speed, km/s	320	850	-
Corresponding flux, $cm^{-2}s^{-1}$	2.6×10^{8}	10^{10}	R^{-2}
energy, cV	534	4000	-
energy density, erg/cm^{3}	6.8×10^{-9}	7×10^{-7}	R^{-2}
energy flux, $erg/cm^{2}s$	0.22	60	R^{-2}
Proton temperature, K	4×10^{4}	10^{6}	-
Corresponding flux, $cm^{-2}s^{-1}$	2.5×10^{7}	2×10^{9}	R^{-2}
energy, eV	5.2	130	-
energy density, erg/cm^{3}	6.6×10^{-11}	2×10^{-8}	R^{-2}
energy flux, $erg/cm^{2}s$	7.0×10^{-5}	0.2	R^{-2}
Electron concentration, cm^{-3}	8	120	R^{-2}
Electron flow speed, km/s	320	850	-
Corresponding flux, $cm^{-2}s^{-1}$	2.6×10^{8}	10^{10}	R^{-2}
energy, eV	0.29	2	-
energy density, erg/cm^{3}	3.7×10^{-12}	4×10^{-10}	R^{-2}
energy flux, $erg/cm^{2}s$	1.2×10^{-4}	0.03	R^{-2}
Electron temperature, K	1×10^{5}	10^{6}	-
Corresponding flux, $cm^{-2}s^{-1}$	1.7×10^{9}	2×10^{11}	R^{-2}
energy, eV	13	130	-
energy density, erg/cm^{3}	1.7×10^{-10}	2×10^{-8}	R^{-2}
energy flux, $erg/cm^{2}s$	0.012	6	R^{-2}
Magnetic field strength, gauss	5×10^{-5}	16×10^{-5}	R^{-3}
Corresponding energy density, erg/cm^{3}	1.0×10^{-10}	1×10^{-9}	R^{-2}

[a]Observed. Maximum disturbed values considered very conservative.

[b]Theoretical; a dash indicates that no major R dependence is expected for $0.3 < S < 30$ au.

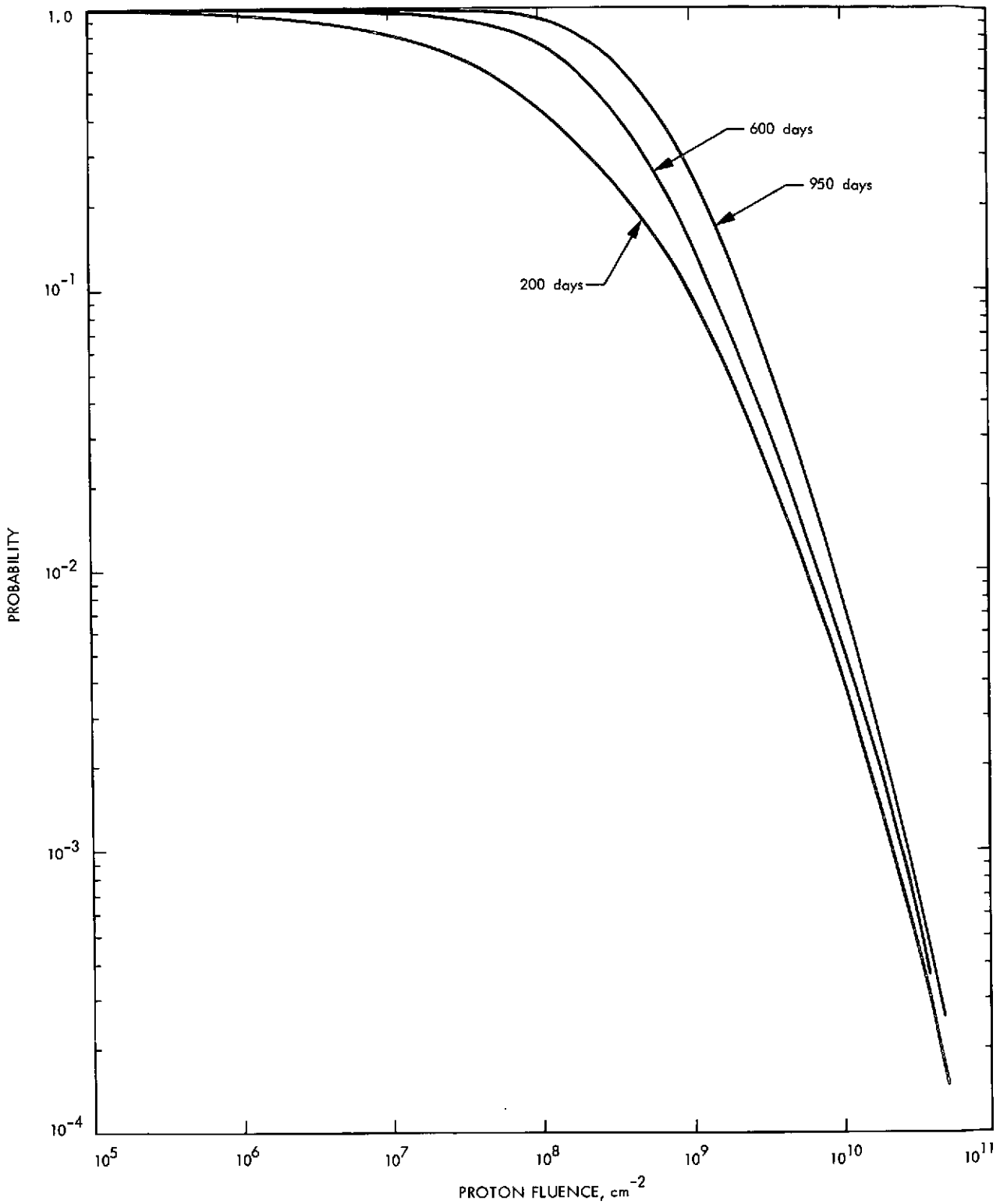

Fig. A-7. Solar flare proton fluence F of protons having energy E > 30 MeV

15. Magnetic field constraints. Magnetic fields generated by subsystems of the space vehicle must not interfere with the performance of science instruments. The following constraints are extracted from Viking or MJS requirements and should be considered as guidelines with additional constraints to be determined (TBD).

Sensitive instrument	Constraining level, nT	Locations of constraints
TV vidicon	5000	Science scan platform
Magnetometer	0.2	At magnetometer
Others	To be determined	

Allowable magnetic fields from subsystems/assemblies depends on distance from the sensitive instrument. MJS requirements for magnetometer compatibility are recommended as design guidelines for SEPSIT. That is, magnetic fields generated by an electronic assembly at 1 m from the assembly should be:

<40 nT	Static
<4 nT peak and <4 nT/$\sqrt{}$ Hz broadband <10 Hz	Dynamic

16. Electromagnetic compatibility

a. Conducted noise immunity. Input and output end-circuits identified in the following subsection shall be immune to (i.e., operate acceptably in the presence of) transient pulses as defined. That voltage or current value applies which is first reached as pulse amplitude increases.

Type 1 digital circuits. Type 1 digital circuits shall be immune to pulses of Table A-13 superimposed on the signal "1" state, "0" state, and "1-0" and "0-1" transitional states. Digital circuits, Type 1, are circuits which carry digital signals of less than 5 kbits (transitions) per second consisting of single pulses, binary levels, multibit words, clock signals and synchronizing signals, with voltage/current excursions greater than 200 V/A.

Table A-13. Conducted noise susceptibility

Circuit	Transient pulse amplitude voltage or current (whichever constraint is reached first; minimum, peak)	
Quiet	+1 V, -1 V	+100 mA, -100 mA
Noisy	+3 V, -3 V	+300 mA, -300 mA
Direct access and umbilical	+3 V, -3 V	+300 mA, -300 mA

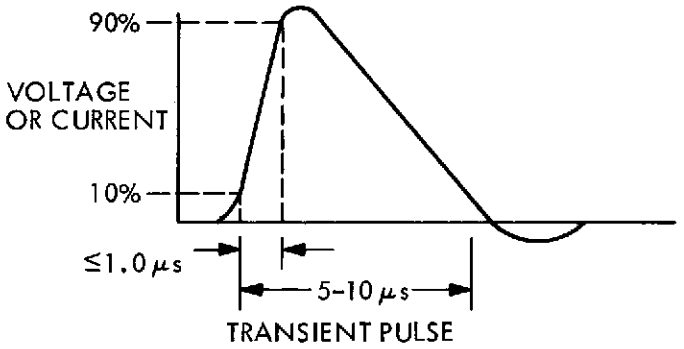

Analog circuits. All unshielded analog circuits, including direct access and umbilical, shall be immune to the transient pulses defined above.

Ground line noise immunity. Each externally referenced subsystem or electronic assembly shall operate acceptably when transient pulses of either the voltage or the current given in Table A-14 are injected between subsystem circuit common and chassis. Characteristics of the pulses shall be as defined in the above sketch.

Subsystems wherein the circuit common is internally referenced to chassis are not subject to this requirement.

b. Conducted noise generation. Conducted noise is defined as any voltage emitted from the output end-circuit (measured between signal and return line) instead of or superimposed on the intended signal. Such noise shall be controlled to the levels of Table A-15.

Ground line noise. No subsystem or electronic assembly shall develop more than 1.0 V (peak) of electrical noise between subsystem circuit common and chassis, when the two points are connected together only by means of a 183-cm (72-in.) length of 24-gage test wire. Subsystems wherein the circuit common is normally referenced internally to chassis are not subject to this requirement.

c. RF radiated noise immunity. Equipment shall be capable of satisfactory operation in the RF environment defined in Table A-16 as a minimum.

d. RF radiated noise generation. Equipment shall not generate RF noise which interferes with communications or science measurements. As a minimum, the Table A-17 constraints adopted from Viking Orbiter must be met. Additional science-dependent constraints are to be determined.

Table A-14. Ground line noise susceptibility

Subsystem	Transient pulse amplitude voltage or current (whichever constraint is reached first; minimum, peak)	
Externally referenced	+3 V, -3 V	+3 A, -3 A
Internally referenced	NA	NA

Table A-15. Conducted emission (noise generation)

Circuit	Amplitude (maximum peak)
Quiet	0.3 V
Direct access	1.0 V
Umbilical	1.0 V

Table A-16. RF radiated susceptibility (noise) levels

Frequency range, GHz	RF power density, W/m^2
2.1 - 2.3	10 avg
5.5 - 5.8	60 peak
8.3 - 8.5	0.5 avg

Table A-17. RF radiated emission levels (noise)

Frequency range, GHz	RF power density at 1 m, dBm/m^2
2.1 - 2.3	-140
5.5 - 5.8	-40

II. EMI DATA ON SEP POWER CONDITIONING UNIT

Figures A-8, 9, and 10 are from a presentation to the SEPSIT Study Team by Tad W. Macie (see also Ref. 3).

A summary of EMI test results (FY '72) is as follows:

(1) Radiated and conducted EMI greatly exceeds acceptance levels.

(2) Most EMI generated by 5-kHz ac power.

(3) Arcing produces breadboard interference with 20-dB peak at 150-kHz.

(4) PC harness radiates EMI.

(5) Panel shielding as provided not sufficient to suppress radiation.

III. STATIC MAGNETIC FIELDS FROM THRUSTERS VS SEPARATION AND GENERAL MAGNETIC CONTROL CONSIDERATIONS

A graph (Fig. A-11) has been adapted here from Ref. 11, to which has been added Bastow's 16 November 1972 measurement of the dipole moment of an inactive 30-cm permanent magnet engine (lower solid line), replacing Sellin's r^2 scaling estimate (upper dash-dot line), which turns out to be too high by a factor of 2. (It is not clear why the magnetic field of Sellen's estimate of the 20-cm engine is 6 times higher than the Bastow measurement of a 30-cm engine field at any separation distance, that is, whether there are real variations due to fabrication, design, etc., or merely difficulties in the analysis.) A magnetometer with a 6-m separation would see a 5.6 γ B_θ field from a single engine if it were deployed in the thruster array plane perpendicular to the thruster axis. It would see a 0.1 γ field if the magnetometer were located on a short boom at the tip of a solar array, assuming negligible fields from the array itself. (Unfortunately, thermal deflection and possibly vibration of the array is expected to considerably exceed the 1-deg pointing accuracy requirement of the magnetometer. If the deflection could be monitored and therefore known, then the array tip might be a satisfactory magnetometer location.)

Now consider the technique of achieving a degree of magnetic cleanliness in Mariner programs (i.e., no magnet for thrusters). There are two problems: (1) The three S/V field components at the magnetometer should be lower than,

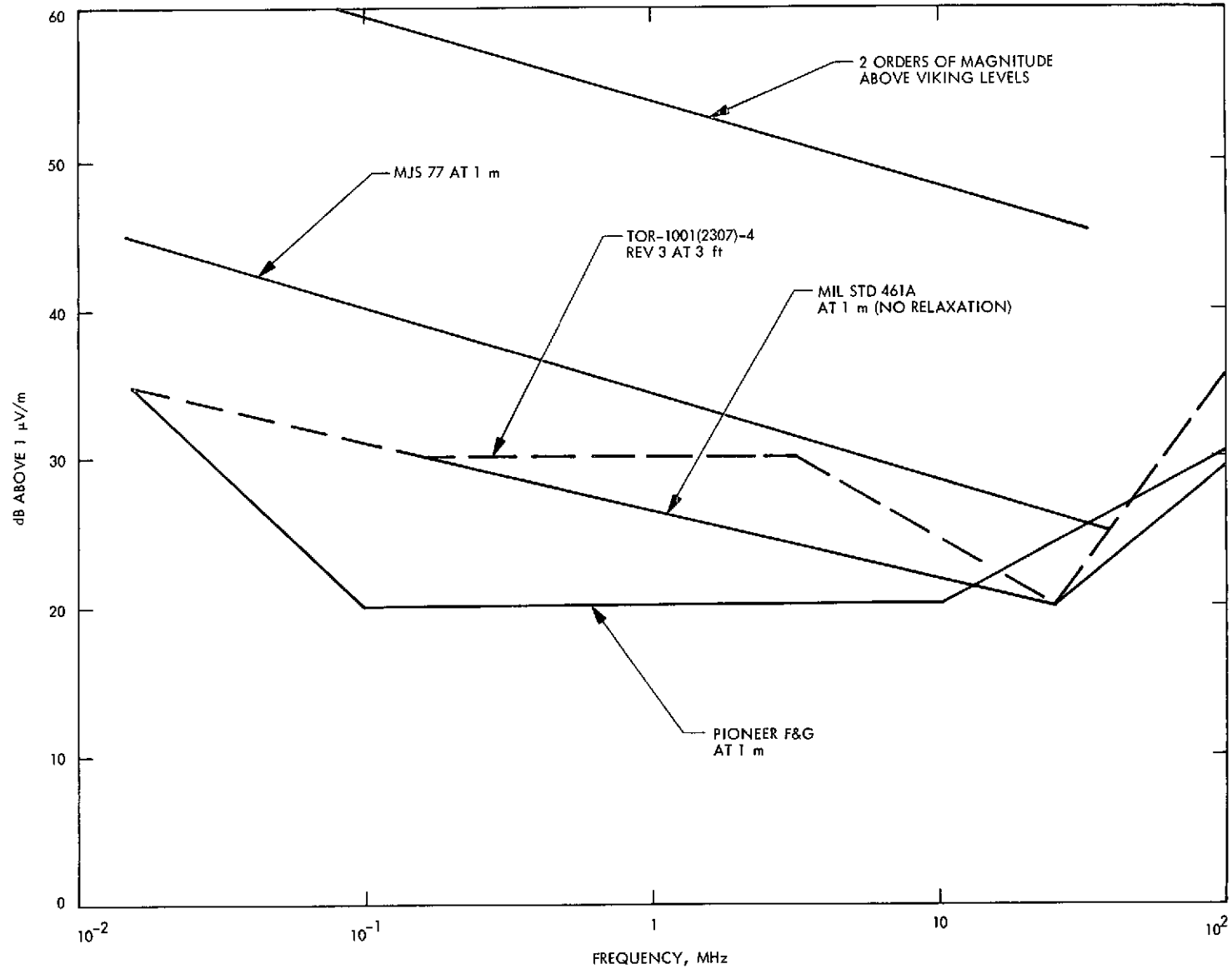

Fig. A-8. Narrowband CW radiated interference limits

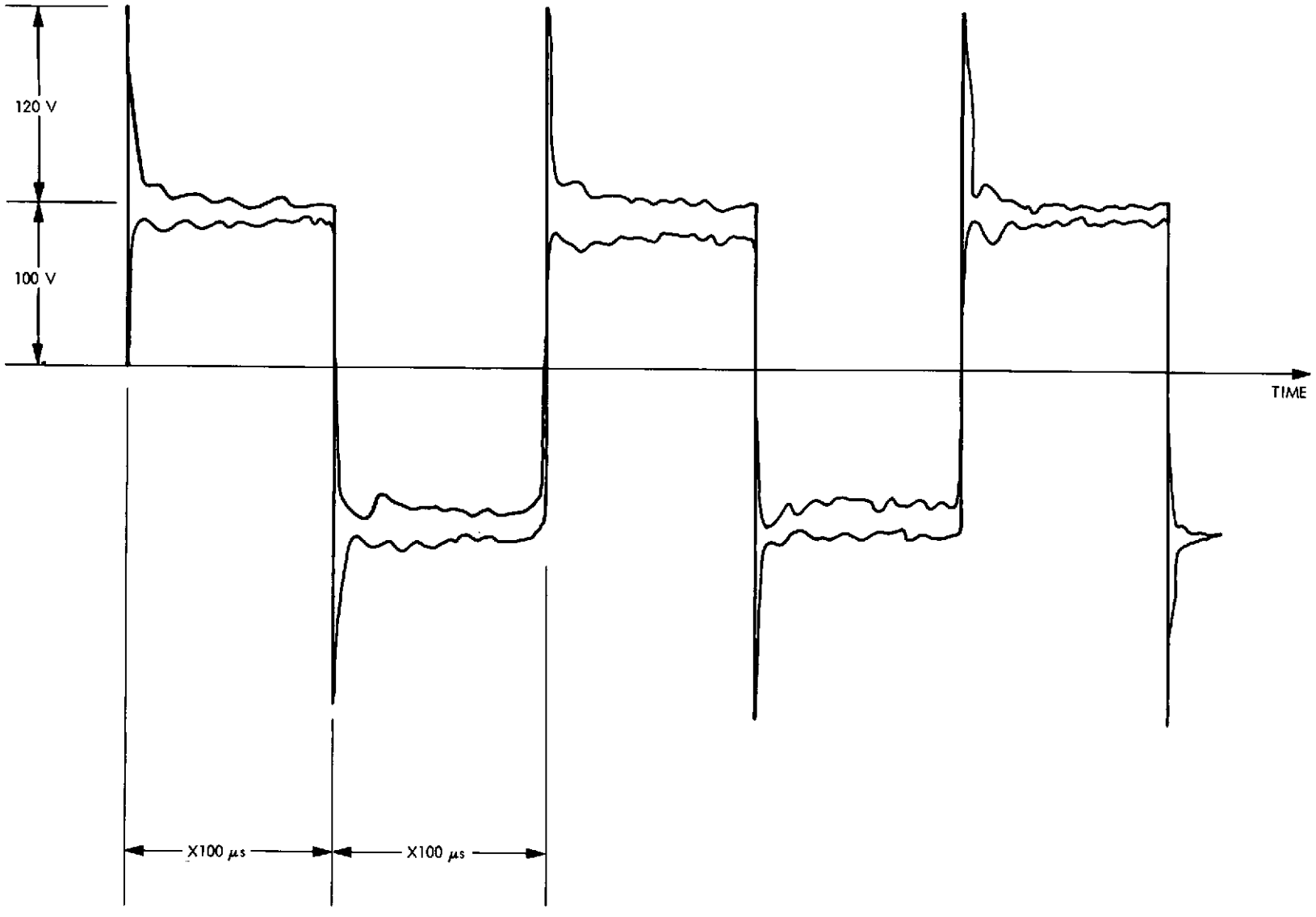

Fig. A-9. Auxiliary power 5 kHz inverter voltage waveform

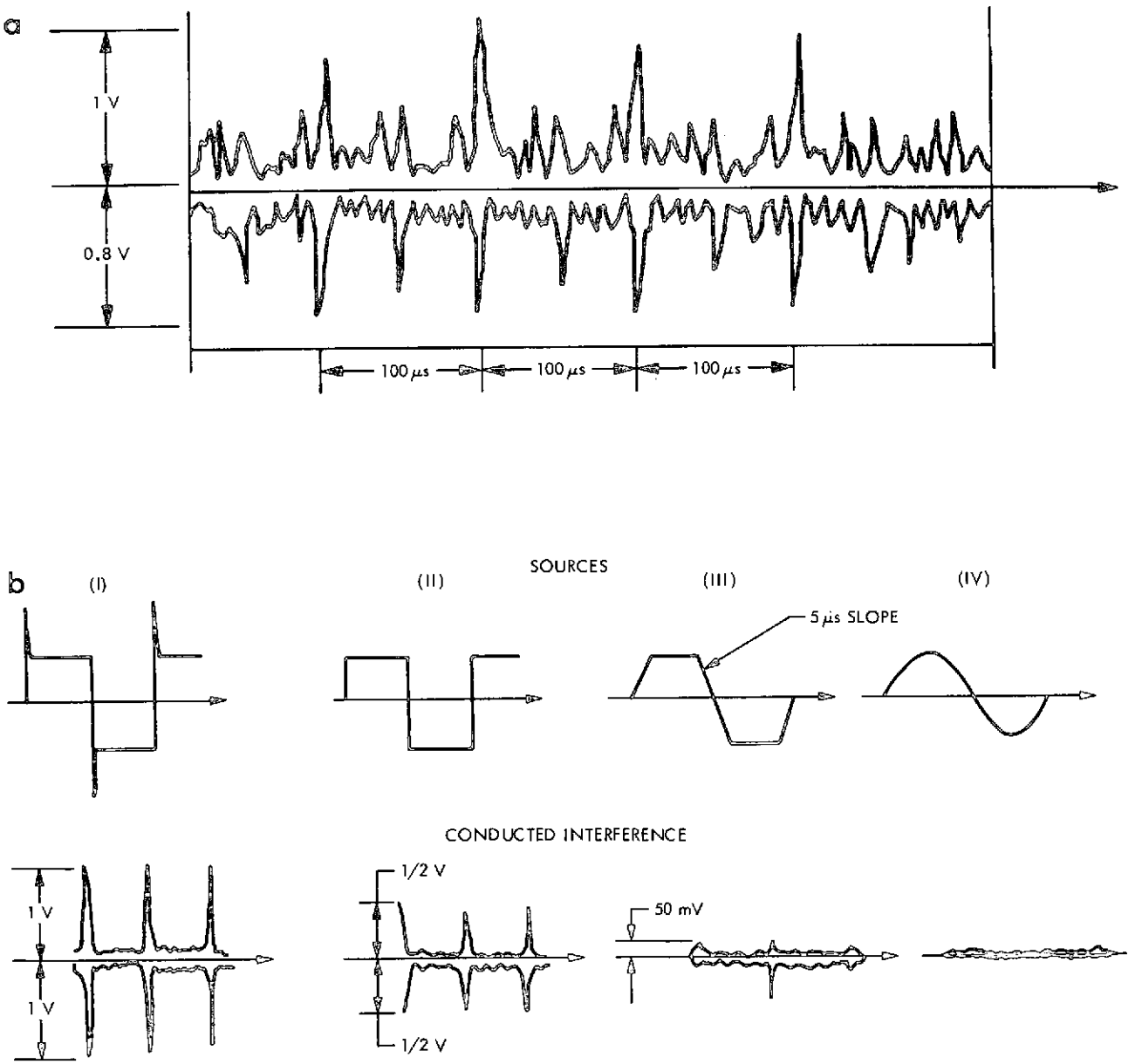

Fig. A-10. Measured EMI levels from a power conditioner

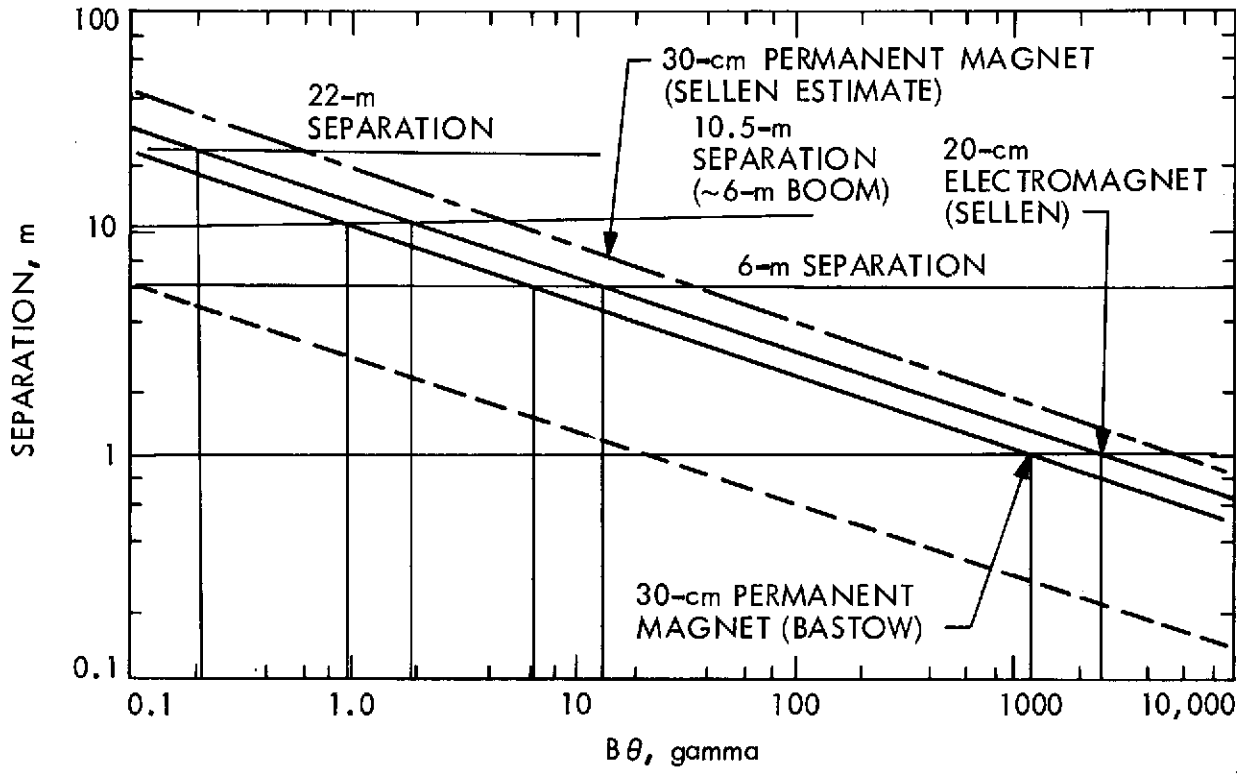

Fig. A-11. Thruster magnetic field vs separation distance

or at the very most not greater than, the variations of the interplanetary fields to be measured, i.e., 1γ ±0.1γ, and they must be known; (2) the field components must be stable for extended periods of time. There are, however, techniques to determine them in flight, at least approximately. A magnetic cleanliness procedure has worked in the past. First, every effort is made to exclude magnetically soft material, that is, material that is easily permed from S/V construction including all subsystems. Where these materials cannot be avoided (relays motors, etc.), their use is kept to a minimum. In any case, all subsystems are depermed prior to assembly except only in cases where this procedure is detrimental to the unit's performance. Second, each subsystem is assumed to contribute the field of a dominant dipole at the magnetometer (higher magnetic moments are neglected). Each subsystem is then surveyed to determine the strength and direction of its dipole moment (the procedure is relatively simple except in case of solar arrays), and the exact location and orientation of each subsystem is noted. With this information, and in the absence of, or to the extent that, the use of magnetically soft material is minimal, the dipole moments can be summed in a computer to give the field at the magnetometer.

Magnetic materials render this process inaccurate through nonlinear effects. Since the individual dipoles are virtually randomly distributed in position and orientation they sum to a surprisingly low value due to cancellations.

Past experience tells us that the Command and Control Subsystem (CCS) is the magnetically dirtiest subsystem, with the star tracker running second. But we must now also contend with the thrust subsystem, with its necessary magnetic field and the solar arrays which develop 40 times more than the customary power. Also, there are translations and gimballing of the thrusters and their magnets. To complicate matters still further, we must contend with a large number of possible active thruster configurations (see Appendix C), each with its own characteristic dipole field contribution.

APPENDIX B

OPTICAL EFFECTS IN ELECTRIC PROPULSION THRUSTER PLUMES

I. CALCULATION OF COLUMN DENSITY OF PLUMES

The following uses the formula (3-2) presented in Ref. 4 to calculate the column density of atoms in plume as seen from a location consistent with the field of view for science instruments on the configuration shown in Fig. 1 and with the geometry in Fig. 28

$$j(z) = j_0 \left[1 + \frac{2z}{r}\tan\beta + \frac{\tan^2\beta}{r^2} z^2\right]^{-1}$$

or

$$j(z) = j_0 \frac{1}{(1 + \frac{\tan\beta}{r} z)^2}$$

$$\int j(z)\, dz = j_0 \int \frac{dz}{(1 + \frac{\tan\beta}{r} z)^2}$$

If the FOV begins to intersect the plume at z_1, we obtain from the standard integral tables

$$\therefore \int_{z_1}^{\infty} j(z)\, dz = \left[-\frac{1}{\frac{\tan\beta}{r}(1 + \frac{\tan\beta}{r} z)}\right]_{z_1}^{\infty} = \frac{1}{\frac{\tan\beta}{r}(1 + \frac{\tan\beta}{r} z_1)}$$

For tan = 0.268 (i.e., $\beta = 15^{\circ}$),

$$\int_{z_1}^{\infty} j(z)\, dz = \frac{r}{\frac{0.0719 z_1}{r} + 0.268}$$

For $z_1 = 5r$,

$$\int_{5r}^{\infty} j(z)\, dz = j \frac{r}{0.0719\,(5) + 0.268} = j_0 \frac{r}{0.622}$$

For r = 30 cm and j_0 = 4 mA/cm^2 (5r = 1.5 m)

$$\int_{5r}^{\infty} j(z)dz = 193 \text{ mA/cm } (\times 6.25 \times 10^{15} \text{ ions/mA})$$

$$1.21 \times 10^{18} \text{ ions/s-cm}$$

but ion column density is also current density integrated along the view line divided by the ion velocity (assume constant velocity to infinity) 3×10^4 m/s.

$$1.21 \times 10^{18} \text{ (ions/s-cm)} / 3 \times 10^6 \text{ (cm/s)}$$

Therefore, 4×10^{11} ions/cm^2 is the column density looking parallel to the thrust axis. This actually is atoms and ions, since some fraction will be already neutralized.

II. CALCULATION OF MERCURY EMISSION INTERFERENCE ON SEP SPACE VEHICLE FOR UV INSTRUMENTS OBSERVING 1849 Å LINE

For the purpose of calculating the detectability of Hg atoms in the vicinity of the SEP spacecraft we will consider the MJS UV spectrometer. This instrument is optimized for measuring a solar occulation at a distance of $5R_J$ (Jovian radii). However, it can be used to make an order-of-magnitude estimate to the maximum allowable column density of Hg atoms in the line of sight illuminated by the Sun. The Hg atoms will resonate at 1849 Å and might interfere with a UV photometric measurement (see Appendix B-V).

In this exercise it is assumed that the UV spectrometer has a rectangular field of view 3×10^{-4} by 4×10^{-4} rad. The counting rate is given by

$$P = B_\lambda WAN_1N_2Qe$$

where

B_λ is the source brightness in photons cm^{-2} s^{-1} ster^{-1}

W is the angular field of view (1.2×10^{-7} sr)

A is the area of the grating (60 cm^2)

N_1 is the efficiency of the collimator (0.3)

N_2 is the efficiency of the grating (0.1)

Qe is the quantum efficiency of the detector for the instrument defined

$P = 5 \times 10^{-8} B_\lambda$ cts/s

$$B_\lambda = \frac{\Pi F\lambda}{\psi \Pi} \frac{\Pi e^2}{mc^2} \lambda^2 g f_\eta$$

where

ΠF_λ is the solar flux in photons/cm^2-s-Å at 1849 Å or about 2.5×10^{10}

$\frac{\Pi e^2}{mc^2} \lambda^2$ gf is the integrated absorption crossection in cm^2-Å or

8.9×10^{-13} cm $\times 1.8 \times 10^{-5}$ cm $\times 1.8 \times 10^3$ Å $\times 1.3$

η is the column density of ground state mercury atoms

Substituting these values into the equation for B_λ, we find $B_\lambda \cong 10^{-3}$

or $P = 5 \times 10^{-11} n$ cts/s.

If the counting rate exceeds the dark count of 1 ct/s, the signal is detectable. Thus a column density of $n < 10^{11}$ atoms/cm^2 is a safe number of Hg atoms in the line of sight illuminated by the Sun, and still is not detectable. Even for an order-of-magnitude increase, the inference is negligible for most conceivable instruments and objectives. The fact that a factor of 50 exists in the estimated/detectable ratio represents a potential marginal problem at the emission line wavelength.

III. SELECTED POSSIBLE UV EMISSIONS FROM COMET ENCKE IN THE RANGE 500 to 5000 Å

Diatomic species			
CH	3145Å		Strong
CO	2063	Cameron bands	Strong
	1544	4th positive	Strong
	1804	Hopfield-Birge	Strong
CS	2577		
H_2	1109-1600	Lyman bands	Weak
	3400	A - X	
HCl	1291, 1331		
HS	3262		
N_2	1450	Lyman-Birge-Hopfield	Strong
	2010	Vegard-Kaplan	Strong
	3370	2nd positive	Strong
	2173	γ bands	Strong
	and various others		
N_2^+	3570, 3911	1st negative	Strong
	1549	2nd negative	Strong
CO^+	2191	1st negative	Strong
NH	2531, 3300		
OH	3064		Strong
OH^+	3578		
NO	2262, 1909, 2198	γ, Δ, β	
NO^+	1368	1st negative	
O_2	2026	Schumann-Runge	Strong
	2885	Herzberg	
O_2^+	2610	2nd negative	Weak
NS	2310	γ bands	Weak
	2510	β bands	
SiO	2345		Weak
SO	2557		Weak

Polyatomic species		
H_2O	1200Å-1900Å	Broad
	1115, 1128	Single bands
CH_2	1414	Weak
HCN	<1120	Strong, diffuse
	1350-1550, 1535-1830	Weaker, discrete
HCO	2600-4100	Hydrocarbon flame bands
CO_2^+	2875-2905	Strong band
	2900-4900	Extensive band
CO_2	1122-1129	Very strong bands
	1130-1770	Strong
	1220-1390	Distinct
CH_3	1408, 1497, 1503, 2160	
NH_3	1150-1210, 1220-1290	Strong bands
	1270-1330, 1270-1435	Strong bands
	1480-1570, 1400-1690	Strong bands
	1700-2170	Diffuse
C_2H_2	1160-2400	Strong bands
H_2CO	1288-4000	Bands
C_2N_2	1250-1320, 1450-1680	Extensive band systems
	1820-2260, 2400-3020	
CH_4	500-1455	Diffuse
HCO_2H (formic acid)	1180-1225, 1280	
	1320-1410	
HC_2-CN (cyanoacetylene)	2100-2300, 2300-2715	Sharp bands
C_2H_4	1335-2100	Bands
CH_3CN	1101-1600	
CH_3NH_2	2000-2450	Diffuse
C_3H_4 (allene)	1350-2000	Bands
C_3H_4 (propyne)	1350-2000	Bands
C_3H_6 (propylene)	1350-2000	Bands

IV. EQUATIONS TO PREDICT CAMERA SIGNAL-TO-NOISE RESPONSE (by T. E. Thorpe)

1. Illuminance received by telescope aperture A

$$E = B\omega = \frac{\mathscr{P} E s \phi}{\Delta^2 \pi} \frac{K r^2}{R^2} = \frac{E s}{\Delta^2} \frac{p\phi}{4N^2}$$

where

$$\omega = \frac{s}{R^2} \frac{r^2}{R^2} = \frac{D^2}{4\lambda^2} = \frac{1}{4N^2}$$

2. Extended source signal

$$\text{Signal} \propto ETt \text{ or } = \gamma ETt$$

3. Point source signal

Illuminance per image area A' at sensor

$$\epsilon = \frac{F}{A'} T = E \frac{A}{A'} Tt = \frac{Bds}{R^2} \frac{A}{A'} T$$

$$\text{Signal} = \frac{Es\mathscr{P}\phi}{\Delta^2 4N^2} Tt \frac{D^2}{d^2} f$$

where signal $\frac{A'}{a}$ or $= f \frac{d'^2}{d^2}$

4. Encke nucleus signal

$$\text{Signal} = \gamma tT \; 10^{-(8.5+.4M)} \frac{D^2}{d^2} f \int H_\lambda \mathscr{T}_\lambda T_\lambda S_\lambda d_\lambda$$

where

H = irradiance

0th magnitude star = 10^{-8} ergs/cm^2 s 100 Å

5. Encke coma signal

$$\text{Signal} = \gamma tT \frac{\pi}{4N^2} \int Bds = \gamma tT \frac{\pi}{4N^2} B_0 \int_0^{r=\frac{d}{2}\frac{R}{\ell}} \frac{r_0}{r + r_0} 2\pi r dr$$

where

$$\frac{B_0 r_0}{r + r_0} = \text{coma photometric model } (\frac{\alpha B_0}{r})$$

$$\text{Per emission line } B_0(n) = \int C_\lambda S_\lambda \mathscr{T}_\lambda T_\lambda d_\lambda$$

$$C_\lambda = \text{photons/s cm}^2 \times 3.4 \times 10^{-12} \text{ ergs/photon} \times \frac{5165}{\lambda}$$

$$\text{Broadband } B_0 = \sum_{\text{lines}}^{n} B_0(n)$$

Definition of terms			
Symbol	Definition	Units	MM'71
A	area of telescope objection	cm^2	466
A'	area of image at sensor	cm^2	
a	area of a picture element	cm^2	6.25×10^{-6}
B	luminance (I/A)	lumens/ ft^2-str	
B_0	luminance at center of coma (r=0)	lumens/ ft^2-str	
C_λ	radiance per emission line	W/cm^2-str	
D	diameter of telescope objective	cm	21.6
d	diameter of a picture element	cm	2.5×10^{-3}
d'	diameter of optics point spread (50%)	cm	1.5×10^{-3}
E	illuminance received at telescope	lumen/ft^2	
E_s	illuminance received at comet nucleus	lumen/ft^2	
ξ	illuminance received at sensor	lumen/ft^2	
F	flux received at telescope	cd	
f	efficiency factor of read beam for sub-beam diameter images	-	0.7
g	phase angle at nucleus	deg	
H	irradiance of comet nucleus	W/cm^2 or erg/cm^2s	
I	intensity of comet nucleus (F/W)	cd/str	
ℓ	telescope focal length	cm	50.1
M	visual magnitude	2.5 log B	
N	focal ratio (ℓ/D)		2.35
R	spacecraft-comet range	km	
r	radius of nucleus or coma	km	
r_0	constant	1.1 km	
s	area of comet nucleus	km^2	
S_λ	vidicon relative spectral sensitivity		
T_λ	transmission of optics (including obscuration)		0.45 @ 550 nm
$\mathscr{T}_\gamma$	transmission of filter		

Definition of terms (contd)			
Symbol	Definition	Units	MM'71
t	shutter speed	s	
γ	television system gamma, e.g., DN/FCS		
Δ	ratio of comet-sun distance to 1 au		
λ	wavelength	Å	
$\mathscr{P}$	geometric albedo		
$\phi(g)$	phase function (relative luminance vs phase)		
ω	solid angle of target observed at telescope	str	

V. SELECTED STRONG MERCURY AND MOLYBDENUM EMISSION LINES FOR NEUTRALS AND SINGLY IONIZED ATOMS[a]

Atom	Ionization level	Wavelength, Å	Intensity	
			Arc	Spark
Hg	Singly	1649.8	No data	No data
Hg	Neutral	1849.68	Most sensitive	Most sensitive
Hg	Singly	1942.3	No data	No data
Hg	Neutral	2536.519	2000	1000
Mo	Singly	2816.154	200	300
Mo	Singly	2848.232	125	200
Mo	Singly	2871.508	100	100
Mo	Singly	2890.994	30	50
Mo	Singly	2909.116	25	40
Hg	Neutral	3650.146	200	500
Hg	Neutral	3654.833	No data	D200[b]
Hg	Neutral	3663.276	500	400
Mo	Neutral	3798.252	1000	1000
Mo	Neutral	3864.110	1000	500
Mo	Neutral	3902.963	1000	500
Hg	Neutral	4046.561	200	300
Hg	Neutral	4358.35	3000	500
Hg	Neutral	5460.740	No data	D2000[b]

[a]Data is from the 53rd Edition of the Handbook of Chemistry and Physics.

[b]Indicates a discharge tube spectrum.

APPENDIX C

AN OPTIMUM MAGNETIC FIELD CANCELLATION STRATEGY

To mitigate the problem associated with the set of active thruster configurations, it is possible to adopt a strategy which might be called optimum field cancellation. The strategy takes two general forms, depending on the type of thruster selected in the S/V design. At the time of writing, final choices have not been made between thrusters with permanent magnets (PMT) and thrusters with electromagnets (EMT).

Cancellation strategy for EM thrusters can be accomplished through a thruster field switching program. It should be noted that thruster performance is not dependent on the polarity of the thruster field. If we can accept the addition of DPDT switches in the magnet circuits, controlled, for example, by a simple on-board computer routine, the magnetic polarity of each active engine can be optimally selected to produce the minimum summed field after the manner shown in Fig. C-1 for a few of the possible configurations (the values in parentheses are the fields seen by the magnetometer in the case all polarities are the same). A still greater improvement can be achieved by appropriately activating the field windings of selected inactive engines also. A disadvantage of EM thrusters which deserves consideration is the presence of soft iron cores in the electromagnet design. Soft iron, which introduces nonlinearities into the dipole summing process, diminishes the prediction reliability of this method and increases the S/V field variability due to temperature and vibrational dependencies on permeability.

Cancellation strategy for permanent magnet thrusters can be accomplished by installing the set of thruster magnets in such a way that their dipole moments produce a minimum field at the magnetometer location. Clearly, for reasonable separation distances, a sufficiently reduced field cannot be achieved by this means alone, particularly if an odd number of thrusters is involved in the design. Because of the finite size of the thruster array and the inverse cube law for dipole moments, an even number of thrusters brings with it only a moderate improvement. Additionally, there is the dispersion in the thruster magnet field strengths due to manufacturing processes. Therefore, a bucking or trimming coil (possibly a programmable electromagnet) is needed to reduce the thruster magnetic field to

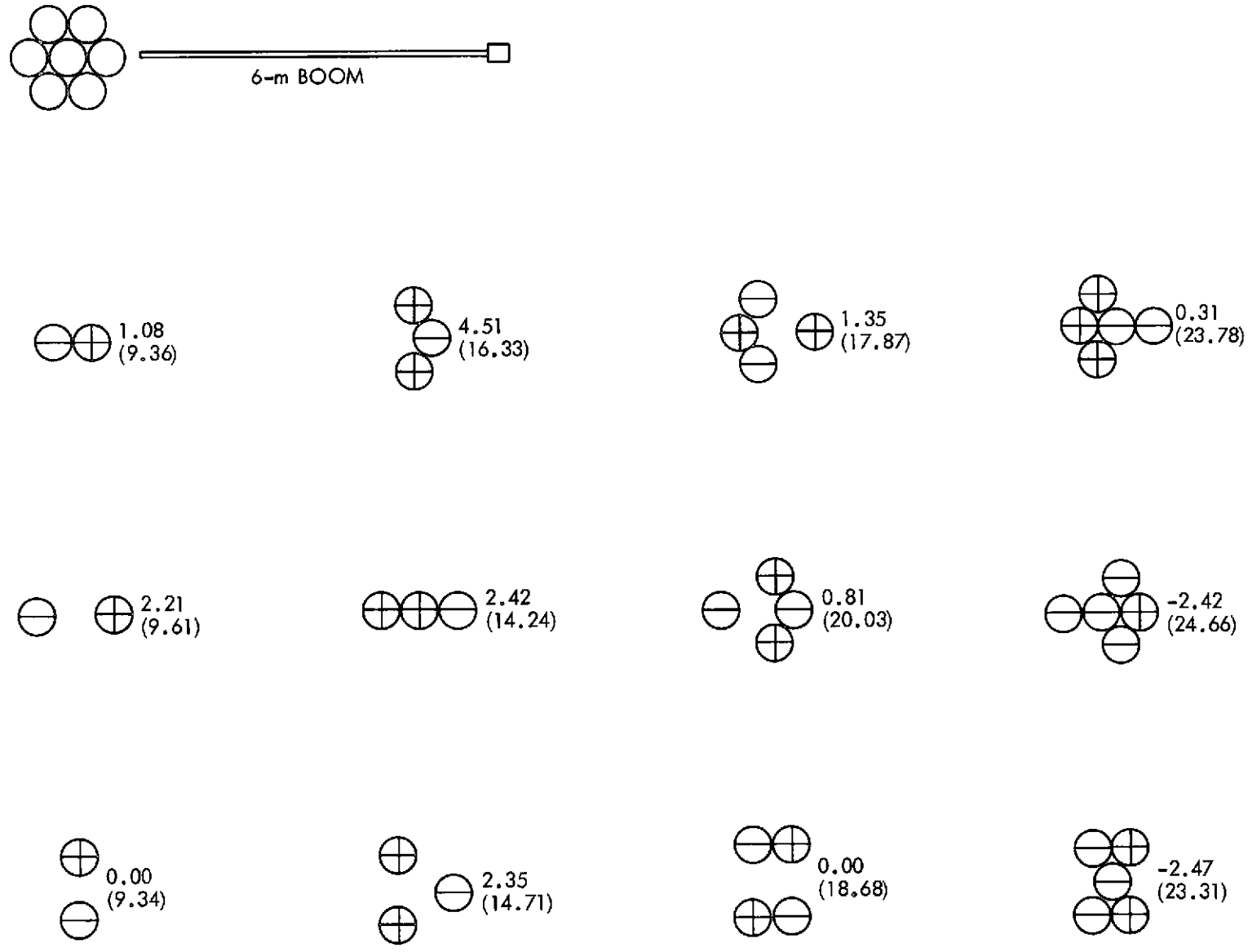

Fig. C-1. Thruster dipole orientation schemes

acceptable values at the magnetometer. If optimum thruster magnet poling is undertaken, then at the very most, the power and weight penalty of a bucking coil is no greater than that required for a single EM thruster magnet system, and if properly designed can be far less.

At least two disadvantages of the PM thruster are evident:

1. The fields cannot be switched off for "magnetically clean" periods to support magnetometer measurements
2. Permed field sources are inherently unstable, particularly in the high-temperature regime in an active thruster. Magnetometer measurement reliability is dependent upon fields which do not change unpredictably.

REFERENCES

1. Gardner, J. A., Solar Electric Propulsion System Integration Technology (SEPSIT) Final Report, Vols. I-III, Technical Memorandum 33-583, Jet Propulsion Laboratory, Pasadena, Calif., Nov. 15, 1972.

2. Newburn, Jr., Ray L., et al., Preliminary Information on a Science Rationale and a Science Instrument Package for a Slow Flyby of Comet Encke, Jet Propulsion Laboratory, Pasadena, Calif., (to be published).

3. Whittlesey, A. C., and Macie, T. W., Electromagnetic Interference of Power Conditioners for Solar Electric Propulsion, Technical Memorandum 33-623, Jet Propulsion Laboratory, Pasadena, Calif., July 1, 1973.

4. Hall, David F., Electrostatic Propulsion Beam Divergence Effects on Spacecraft Surfaces, Final Report, Vol. II, Report 11985-6002-RU-00, TRW Systems, Redondo Beach, Calif., Jan. 17, 1973.

5. Huberman, Marshall, TRW, personal communication, Mar. 1973.

6. Sellen, Jr., J. M., et al., Solar Electric Propulsion/Instrument/Subsystems Interaction Study, Final Report, Report 22878-6007-RU-00, TRW Systems, Redondo Beach, Calif., Mar. 30, 1973.

7. Taylor, F. W., A Model of the Physical Properties of the Comet Encke, Technical Report 32-1590, Jet Propulsion Laboratory, Pasadena, Calif. (in press).

8. Metzger, A. E., et al., "Lunar Surface Radioactivity: Preliminary Results of the Apollo 15 and Apollo 16 Gamma-Ray Spectrometer Experiment," Science, Vol. 179, 800, Feb. 23, 1973.

9. Metzger, A. E., and Arnold, J. R., "Gamma-Ray Spectroscopic Measurements of Mars," Appl. Opt., Vol. 9, 1289, June 1970.

10. Scarf, F. L., et al., A Preliminary Report on the IMP-7 Plasma Wave Investigation: Instrumentation and In-Flight Performance, Report 22751-6001-RU-00, TRW Systems, Redondo Beach, Calif., Mar. 1973.

11. Sellen, J. M., Jr., personal communication, Sept. 19, 1972.

12. Hanson, W. B., Sanatani, S., Zuccaro, D. and Flowerday, T. W., "Plasma Measurements with Retarding Potential Analyzer on OGO6," JGR Space Physics, Vol. 75, No. 28, 5483, Oct. 1, 1970.

13. Metzger, A. E., and Trombka, J. I., "Identification and Control of Spacecraft Radiation Sources of Interference to X-Ray and Gamma-Ray Experiments," Proceedings of the National Symposium on Natural and Manmade Radiation in Space, E. A. Warman, Ed., NASA TM-XL, 2440, 714, Jan. 1972.

14. Strong, J., et al., Procedures in Experimental Physics, Prentice-Hall, Inc., Englewood Cliffs, N.J., 1945.

15. Milder, N. L., and Sovey, J. S., "Optical Radiation from Regions Downstream of Mercury Bombardment Thrusters," Paper 72-441, AIAA Ninth Electric Propulsion Conference, Bethesda, Md., April, 1972.

16. Thomassen, K. I., "Radiation From Pulsed Electric Thrusters," Paper 73-263, AIAA Eleventh Aerospace Sciences meeting, Washington, D.C., Jan. 10-12, 1973.

17. Danilowicz, R. L., "Magnetic Flux Density Environment of Several Electron-Bombardment Ion Thrusters" NASA-TM X-68239 Lewis Research Center, May, 1973.

18. Functional Requirement, Viking Orbiter 1975 Environmental Design Criteria, Project Document VO75-3-240, Jet Propulsion Laboratory, Pasadena, Calif., June 25, 1973.

19. Functional Requirement, Viking Orbiter 1975 Electrical Grounding and Interfacing, Project Document VO75-3-260, Jet Propulsion Laboratory, Pasadena, Calif., Dec. 29, 1972.

NASA — JPL — Coml., L.A., Calif.